Cloud Forest Hydrology in a Changing Context

An approach to understanding the impact of
Climate Change and Deforestation
on the Water Balance of the Sierra Yalijux
Alta Verapaz, Guatemala

MultiDisciplinary Project 2023

TU Delft

Cloud Forest Hydrology in a Changing Context

An approach to understanding the impact of
Climate Change and Deforestation
on the Water Balance of the Sierra Yalijux
Alta Verapaz, Guatemala

by

Students:	Diana Arias - 4911865
	Femke Bulsing - 5415047
	Jelle Schrijver - 4581687
	Maxine Luger - 4494555
	Linnaea Cahill - 5543665
Institution:	Delft University of Technology
Faculty:	Civil Engineering and Geosciences
Course:	Multidisciplinary project
Place:	Delft, Netherlands
Date:	Wednesday 19th April, 2023

TU Delft

Executive Summary

This project is a consulting project for Community Cloud Forest Conservation (CCFC) on how to obtain and communicate to relevant stakeholders an understanding of **the impact of land use change and climate change on the hydrological balance of the cloud forest ecosystem in the Sierra Yalijux**. The outcomes of the project will be used by CCFC and partners in four areas: Rural water committee capacity building with municipal and village leadership groups, environmental education with the ministry of education, reforestation, and conservation carbon/water credit prioritization with the national forestry institute, and to create thesis topics for bachelors level students with Universidad Rafael Landívar and Universidad de San Carlos.

In order to achieve this goal, we divided our efforts in four areas: First, a description of the situation and a review of literature to identify gaps in scientific and practical understanding of local cloud forest hydrology (Chapter 2). Second, an analysis of the situation at a regional scale using publicly available historical data such as remote sensing data and data from the national meteorological authority (Chapter 3). Third, identifying important hydrological processes in the Cloud Forest micro-climate (Chapter 4) and prototyping and testing measurement setups (Chapter 5). Fourth, making suggestions on how to apply the results to the intended impact areas that CCFC has (Chapter 6).

Our recommendations to CCFC for capacity building with water committees are based on a literature review, we found that the presence of Cloud Forest is expected to increase base flow in springs due to its ability to capture additional hydrological inputs in the dry season, increase moisture recycling after heavy rain events, and store water in the soil. We recommend working with water committees to outline the recharge zones of their springs, run some simple calculations on water availability based on precipitation, and develop management plans for the area.

Our recommendations for further research are based on the research approaches we describe at the regional scale and the prototyping of field methodologies that we tested. A more permanent setup for data collection is being developed jointly with the Universidad de San Carlos at CCFC's nature preserve.

Acknowledgements

This project would not have been possible without the financial support of Students4Sustainability, FAST Fund, Delft Global Initiative, and MC de Visser Fonds.

We would like to express special thanks to our supervisors: Dr. Saket Paned, Dr. Ir. Marc Schleiss, and Prof. Dr. Ir. Bas van de Wiel for their guidance, and to many current and former members of the Water Management Department at TU Delft for always having their door open or for not minding an interruption to their coffee break, especially Dr. Ir. Miriam Coenders and Dr. Ir. Ruud van der Ent, Dr. Ir. Martine Rutten, Dr. Cesar Jimenez Rodríguez. Also thanks to the Water Lab staff for lending us the equipment we needed.

We are grateful to Dr. Wener Ochoa of Universidad de San Carlos de Guatemala for the advice and feedback throughout the project; to Dr. Fredy Archila for introducing our team to the botany of the Sierra Yalijux Cloud Forest; and to Dr. Rowland Griffin for the advice and loan of measurement equipment.

For hosting us in Guatemala, we thank Community Cloud Forest Conservation, particularly, Elsi Mucú, and Ana Cabnal, who accompanied us on field work, and Delia Valdizón for sharing her knowledge on local water management systems. For welcoming us to Satex and allowing us to complete our fieldwork on his property: Ismael Caal Quib.

During our fieldwork, Boris Llamas and Juan Pablo Pinto of Tree Climbing Guatemala, were key members of our team, thanks for helping us reach the canopy!

And finally, thanks to many members of the tropical montane cloud forest and páramo hydrology research community for the wealth of knowledge and inspiration to continue studying the complexity of this special ecosystem, especially to Laurens Poorter, Hans Vester, Erik Veneklaas, Sybil Gotsch, Robert Hofstede, and Conrado Tobón Marín, for their comments.

Contents

1

Project Definition and Objectives

Alta Verapaz, a mountainous department in the central highlands of Guatemala, has documented the highest poverty and inequality rates in the country (99; 94). The majority of the population belongs to the predominantly rural Maya ethnic group, Q'eqchi'. In southern Alta Verapaz, the Sacranix and Yalijux mountain ranges are a patchwork of indigenous smallholder farming villages, larger farms 'fincas', and forested areas. The exploitation of land for agriculture or other economic activities has been expanding constantly, with little regard for preserving natural ecosystems. Recognizing the importance of the ecosystem services that forests can lead to valuing their presence in the landscape.

With population growth and subdivision of land, Alta Verapaz has seen an expansion of agriculture and large-scale logging as key factors behind the deforestation of cloud forests (76). As these cloud forests rapidly disappear from Guatemala's rural highlands in recent decades, the freshwater resources that supply the potable water systems in the region, also deteriorated (75).

Across the planet, tropical forests are the guardians of ecosystem services, including clean water, biodiversity, healthy soils, and carbon sequestration (105; 5). Tropical montane cloud forests (TMCF) carry a critical hydrological significance in the highlands of Alta Verapaz: drought and erosion prevention, provision of water availability, horizontal precipitation interception, and deep groundwater recharge (10). Springs fed by the cloud forest in the region typically flow year-round, however in the last couple of decades, less to no flow in springs during the dry season and flooding during rainy and hurricane seasons may be attributed to global, regional, or local changes in the hydrological system (13).

Global changes could include those due to the increase of greenhouse gases in the atmosphere, such as alterations in the Intertropical Convergence Zone (ITCZ) and North Atlantic, Pacific Decadal, or El Niño-Southern Oscillation (NAO/PDO/ENSO) (14). Regional changes could include lowland deforestation resulting in higher cloud elevations (79; 57) and local deforestation affecting cloud formation, local recycling, and precipitation processes (7).

Cloud forests and their role within the hydrological context have been a topic of increasing research interest over the past few decades. The unique characteristics of cloud forests, such as persistent fog, high levels of precipitation, and high biodiversity, make them important sites for understanding the hydrological cycle and the impact of environmental change on water resources. While there is significant research on cloud forests and their role in the hydrological context, the amount of research specific to cloud forests in Guatemala is more limited. Further research is needed to better understand the functioning of cloud forests in Guatemala and to inform management strategies that promote their sustainability and conservation (10; 67).

1.1. Defining the Project Objectives and Research Questions

Based on a review of relevant literature and discussions with CCFC on the situation and needs in the region (see Chapter 2), the question driving the project is:

How can the impact of land use change and climate change on the hydrological balance of the

cloud forest ecosystem in the Sierra Yalijux be studied in order to improve the local operational understanding of threats to water availability in the dry season?

In order to answer this question, the following directions of inquiry and action were defined:

- Regional Scale: Change Driver Analysis
  - Objective A: Identify continental-scale climate change and land use change patterns that influence the spatial and temporal distribution of precipitation in highland Cloud Forests (Chapter 3.1).
  - Objective B: Identify changes in meteorological conditions and land use in the Sierra Yalijux, and the impact these are expected to have on the hydrological balance of the Cloud Forest ecosystem (Chapter 3.2).
- Local Scale: Hydrological Balance
  - Objective C: Outline the most important processes to model in a hydrological balance in the cloud forest ecosystem, and how they interact with each other.
  - Objective D: Prototype in-situ setup for data collection to calibrate and validate the canopy hydrological balance.
- Operational Scale: Applying Knowledge
  - Objective E: Identify measures that could be encouraged by advocates for water security and forest conservation in order to adapt to the changing global climate through the preservation of microclimates.
  - Objective F: Suggest topics for research on the Cloud Forest of the Sierra Yalijux.

1.2. Target Impact Areas

The objective of this research is to contribute to the development of sustainable water management practices that support both the natural environment and human well-being in Guatemala and beyond.

1.2.1. Scientific

The scientific objective of research on the hydrological context of Guatemalan cloud forests is to understand the complex interplay between the forest ecosystem and water resources. These cloud forests are known for their high biodiversity and unique hydrological characteristics, including high levels of rainfall interception, storage, and release. However, human activities such as deforestation and land-use changes have led to the degradation of cloud forests and altered their hydrological cycles. Cloud forests are particularly sensitive to changes in temperature and precipitation, and understanding their hydrological cycle can help improve the understanding of the impacts of climate change on freshwater availability and ecosystem services. The findings of this project will help identify the key drivers of hydrological changes and inform conservation and management strategies. The research will hopefully have implications for the broader scientific community, including researchers studying climate change impacts, hydrology, ecology, and biodiversity. The findings of this research will be of interest to scientists working in these fields and can help advance scientific knowledge in these areas.

1.2.2. Societal

From a societal perspective, the research has significant relevance as well. Cloud forests are critical ecosystems that provide a range of important services, including freshwater supply, carbon sequestration, and biodiversity conservation. The research on the hydrological cycle of cloud forests will provide policymakers, conservationists, and other stakeholders with crucial information needed for making informed decisions about land use, water

management, and conservation efforts. The research will also help support sustainable development and improve the quality of life for local communities that rely on cloud forests for their livelihoods and well-being. Thereby, members of local communities will be involved in the research, providing them with the tools to gain an understanding of the functioning of the cloud forest.

1.3. Project Team

- TU Delft MDP Team (Maxine Luger, Jelle Schrijver, Femke Bulsing, Diana Arias, Linnaea Cahill), advisors (Dr. Saket Pande, Dr. Marc Schleiss, Prof. Dr. Ir. Bas van de Wiel)
- Community Cloud Forest Conservation (Ing. Delia Valdizón, Elsi Mucú, Ana Cabnal)
- Tree Climbing Guatemala (Boris Llamas-Menchú, Juan Pablo Pinto)
- Archilarum (Dr. Ing. Fredy Archila, Javier Archila)
- Universidad de San Carlos de Guatemala (Dr. Ing. Wener Ochoa)

Figure 1.1: Members of Project Team from TU Delft MDP group, Tree Climbing Guatemala, and Community Cloud Forest Conservation.

2

Background

2.1. Project Area

The studied area lies in the department of Alta Verapaz in Guatemala. Guatemala is mountainous and borders the Pacific Ocean to the south, Honduras, El Salvador, Belize, and the Gulf of Honduras to the east, and Mexico to the west and north. The country is divided by two mountain chains, creating distinct regions: the lowlands of the Atlantic slope (Peten) region north of the mountains, the highlands in between the mountains, and the pacific slope south of the mountains. Peten was once covered in rainforests, but deforestation has turned big parts of the southern part of Peten into savanna grasslands. The lowlands on the pacific coast have been cleared of their rainforest and now consist of agricultural landscapes. Alta Verapaz is located in the north-central part of the highlands, bordering Peten. Alta Verapaz is characterized by its rugged mountainous terrain and diverse ecosystems. The region is situated on the southern edge of the Sierra Madre mountain range and is home to several peaks that exceed 2,000 meters in elevation. The geological formation of the region is dominated by Mesozoic sedimentary rocks, which are interspersed with volcanic rocks of varying ages. The area experiences a tropical climate, with high temperatures and precipitation throughout the year, although there is a marked dry season from November to April. The region is also characterized by a high degree of biodiversity, with numerous species of flora and fauna inhabiting its forests, rivers, and caves. The mountainous area has an elevation range of 200 meters to 2800 meters.

2.2. Community Context

2.2.1. History of Maya Culture

The Maya built a highly advanced Mesoamerican civilization that flourished in the pre-Columbian era from around 2000 BC to 1500 AD. The Maya civilization was primarily located in present-day Mexico, Guatemala, Belize, Honduras, and El Salvador, and was known for its highly sophisticated architecture, art, mathematics, astronomy, and writing system. (81). The decline of the Maya civilization is still debated, but environmental factors, such as drought and deforestation are likely to have played a role (26). Despite the decline of the Maya civilization, their culture and traditions have survived to the present day, and the Maya people continue to practice their ancient customs and beliefs. Today, the Maya culture in Guatemala is a vibrant and dynamic part of the country's social fabric, with many communities continuing to practice their traditional customs and beliefs. One important aspect of Maya culture in Guatemala is the use of traditional agricultural practices. Many Maya communities rely on subsistence farming, using sustainable methods such as crop rotation and intercropping to maintain soil fertility and biodiversity. Maya farmers also have an intricate understanding of local weather patterns and ecological systems, which allows them to make informed decisions about when and how to plant and harvest their crops. However, despite the resilience and importance of Maya culture in Guatemala, many Maya communities continue to face social, economic, and political challenges. Discrimination and marginalization are still common, and many Maya people struggle with poverty and limited access to

education and healthcare. Efforts to promote cultural preservation and promote the rights and well-being of Maya communities are ongoing and involve collaboration between Maya leaders, civil society organizations, and government agencies (59).

2.2.2. Village-level governance and water issues

Villages in Guatemala are under the administrative political jurisdiction of municipalities, however, many governance tasks are the responsibility of village-level councils and committees. Typically, the village governance structure includes a council (Consejo Comunitario de Desarrollo or COCODE), and a handful of committees responsible for areas including Education, Health, Access, and Water; some villages have a Women's committee or an Environment committee as well. Each committee works together with all the families in the village to establish objectives and execute them. For example, if a village needs to build or repair its access road or water distribution system, the access/water committee will make a proposal and budget which may be submitted to the municipality to ask for support, or to collect the necessary funds from each family if machinery or materials are needed, regardless of municipal support, the committee would typically organize the men in the village to work on the road/water system. Village water committees in the municipalities of Alta Verapaz oversee the construction of water tanks and piped distribution systems, however, a concern for maintaining water quality or water availability is not within the scope of practical responsibilities.

Water quality is occasionally monitored by the Ministry of Health, which provides guidance on boiling water before consumption. Meanwhile, concerns for water quantity/availability are dealt with at a household level, when the primary source of water is not available (such as piped water, or a nearby spring), women will walk farther to another spring or to a nearby river to collect water. Most families in Guatemala have a water storage basin of around 100 liters in their 'pila' a sort of sink with storage in the middle, and washboards on either side (see Fig 2.1a). Additionally, some rural families may have a larger storage tank (Fig 2.1b) for rainwater collected from their roof, however, this remains economically inaccessible for many families (27).

(a)

(b)

Figure 2.1: Household water storage

COCODE's of villages located in the headwaters of the Cahabón and Polochic rivers have expressed concern for water availability among their constituents, mentioning meteorological drought, deforestation, and population growth as causes of water stress (85). In order to tackle this issue, CCFC considers it important to study the situation and work together with COCODEs, water committees, and other stakeholders to come up with solutions.

Figure 2.2: Houses in The Village Satex 1

2.2.3. Involvement of local communities with NGO CCFC

Community Cloud Forest Conservation (CCFC), also known as Comunidad de Conservación Tz'unun is a non-governmental organization (NGO) that works in the rural area of the northern region of Guatemala in Q'eqchi' and Poqomchi' villages. The founding objective of CCFC is conservation through humanitarian development. In practice, this is achieved by working with local and international partners in five focus areas: Women's empowerment, Environmental Education, Agroecology, Reforestation, and Research. Education programs and capacity-building materials are based on a combination of local knowledge and internationally acknowledged best practices. In order to value and conserve the Cloud Forest, CCFC encourages research on its biodiversity, ecosystem services, and vulnerability to climate change and human actions. This project on the hydrology of the Cloud Forest adds to a bank of knowledge that is used across CCFC's focus areas (Figure 2.3) (20).

(a) **(b)**

Figure 2.3: CCFC Work areas

2.3. Cloud Forests

2.3.1. Cloud Forest Characteristics and Functions

A Cloud Forest is a unique ecosystem characterized by its high levels of moisture and mist. This type of forest is found in high-altitude areas, in Guatemala, it typically occurs between 1,500 and 3,000 meters above sea level, where moist air from the Caribbean meets cool air from the highlands, creating a misty and humid environment. Cloud forests are found to be wetter, cooler, and less seasonally variable than other montane forests not affected significantly by fog and low clouds (47). The functioning of a cloud forest can be explained through several key processes that contribute to its ecological dynamics (48). One of the primary functions of a cloud forest is its role as a carbon sink. Cloud forests have a high density of vegetation, including tall trees, ferns, mosses, and epiphytes (plants that grow on other plants). These plants absorb carbon dioxide from the atmosphere through photosynthesis and store it in their biomass. As a result, cloud forests play a critical role in mitigating the effects of climate change by sequestering carbon (98). Cloud forests have an important role in protecting steep slopes, especially during heavy rainfall events. The soils store the water which reduces runoff and the trees protect the soils from erosion. Another important function of a cloud forest is its contribution to the water cycle. The constant mist and fog that characterize these forests provide a continuous source of moisture that sustains the vegetation and surrounding ecosystems. The plants in the cloud forest act as a sponge, absorbing and storing water in their tissues. This stored water is then slowly released over time, contributing to the flow of rivers and streams that provide water for human consumption and agriculture (10). Cloud forests also support a high level of biodiversity. The unique environmental conditions in these forests create a habitat for many plant and animal species that are adapted to the misty and humid environment, such as the national bird the Quetzal. The flora in the cloud forests is characterized by high-altitude moist forests, with layered vegetation structure that includes shrubs, trees, bromeliads, and orchids. Many of these species are endemic, meaning they are found only in this particular type of forest. The high level of biodiversity in cloud forests makes them important centers of conservation and research (15).

The humid montane forests are characterized by their high levels of rainfall and fog that produce a unique microclimate and soil composition. The high altitude environment provides benefits for local communities as it helps regulate temperature and influence rainfall patterns in the region by intercepting moisture from clouds, helping to conserve water in the dry season (66). Nearly every aspect of the cloud forest is affected by regular cloud immersion, from the hydrological cycle to the species of plants and animals within the forest. Exactly how cloud immersion impacts the forest is unknown, but certain effects are obvious—high relative humidity (RH) and reduced sunshine are two of the most important ones (30).

2.3.2. Cloud Forest in the Guatemalan context

The hydrological context of the cloud forest in the Alta Verapaz region of Guatemala is closely tied to the unique environmental conditions of the area, which are characterized by high levels of rainfall and humidity. The region is located in the northern part of the Sierra de las Minas mountain range, which is the largest remaining cloud forest in Central America. The functioning of the hydrological cycle in this ecosystem is essential for the maintenance of the ecological services it provides (16). An overview of the hydrological system of TMCFs is shown in Figure 2.4. The cloud forest in Alta Verapaz plays a crucial role in regulating the water cycle at local and regional scales. The forest acts as a natural sponge, absorbing large amounts of rainfall and releasing it slowly over time. The dense vegetation of the cloud forest intercepts and captures moisture from the mist and fog, which then drips down to the forest floor. The soil in the cloud forest acts as a reservoir, storing water and releasing it slowly into the rivers and streams that flow through the region. The slow release of water from the forest helps to maintain a stable flow of water throughout the year, even during periods of meteorological drought (18).

The cloud forest in Alta Verapaz is also an important source of water for the local communities and agriculture. The rivers and streams that originate in the cloud forest provide water for drinking, irrigation,

and other human activities. The cloud forest ecosystem helps to regulate the quality and quantity of water in these water sources, preventing erosion and sedimentation and filtering pollutants.

However, the cloud forest in Alta Verapaz is facing threats from deforestation, fragmentation, and climate change. The loss of forest cover reduces the capacity of the ecosystem to regulate the water cycle, leading to increased runoff, erosion, and floods. The degradation of the cloud forest also reduces its capacity to provide clean water, leading to a decline in the quality of water resources. Therefore, it is essential to protect and manage the cloud forest in Alta Verapaz to ensure the provision of water resources for the local communities and maintain the ecological services it provides (83).

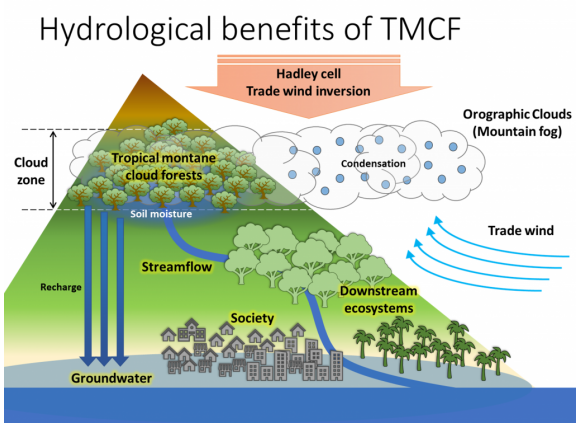

Figure 2.4: Hydrological context of a cloudforest
Source: (1)

2.3.3. Cloud Forest Ecology

Alta Verapaz is one of the richest departments in nature in Guatemala. The high level of biodiversity found in the cloud forest is likely due to the complex topography and diverse microhabitats present in the region, which creates a range of niches for different species to occupy. However, the cloud forest of the Alta Verapaz, like many cloud forests around the world, is threatened by deforestation, climate change, and other anthropogenic factors, which can disrupt the delicate balance of the ecosystem and threaten the survival of its inhabitants. TMCF are qualified high on the ranking of endangered ecosystems. Cloud forests typically occur in tropical climates. They are characterized by their distinctive floristic and structural form and occur on a relatively narrow altitudinal zone.

Flora

The flora in the cloud forest is very rich. One of the most striking features of cloud forests is the presence of numerous epiphytes, which are plants that grow on other plants without harming them. These include bromeliads, orchids, ferns, and mosses, which can be found growing on the trunks and branches of trees, as well as on rocks and other surfaces (92). The diverse array of orchid species is highly valued for their beauty and cultural significance (32). Among these is the endangered Monja Blanca, the national flower of Guatemala. In addition to the epiphytes, the Alta Verapaz cloud forest is home to a diverse assemblage of trees, including species of oak, pine, cedar, and cypress. Many of these tree species are evergreen, and their leaves are adapted to capture and retain moisture from fog and mist. Other important plant groups in the Alta Verapaz cloud forest include palms, lianas, and understory shrubs (95). Aside from the natural flora in the study area, a variety of heirloom crops thrive in the cloud forest microclimate. While some are intentionally cultivated, others still grow naturally and are collected in the forest for consumption, such as wild mushrooms and some herbs.

Fauna

Mammals found in the cloud forest of the Alta Verapaz include species such as the Central American agouti (Dasyprocta punctata), the white-lipped peccary (Tayassu pecari), and the jaguar (Panthera onca) (36). The bird community in the cloud forest is particularly diverse, with over 200 species recorded, including the resplendent quetzal (Pharomachrus mocinno) and the azure-rumped tanager (Tangara cabanisi) (50). Reptiles and amphibians found in the cloud forest of the Alta Verapaz include species such as the Guatemalan spiny-tailed iguana (Ctenosaura palearis), the emerald glass frog (Espadarana prosoblepon), and the variable harlequin frog (Atelopus varius) (17). Invertebrates are also abundant in the cloud forest, including numerous species of butterflies, moths, and beetles (51).

2.4. Climate

Guatemala sees a variety of different climates, as the different environments like the oceans, lowland jungle, and mountainous areas are all subjected to their own meteorological effects. When considering the Köppen-Geiger climate classification, we mainly see a mix of tropical and oceanic climates. The tropical savanna (Aw) and tropical monsoon climate (Am) are the ones that dominate, with respect to the oceanic climates that make up for one-third of the country's climate (64).
One last aspect to be well aware of is the fact that the mountainous/hilly region in Alta Verapaz is very much affected by its own microclimates.

2.4.1. Tropics

The climate that best describes the region of interest, situated in the region of Alta Verapaz, is a mixture of oceanic climate (Cfb) and tropical rainforest climate (Af). This mixture can be explained by the fact that the landscape is very much dominated by cloud forests, which can get very wet and humid through the clouds that are brought by the winds coming from the Atlantic ocean. The average temperatures and precipitation per month can be seen in Figure 2.5. For this project, the month of January is of particular interest, where an average temperature of $14.4°C$ and an average accumulated precipitation of 172 mm, as obtained from (65). In addition, the average relative humidity is measured at 88% and it rains for 13 days in the month of January. This makes January significantly wetter than the months of February, March and April, but not as wet as the months which are during the wet season.

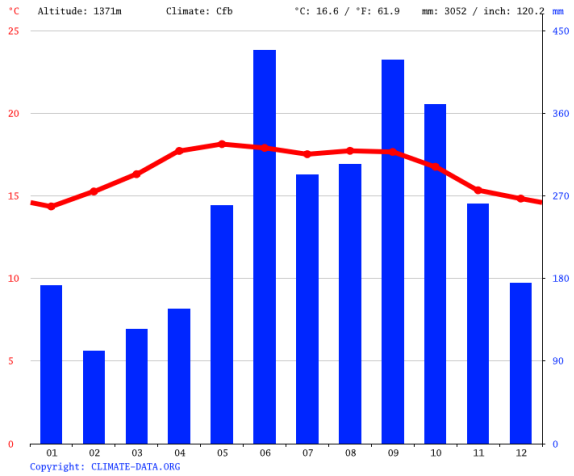

Figure 2.5: Average temperature and precipitation in the town of San Juan Chamelco. Gathered over the years 1991-2021 (65).

2.4.2. Seasonal

As could already be seen in Figure 2.5, precipitation amounts are highly seasonal and mostly depended on the timing of the dry and wet seasons. Figure 2.6 shows the average accumulated precipitation amounts for the described months in millimetres. Despite the fact that Figure 2.6c shows 1 month more than the preceding 2 figures, it still shows significantly lower amounts of accumulated precipitation. The months from December to March are typically being described as the dry season, as opposed to the months from May to October which show more precipitation and is therefore seen as part of the wet season.
These seasons are controlled by the North-South movement of the Inter-Tropical Convergence Zone (ITCZ), as well as the El Niño-Southern Oscillation (ENSO).

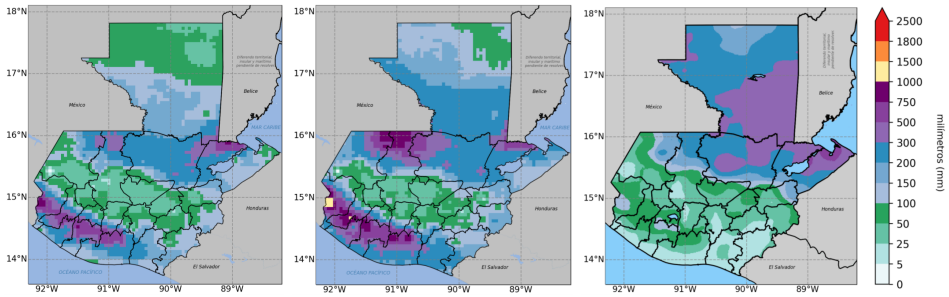

Figure 2.6: Multimonthly precipitation accumulation rates, averaged over the years 1991-2020. (a) May-June-July, (b)August-September-October, (c) December-January-February-March, (45)

Dry and wet seasons

The dry and wet seasons are mainly controlled by the Inter Tropical Convergence Zone (ITCZ). This zone of low pressure is situated around the equator and shows a North-South movement which is related to the position with respect to the sun (107). This results in the ITCZ being more North in the summer, compared to the more Southern position in the winter. Figure 2.7 shows this, where the ITCZ in July is shown in red and fully covers the country of Guatemala.
The ITCZ is also the boundary between the trade winds from both the North and the South. The trade winds therefore also, from both sides, converge to the ITCZ, which results in northeast trade winds from the North and southeast trade winds from the South.

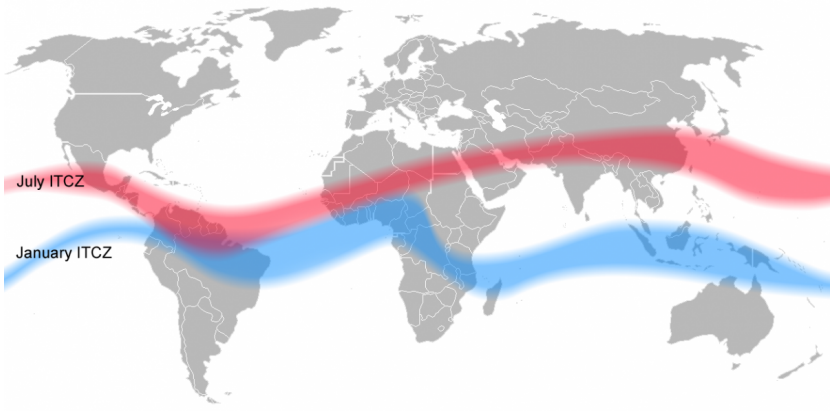

Figure 2.7: Inter Tropical Convergence Zone, positions in July (red) and January (blue) (41).

The combination of the two above-mentioned factors makes up for the wet season during the summer and the still humid but dryer season during the winter in the region of interest. The ITCZ is a zone of low pressure and with very low wind speeds, therefore all the air being delivered by the trade winds are collected and transported upwards. During the upward forcing of the air, containing a lot of moisture from the oceans, cumulonimbus clouds are formed and finally result in heavy precipitation events (107). This mainly

accommodates the intense rainfall events during the wet season. During the dry season, which in the region of Alta Verapaz is still relatively humid, the trade winds North of the ITCZ, coming from the northeast direction, make sure there is still some moist air and so clouds being delivered. The northeast trade winds bring the moisture-containing clouds from the Atlantic Ocean towards the mountainous area of Alta Verapaz. Having a significant amount of cloud forest on these mountains and hills, the moisture is then transferred from air to land as the clouds hit the mountains and hills. Figure 2.8a shows the direction of the trade winds being described, with in addition Figure 2.8b showing the incoming trade winds on the map of Guatemala.

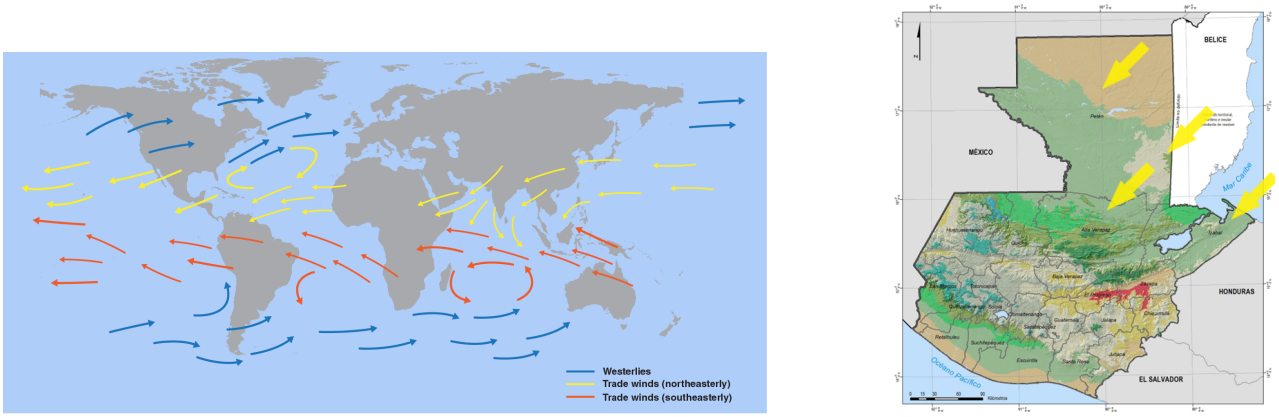

(a) (b)

Figure 2.8: Trade winds, (a) visualized on the world map (71), (b) visualized on the map of Guatemala (42).

ENSO

Another phenomenon that has an impact on the weather in Guatemala is the El Niño Southern Oscillation (ENSO). This oscillation is related to specific atmospheric circumstances where the air pressure patterns at sea level change simultaneously with the temperatures of the ocean at surface level (103). The ENSO can result in two different opposing states, known as El Niño and La Niña (Figure 2.9).

From an atmospheric circulation point of view, the Walker circulation should first be understood to explain the process of ENSO. The Walker circulation is the loop of airflow connecting the western warming and rising of air to the eastern falling and cooling of the air. Along the Pacific Ocean, an airflow is connecting the east and the west through the easterly trade winds, while at the top of the troposphere, it is encountered airflow from the west Pacific to the east Pacific (24). Subsequently, a pressure difference between the west Pacific and east Pacific is present, which in its turn has an effect on the water in the Pacific. A thermocline with warmer water in the east and colder water in the west is the result of this and forms the basis of the neutral ENSO conditions.

El Niño is the state wherein the ocean is warmed up and atmospheric circulation in the opposite direction of the trade winds is enhanced. This results in weaker trade winds or even reversing the direction of the trade winds towards the east (60). The influence of El Niño will mean that the wet season in Guatemala will be relatively dryer and warmer, due to the fact that the weaker trade winds will bring less moisture over to the ITCZ. La Niña is the state wherein the ocean is cooled and atmospheric circulation is enhanced in the naturally occurring direction. The result is even stronger trade winds and thus the wet season will become even wetter and cooler as an increase in moisture is seen in the ITCZ.

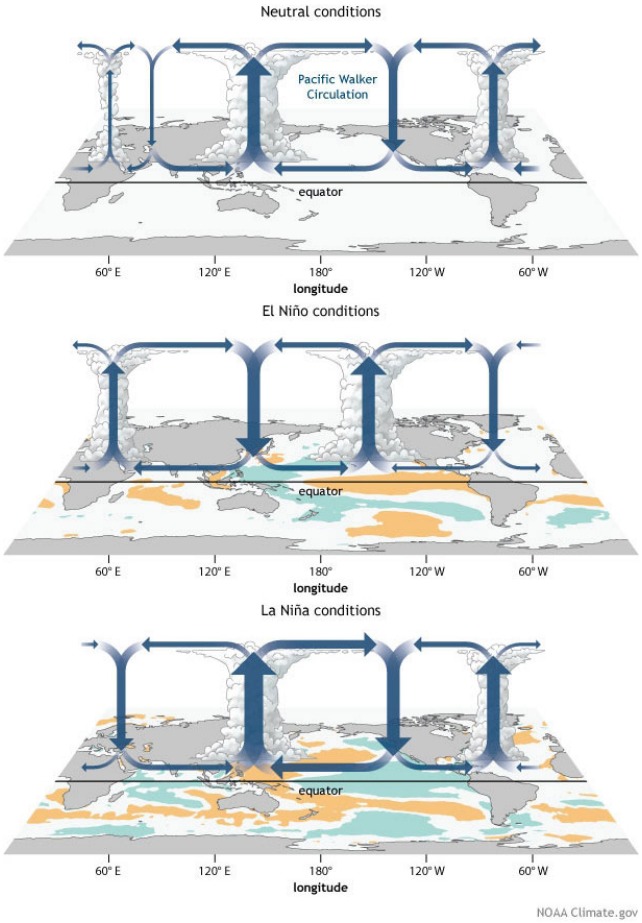

Figure 2.9: ENSO and Walker Circulation impact on moisture availability in Neutral, El Niño and La Niña conditions (21)

2.5. Change Drivers

2.5.1. Climate change

Guatemala is located on a narrow isthmus between two big oceans. This results in the weather and climate being greatly influenced by the oceans. As the climate is changing, the way of the influence of the two oceans is directly changing the meteorological effects on the country (84). As both the natural ecosystems and farming practices in Guatemala have evolved to fit historic patterns, these upcoming changes pose threats to the functionality of these systems.

Climate change and Cloud Forest

Stable weather patterns are needed for the cloud immersion of tropical montane cloud forests (TMCF). Stable weather will result in a stable moisture balance inside the cloud forest. As the climate is changing, more and more extreme patterns are showing heavy precipitation events followed by extended droughts, which are not favourable conditions for TMCFs. When, for example, the same amount of precipitation will fall but within a smaller period of time, part of the precipitation will acts as excess water and immediately drain from the forest.

Next to the above-mentioned dilemma, there is also the effect of global warming, which is that everything: land, ocean, and atmosphere, will get warmer. This effect induces changes in the relative humidity, as its vertical profile will shift upwards as a warmer atmosphere can hold more moisture before transforming into clouds (91). The uplifting of the cloud base height will be the consequence of this process, which in the end will result in a reduced cloud immersion into the TMCF's as less clouds will be at a low enough elevation to hit the mountainous terrain. With the scenario in mind that CO_2 emissions could double, we are looking at

an increase of the cloud base height of 'hundred of metres during the dry season', as was studied by (91).
In a study from (56), where the effect of climate change on TMCF's in Costa Rica was researched, it was found that longer(>5 days) cloud-free periods were related to higher Pacific ocean temperatures. Higher temperatures in the ocean will also lead to warmer trade winds towards the mountainous cloud forests. Even when effects from El Niño were factored out, still trends could be seen with the abundance of clouds related to the warming of the ocean. Nevertheless, considering El Niño even adds to this equation as well, the overall view on the effects of climate change on the tropical mountain cloud forest doesn't look promising. In the end, mainly during the dry season, this poses to be problematic, as cloud immersion into the cloud forests is a significant contributor to the water balance, as will be further explained in the extent of this paper.

Weakening trade winds & Walker circulation
The weakening of the Walker circulation and therefore also the trade winds are related to the energy balance that is changing because of climate change, where we are especially focusing on the radiative balance of the atmosphere. As ocean and land are warming up, but both at a different paces, a part of the energy which was designated for keeping the circulation going, is now lost into a radiative transfer towards the free troposphere (100). It was found by (100), that since the 1900s a reduction of 3.5% in the strength of the circulation was lost, which was closely related to a rising temperature and this aspect of climate research has been very consistent in climate change models.

Intensification of ENSO
As known climate change, it induces more extreme weather patterns and therefore it is expected that the events related to the El-Niño-Southern Oscillation will also show more extreme effects. First of all, the combination of the earlier mentioned factors of the warming of the ocean and the weakening of the trade winds will already be a firm base for the conditions that will only be exaggerated and enhanced during an El Niño event. More intense El Niño will have the effect of even dryer and warmer conditions as less moisture is brought from the oceans to the land by the atmospheric circulation. When again considering the Walker circulation and the study done by (100), it was found that the moisture concentration in the lower atmosphere increases by roughly 7% per $^{\circ}C$ of surface warming, while the precipitation rate only increases with 2% per $^{\circ}C$, which is including both vertical and horizontal precipitation. Next to this, a reduction in intensity and quantity of hurricanes over the Atlantic Ocean will be seen as the westerly winds in the North Atlantic are significantly stronger compared to neutral ENSO conditions (6).

2.5.2. Change in land use

The functioning of the cloud forest in the Alta Verapaz region is altered due to changes in land use. Land use has a significant impact on the flow regimes of water sources. This can either be in the form of direct abstraction (for example, through irrigation) or in the form of land cover changes that affect infiltration and storage (for example, through deforestation). The specific impacts of land use on flow regimes will vary depending on the local climate, geology, and hydrology. The Cloud forest and forests in the lowlands are cut down and used for agricultural purposes or for wood (see figure 2.10). When forests are cleared, the water flow patterns and moisture levels in the region can be altered, potentially leading to changes in the water supply to the cloud forest ecosystem (12; 28).

One major way that deforestation can affect the hydrological cycle is through increased runoff and soil erosion. Forests help to regulate the water flow by intercepting rainfall, allowing water to infiltrate the soil, and reducing runoff. When forests are cleared, there are fewer trees and vegetation to intercept rainfall, leading to increased surface runoff and soil erosion. This can result in soil compaction and reduced soil moisture, which can reduce the amount of water available to vegetation in the cloud forest ecosystem (53).

Additionally, deforestation can affect the evapotranspiration rates of the region. Forests release water vapour through transpiration, which can help to maintain moisture levels in the atmosphere and support cloud

formation. When forests are removed, the amount of transpiration is reduced, leading to lower atmospheric moisture levels and potentially less cloud cover over the cloud forest ecosystem.

Finally, lowland deforestation can also affect groundwater recharge rates. Forests help to recharge groundwater by allowing water to infiltrate the soil and replenish underground aquifers. When forests are cleared, there is less water infiltration, which can reduce groundwater recharge rates and potentially impact the water supply to the cloud forest ecosystem.

Overall, the alterations to the hydrological cycle resulting from lowland deforestation can have significant impacts on the water supply and moisture levels of the cloud forest ecosystem, potentially leading to changes in vegetation composition, species distribution, and ecosystem functioning.

In Guatemala, it is suspected that the conversion of forest to pasture resulted in a decrease in base flow, but an increase in peak discharge. This led to increased flood risk during the rainy season and decreased water availability during the dry season. In order to mitigate the negative impacts of land use on flow regimes, it is important to consider the potential impacts when planning land use changes. Planning for increased infiltration and storage capacity can help to reduce the likelihood of negative impacts on the flow regime. In addition, monitoring of flow regimes can be used to identify changes that may be indicative of negative impacts from land use change.

(a) **(b)**

Figure 2.10: Deforestation in Satex I, (a) Old growth tree stump on edge of forest fragment, (b) Logs sawed into dimensional lumber.

3

Regional Scale: Change Driver Analysis

In this chapter, the approach, methodology, and results of each research question on the regional scale (Objectives A and B) are presented. Each question is reported separately in order to define unique proposals for future research on the subjects. Both of these questions involve the analysis of publicly available data sets. Further work on each topic could be options for student projects or internships with CCFC working (fully or partially) remotely.

3.1. Objective A: Identify continental-scale climate change and land use change patterns that influence the spatial and temporal distribution of precipitation in highland Cloud Forests

3.1.1. Premise

Lowland conditions impact highland precipitation: the hypothesis of interest for the remote sensing approach relates to the conditions in the lowlands which might influence the spatial and temporal distribution of precipitation in the highlands. Looking at our area of interest, which is part of the highlands in the region of Alta Verapaz, the trade winds bringing the air that reaches these highlands first cross the lowlands located in the northern parts of Guatemala and also Belize. From the 1990s to the 2010s this region has undergone some heavy deforestation which can have a significant response to evaporation. Forests have accessibility to a large amount of water and moisture through their water-containing properties but also through the deep roots being able to access deeper soil layers (78). Consequently, forests can also contribute greatly to the amount of moisture of the passing air through evapotranspiration, this is also known as latent heat flux. Compared to the forest, the corresponding latent heat flux of bare soil or agriculture (for which the latter is mostly the reason to deforest) is far lower as those land uses cannot store as much water as the forest can.

The process of deforestation in the lowlands can in this way negatively affect the moisture availability in the highlands. As air moves over the lowlands, less moisture evaporates and the air contains less moisture, which will eventually result in less clouds and/or thinner clouds. At the time the air and clouds hit the highlands, less precipitation will reach the highlands as less moisture is available from the clouds. This is also visualized in Figure 3.1.

As the dry season is both the period when these trade winds are most dominant and the period when already a relatively low amount of moisture is present, it is the most important period to analyze this phenomenon and its effects. The dry season will therefore experience the greatest effect as also relatively less precipitation is reaching the highlands in comparison to the wet season.

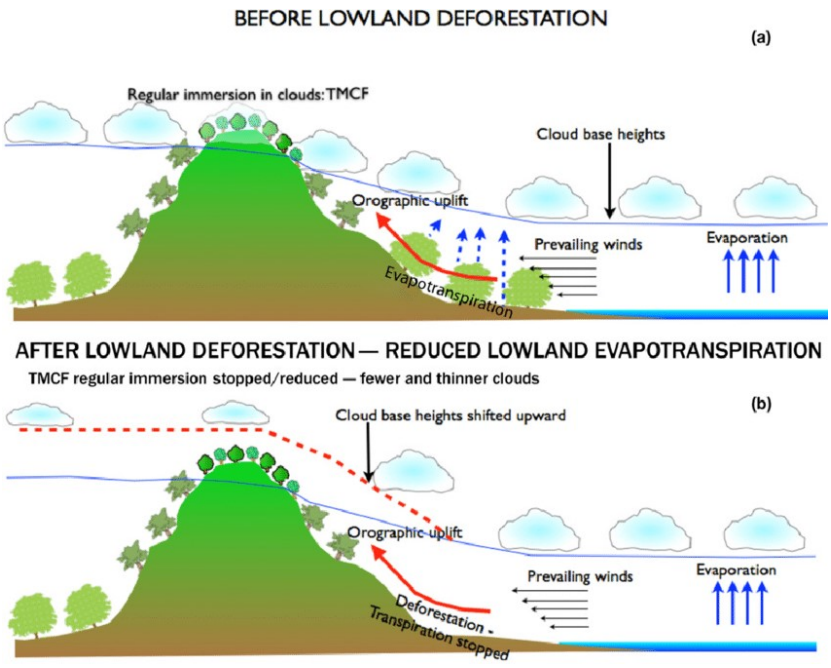

Figure 3.1: Effects of lowland landcover use on the precipitable availability in the highlands (78).

3.1.2. Approach

The approach to the analysis of this hypothesis consists of comparing different parameters between the lowlands and the highlands of Guatemala during the dry season. This is done with the use of a time series where the seasonal El Niño and La Niña will also be addressed. Concerning the areas of interest for the lowlands and the highlands, specific regions are chosen which are related to our research area. The time series could give an indication of the increase or decrease in the amount of precipitation in the highlands in relation to the increase or decrease in the amount of evaporation in the lowlands.

3.1.3. Data Selection/Collection

Satellite data observation

Through the use of satellite data, various variables concerning the climate and the weather can be observed and analyzed. This gives the opportunity to look at a more global scale at the region of interest and from where the different factors arise that influence the climate and weather at a more local scale. These variables are related to the direct inputs concerning the weather and climate, like precipitation, wind direction, and temperature, but also to the responses of the ecosystems on different scale levels. Parameters that can occur due to the combination of the different inputs like evapotranspiration, but also aspects that are related to the vegetation like the Leaf Area Index (LAI) and the reflective properties of vegetation, which can be quantified through the Normalized Difference Vegetation Index (NDVI). With the help of these parameters, through the years trends can be visualized which might contribute to the research of the temporal distribution of lowland conditions and their correlation to the potential for highland precipitation.

ERA5

The ERA5-Land dataset is a fifth-generation ECMWF reanalysis of the climate considering its land variables (22). The dataset is realised with the use of model data, as well as observations, to be combined into a hybrid dataset. The reanalysis of the climate data creates the opportunity to look at the climate of the past, starting in the year 1981. The parameters used from this dataset are the precipitation and evapotranspiration, which in the visualizations of Figure 3.3b, Figure 3.3c and Figure 3.3d are shown as monthly averages of $[mm/month]$ for specific years.

GPP

The Gross Primary Product is used in this case as a measure of the amount of vegetation in the highlands. GPP describes the amount of carbon produced by plants through the process of photosynthesis, where common units are described as grams of Carbon per metre squared per time unit (for example, $[gC\ m^{-2}\ d^{-1}]$) (93). For a dense forest, like a cloud forest, this is a good way of showing the amount of vegetation as all underlying plants are also taken into consideration, which is an aspect where something such as the Leaf Area Index can have issues with. This dataset is produced at a 500-m resolution and runs with an 8-day interval from the years 2002-2017. For the visualized time series in Figure 3.3a, values are downscaled to yearly averages.

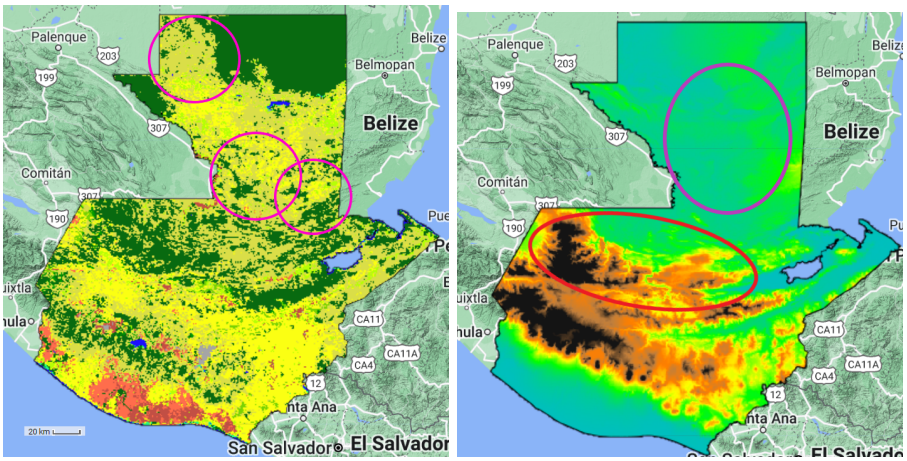

(a) **(b)**

Figure 3.2: Analysis area selection: (a) land-cover map with purple highlighted areas where deforestation has occurred, (b) elevation map with highlighted areas where highlands (red) and lowlands (purple) have been chosen as the regions of interest.

3.1.4. Area of interest

The areas of interest concerning the lowlands and highlands are based on both the elevation and the land cover type for both regions. The landcover types help to distinguish the areas where over time the land has been deforested, as that is of importance for our approach. In Figure 3.2a, the areas are highlighted that have been deforested between the 1990s and 2010s. Because the lowland region is defined as below 1000 *metres* elevation, the area of interest which is chosen is highlighted with purple in Figure 3.2b. The minimum elevation of the highland region should be 1500, as this is the lowest possible elevation to see some cloud forest. Another aspect to consider for the highland region is that it should be in the right orientation to be able to receive the clouds from the trade winds that are coming from the northeast, as shown in Figure 2.8b. This limits us to only using the first band of the mountainous region as seen from the north, which is all with an elevation of above 1500 *metres* for the region of the highlands, which is marked as the red circle in Figure 3.2b.

3.1.5. Analysis

With the use of Google Earth Engine, the dataset ERA5 containing the precipitation and evapotranspiration parameters and the Gross Primary Product could be processed and turned into time series for our regions of interest. For both datasets, averages were computed to easily be able to visualize time series for long periods of time. A direct relationship could be seen between the evapotranspiration in the lowland and the precipitation in the highlands. As evapotranspiration decreases over the years, the precipitation also slowly decreases little by little and where evapotranspiration increases again there is an increase in precipitation. This does not necessarily show a relation between deforestation and the decrease in evapotranspiration, because the pattern in rainfall in the lowlands can also match the pattern in the highlands, however, it does match with the hypothesis that less evapotranspiration will effect in less moisture availability in the continuing airflow towards the mountains and cloud forests where it consequently precipitates less.

3.1.6. Conclusion

Moisture recycling is challenging to identify and quantify using the approach described in this chapter, while the hypothesis is not confirmed, it is also not contradicting it.

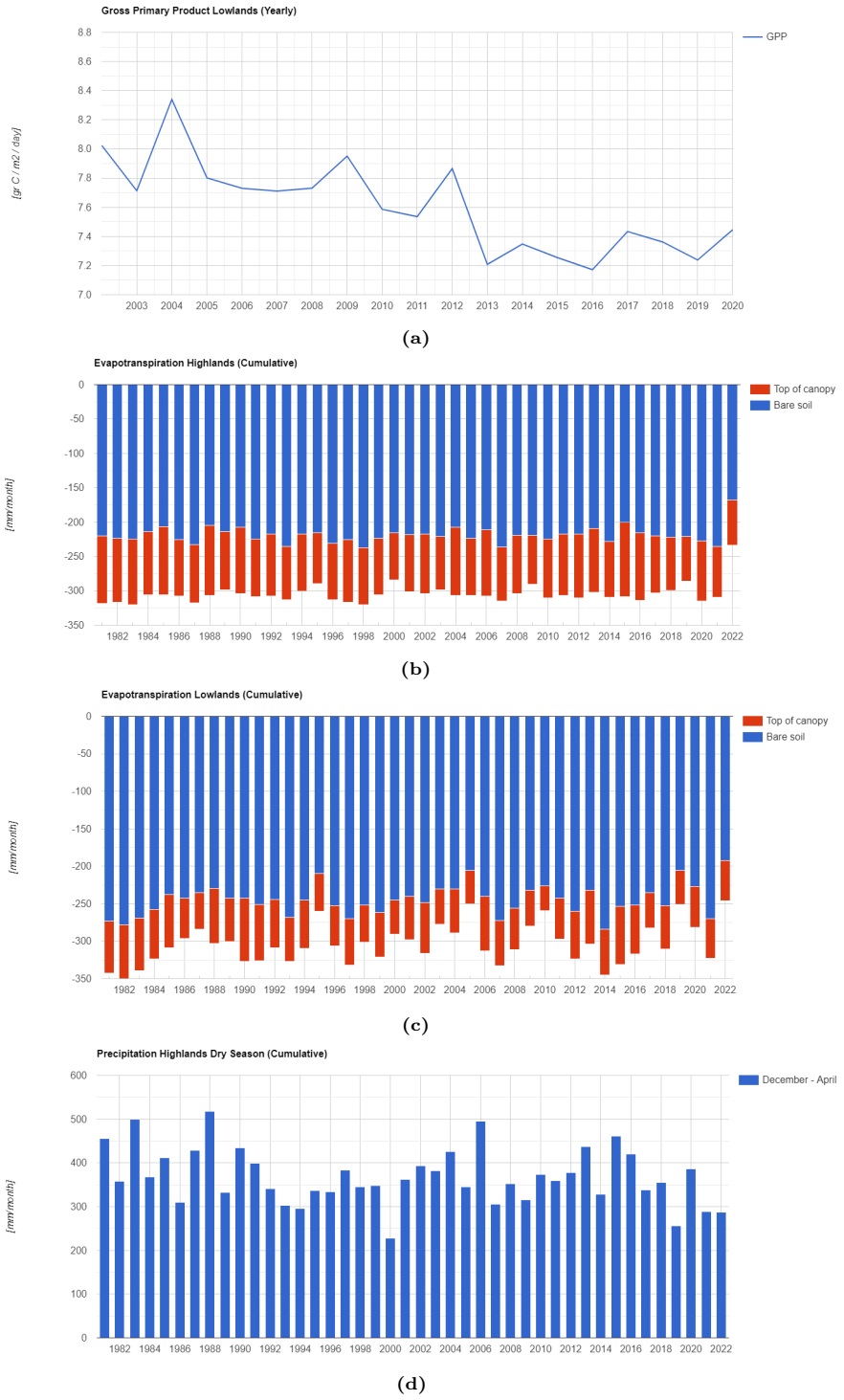

Figure 3.3: Analysis: (a) Gross Primary Product in the lowlands with yearly averages in grams of Carbon per metre squared per day ($gC\ m^{-2}\ d^{-1}$) (108), (b) Evapotranspiration in the highlands with yearly averages in $mm/month$ (22), (c) Evapotranspiration in the lowlands with yearly averages in $mm/month$ (22), (d) Precipitation in the highlands with yearly averages in $mm/month$ (22).

3.1.7. Recommendations for Future Research

As seen from this little remote study of the area and how changes in climate and land influence the conditions of the hydrological balance can be deduced from the results that the parameters that are of importance need to

increase on both spatial and temporal scales. The understanding of aspects like evapotranspiration is also very dependent on many specific variables that are not accurately measured through remote sensing. Combining this with the fact that the region is characterized by microclimates with dynamics at a higher resolution, a more in-depth analysis should be done really focusing on the local scale and local measurements. One thing that should be said about this analysis, is that the yearly trend of the seasons is not taken into account or subtracted from the data as this would have opened a whole new research part which we did not have the resources for. One other aspect that also was discovered during this research is that this specific type of climate analysis is also very much affected by local microclimates. As microclimates, in themselves are already significantly complex to understand, using coarse satellite data actually does not help to better visualize the ongoing processes.

3.2. Objective B: Identify changes in meteorological conditions and land use in the Sierra Yalijux, and the impact these are expected to have on the hydrological balance of the Cloud Forest ecosystem

3.2.1. Premise

Meteorological drought in the Cloud Forest can be attributed to lacking horizontal or vertical precipitation. For the local sub-catchment scale (between 20 and 500 sq km), this section considers the potential contribution to the drought of dry spells in vertical precipitation and the change in cloud base height and fog interception in horizontal precipitation.

3.2.2. Data Collection

For analysis in the region, geospatial information for Guatemala is available online or upon request from Instituto de Agricultura, Recursos Naturales y Ambiente (IARNA) meteorological records are available from the Instituto Nacional de Vulcanología Meteorología e Hidrología (INSIVUMEH), the national weather forecasting and monitoring institute, including:

- Meteorological data from 1990 to 2022 from the INSIVUMEH weather station in Cobán, includes min, max and average temperature (C), precipitation (mm), solar radiation index (-), cloudiness index (-), wind direction (deg) and velocity (m/s), and atmospheric pressure (hPa).
- Stream flow data from 2011 to 2022 from the INSIVUMEH gauge in the Cahabón River in Santa Cruz Verapaz (m3/s).

3.2.3. Area of Interest

While the entire Sierra Yalijux and Sacranix is of interest to understanding water availability in the region, the Cahabón river catchment above Santa Cruz Verapaz is most appropriate for hydrological analysis considering the high percentage of Cloud Forest within the area, and the fact that there is a streamflow gauge located in Santa Cruz, which could be used to model the catchment's water balance, see Figure 3.4.

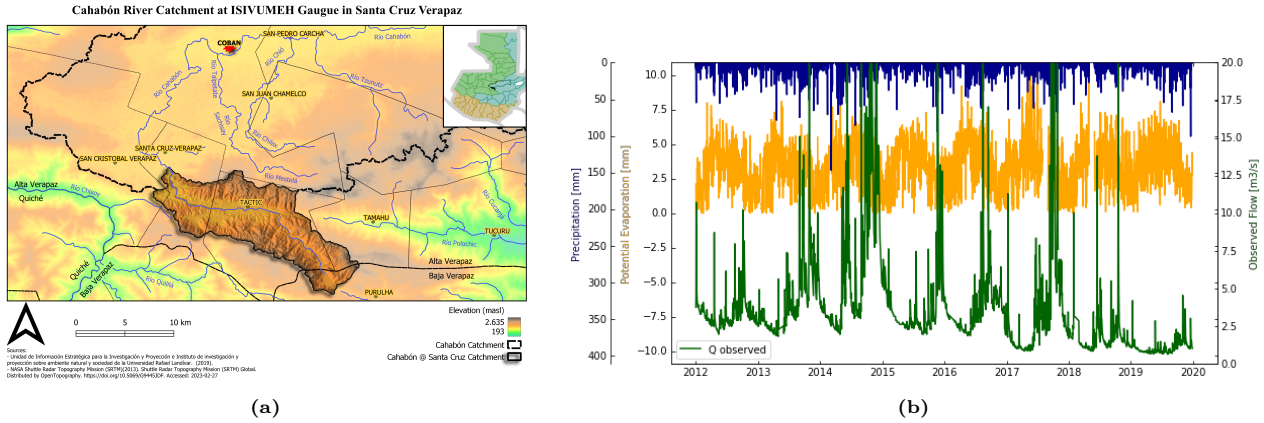

(a) (b)

Figure 3.4: (a) Upper Cahabón Catchment area above INSIVUMEH flow gauge in Santa Cruz Verapaz, (b) Stream flow, Precipitation, and Potential Evaporation for 2012 to 2020. Flow data (Q) is cut off at 20m3/s to focus on the behaviour of flow during the dry season.

3.2.4. Analysis

Vertical Precipitation drought: Dry spell occurrence

In order to measure the severity of drought, various metrics can be used, the Standard Precipitation Index (SPI), for example, compares the precipitation in a period to the historic average of precipitation for the same period (3), whereas the Palmer drought severity index includes precipitation and temperature data to estimate relative dryness (2); these and other indices are used for applications at a variety of spatial and temporal scales.

At a local scale in the villages and towns near the Cloud Forest in Alta Verapaz, the stream flow in the headwaters of the Cahabón is more immediately impacted by periods of little to no precipitation versus longer-term precipitation accumulation, the karst geology gives little storage and rapid hydrological response times. This means that to assess drought risk, understanding the probability distribution of dry-spell frequency and duration can be more indicative than a global drought indicator such as SPI.

Dry spells are periods of consecutive days with rainfall under a threshold, preceded and followed by days with rainfall above the threshold (102). A threshold of 2 mm is chosen because it is a typical upper limit for dew at the location of the weather station.

As mentioned in Section 2.4.2, El Niño Southern Oscillation (ENSO) and the Pacific Decadal Oscillation (PDO) impact Guatemala's weather patterns, therefore, a pattern in dry-spell distribution based on these cycles may be expected.

The frequency of dry spells of four lengths (five, seven, nine and fifteen days) in each year from 1990 to 2022 is shown in Figure 3.5a. There does not appear to be a correlation between El Niño years and the increased frequency of long dry spells, however, dry spells tend to be longer and more frequent in years with a positive PDO phase.

The monthly distribution of dry spells is shown in Figure 3.7b, the longest and most frequent dry spells occur between November and April. Higher drought frequency in PDO-positive phase years is particularly apparent in February through May. The yearly distribution of dry spells in these months is shown in Appendix B.

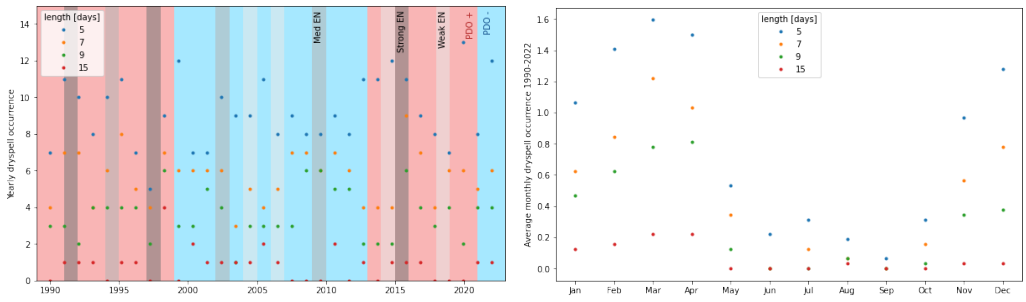

(a) (b)

Figure 3.5: Dry spell occurrence per (a) year and (b) average month from 1990 to 2022. Blue and red shading indicates Pacific Decadal Oscillation (PDO) phase; shades of grey indicate weak, medium and strong El Niño (EN) years.

Horizontal Precipitation drought: Cloud base height estimation

Horizontal Precipitation can contribute significantly to the water balance in Tropical Montane Cloud Forests during the dry months (69), in Fog Interception for the Enhancement of Streamflow in Tropical Areas (FIESTA) Model by Mulligan and Burke, one of the variables determining fog interception is cloud base height or lifting condensation level (Z_{LCL}), where the presence of fog at any point is determined by comparing the modelled cloud height to ground surface elevation (54).

The height of clouds over the upper Cahabón valley appears to be governed by the conditions of the plain between the Sierra Yalijux, Sierra Sacranix and Sierra de Chamá. Observations in the field show uniform cloud base heights over the valley, with clouds intersecting the mountains that are at a higher elevation than the cloud base height. As shown in Figure 3.6a, clouds make contact with the top of Xucaneb mountain (2630 masl). A first-order estimation of the lifting condensation level or cumulus cloud base height (Z_{lcl}) is given by constant times the difference between Temperature (T) and Dew Point Temperature (T_d) (Eq. 3.1), and Dew Point Temperature is a function of Relative Humidity (RH) and Temperature (T) (Eq. 3.2) according to (55), therefore cloud base height varies proportionally to relative humidity. Applying these formulas to historic INSIVUMEH data, a decreasing trend in relative humidity in the month of January translates to an increase in lifting condensation level, as shown in figure Figure 3.7a.

$$Z_{lcl} = 125 * (T - T_d) \tag{3.1}$$

$$T_d = T - \frac{100 - RH}{5} \tag{3.2}$$

The average Z_{LCL} from 1990 to 1996 is 91 meters lower than the average Z_{LCL} from 2017 to 2022. In the upper catchment of the Cahabón river, this means a reduction of the area with a potential for Cloud Forest conditions from 4370 hectares to 2910 hectares, or from 41% of the catchment to 27%, as shown in Figure 3.7.

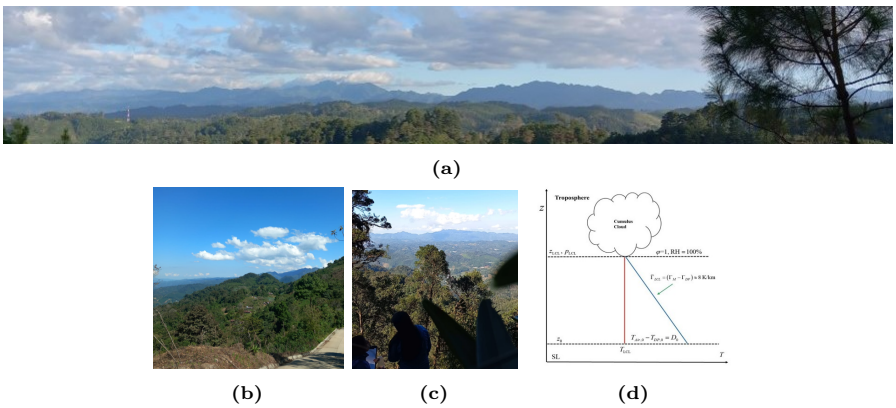

(a) (b) (c) (d)

Figure 3.6: Lifting Condensation Level determines cloud base height. (a) View of Yalijux from Sacranix, (b) View of Yalijux from Satex, (c) view of Sacranix from Yalijux, (d) Z_{LCL} simplified formulation by (23)

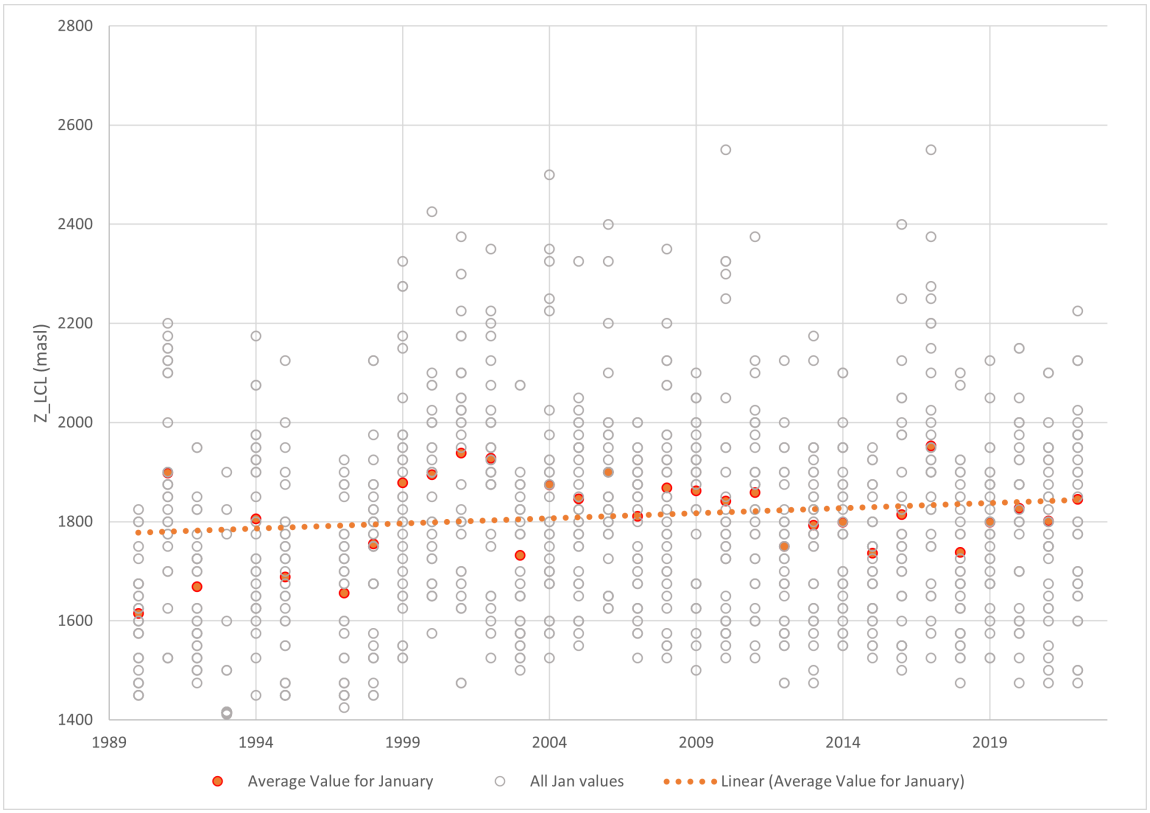

(a)

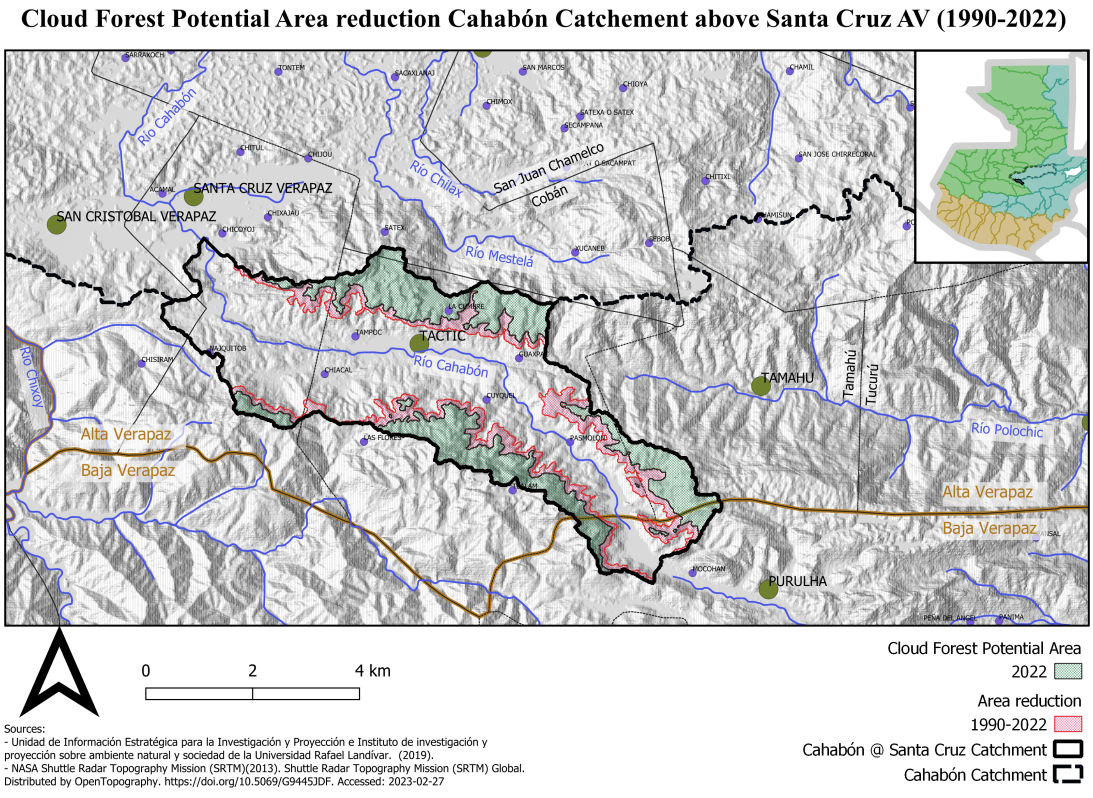

(b)

Figure 3.7: (a) Lifting Condensation Level in January from 1990 to 2022, (b) Cloud Forest potential area reduction in the Cahabón River catchment above Santa Cruz Verapaz from 1990 to 2022.

Fog Interception

The calculation of fog interception potential within the catchment area is calculated following the approach developed by Mulligan and Burke as part of the Fog Interception for the Enhancement of Streamflow in Tropical Areas (FIESTA) project, see Appendix C. The FIESTA model is a process-based, spatially distributed model, which takes topography, land cover conditions, and meteorological variables as input, and outputs a balance of Precipitation, Fog Interception, and Evaporation.

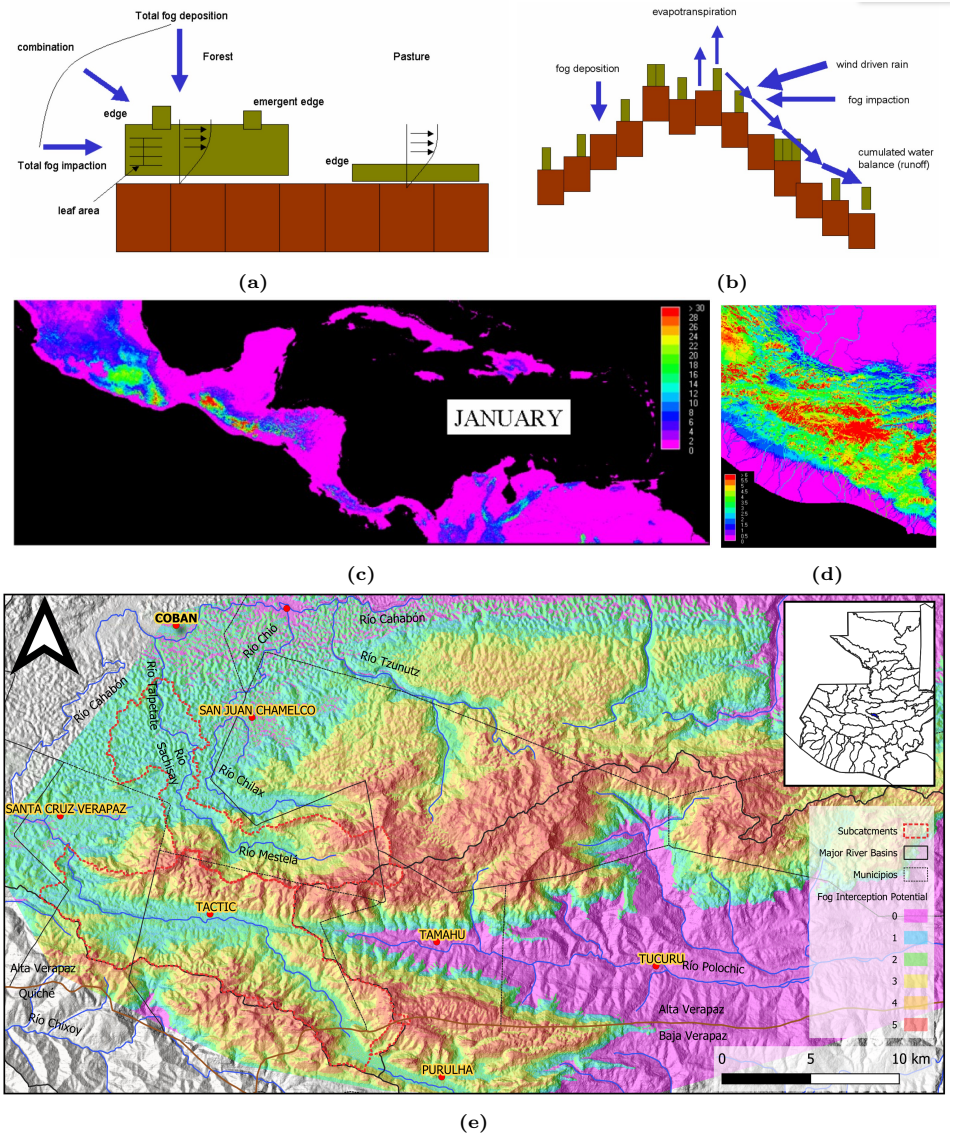

Figure 3.8: FIESTA model Fog Interception Processes (a) fog fluxes, (b) runoff balance, and model Fog Interception Results showing fog inputs as a percentage of vertical precipitation for (c) Central America on a scale of 0 to 30 and (d) zoomed in on Guatemala on a scale of 0 to 6, (69). (e) A rough estimate of the upper bounds of daily fog interception in mm/day from 1991 to 2022 in the Sierra Yalijux, output from the adapted FIESTA algorithm.

FIESTA modeled continental scale fog interception based on yearly averages with prescribed monthly and hourly variations in meteorological conditions. The model setup and results of this analysis for Central America are shown in Figure 3.8. Applying the adapted FIESTA model to the Cahabón catchment (Figure3.9) results in an estimation of fog interception in millimeters per day. Comparing this flux to precipitation (Figure 3.10), the modeled fog interception contributes between nine and fifteen percent of total precipitation.

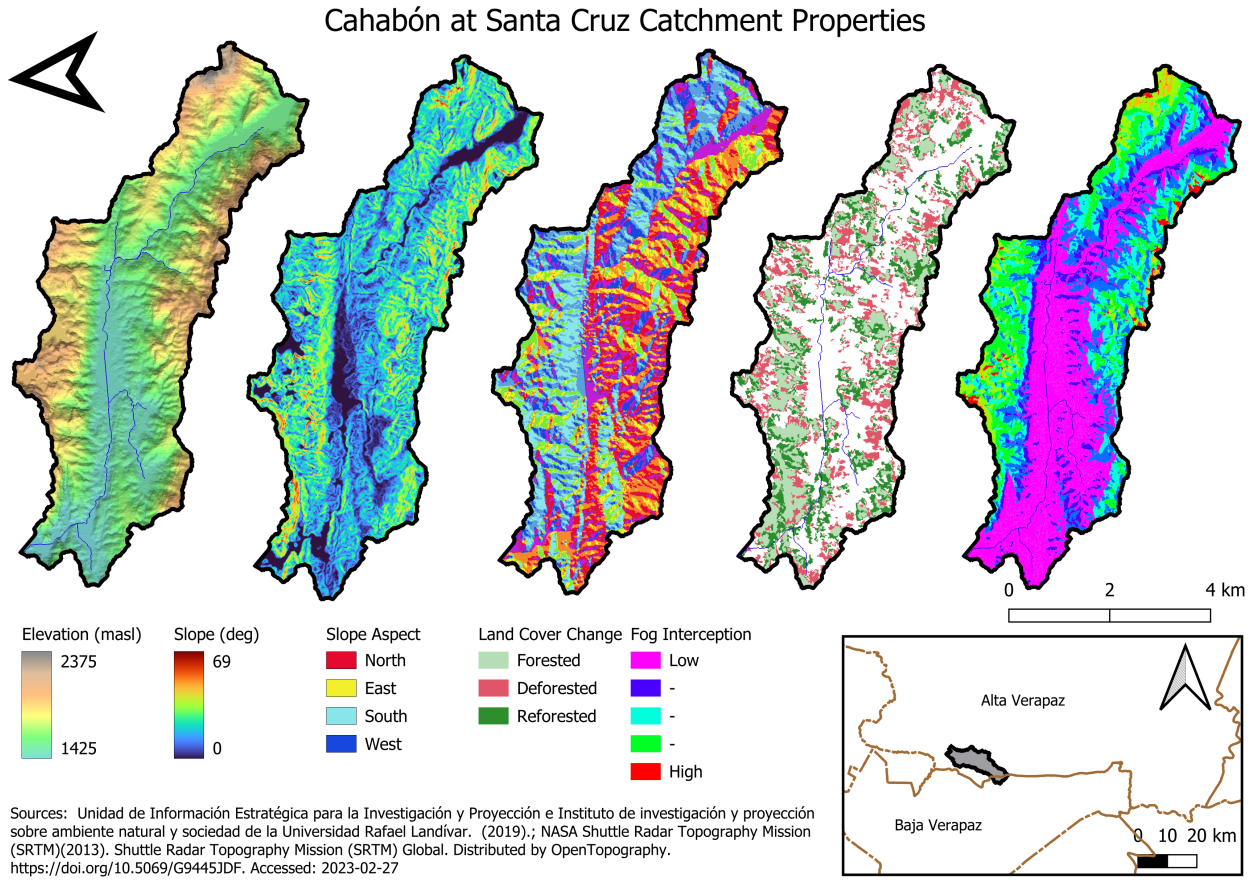

Figure 3.9: Upper Cahabón Catchment area above INSIVUMEH flow gauge in Santa Cruz Verapaz. The left-most map shows the average fog interception from 1991 to 2022, output from the adapted FIESTA algorithm. Higher Fog Interception occurs at higher elevations, and on slopes facing the dominant wind direction

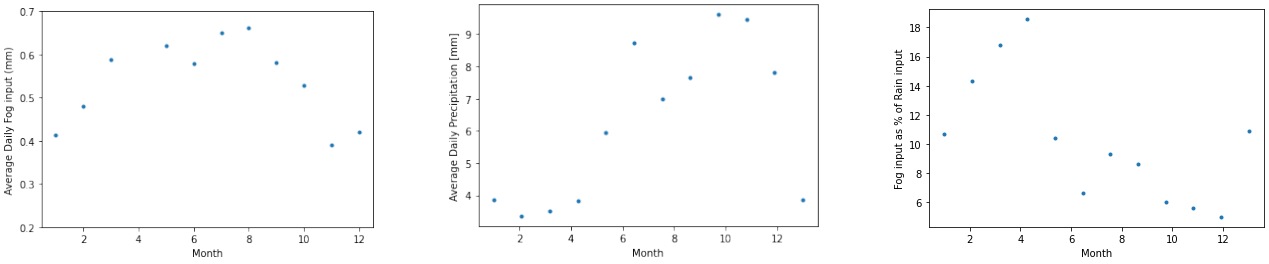

(a) (b) (c)

Figure 3.10: For the upper cahabón catchment above Santa Cruz, (a) average daily fog interception, (b) rainfall, and (c) fog as a percentage of rainfall

3.2.5. Conclusion

Dry spells in vertical precipitation occur most frequently from November to May, during these months, horizontal precipitation from fog interception can contribute significantly to the water balance, however, a decrease in relative humidity in the last 32 years has decreased the area of land where fog occurs regularly. While there is no trend in the data available from 1991 to 2022 showing an increase in dry spell length or frequency, global climate change trends indicate an intensification of extremes in ENSO and PDO oscillations which do appear to correspond to more intense dry spells.

3.2.6. Recommendations for future research

- The adaptation of the FIESTA model for this project can be applied to other catchments and calibrated using in-situ measurements. In order to quantify the historic and projected fog interception deficit, future research could apply the FIESTA model to the Upper Cahabón, Mestelá, Chilax, or Upper Polochic catchment areas. Other factors contributing to a reduction in fog interception such as deforestation should also be included in further analysis.
- Hydrological model for Cahabón above Santa Cruz including cloud water inputs.
- Time series analysis to identify frequency and magnitude of probable fog inputs during dry spells in vertical precipitation.

4

Local Scale Hydrological Balance, Objective C: Outline the most important processes to model in a hydrological balance in the cloud forest ecosystem, and how they interact with each other.

4.1. Premise

The Cloud Forest Canopy and its role in catchment hydrology can be modelled using a conceptual model.

4.2. Modeling Setup

4.2.1. Hydrological balance of the Cloud Forest Canopy

Conceptual hydrological models use an understanding of the fundamental mechanisms that determine the movement of water through a system in order to describe flow paths, storages, and residence times. Hydrologiska Byråns Vattenbalansavdelning (HBV) Models are a semi-distributed conceptual model which is often used to describe catchment behaviour, a variety of processes can be included such as snow melt, canopy interception, evaporation, throughfall, unsaturated zone, transpiration, percolation, groundwater flow, preferential flow paths, upwelling, overland flow, and any other process that describes important storages and fluxes (88). The hydrological dynamics of forest canopies are important processes in the hydrological models at any scale. The canopy is the first point of contact between water in the atmosphere and water in the terrestrial system. The interception reservoir receives the precipitation flux and it is partitioned between throughfall and evaporation (70). The proportion of precipitation that evaporates from the canopy can represent up to a quarter of total precipitation in some parts of the world (25), while in others, such as in Tropical Montane Cloud Forests, throughfall can account for over 100 percent of vertical precipitation (11). In the Tropical Montane Cloud Forests (TMCF), in addition to the three roles that typical forest canopies play (interception, storage, release), the canopy also traps fog as an additional input called horizontal precipitation. Due to the presence of epiphytes, the interception and storage capacity of a TMCF can be higher than that of other types of forests. A uniform canopy structure of branches and foliage, which can easily be captured in a single parameter: maximum interception storage (Imax), meanwhile, an epiphyte-rich forest may have various interception reservoirs with different storage capacities and resistance, mosses that act as sponges, that keep water shaded so it does not evaporate as quickly as it would on the surface of a leaf or branch, while bromeliads can capture precipitation over a wide area and store it in a column with a much smaller surface area for evaporation, canopy soils

also store water in an unsaturated zone that rooted epiphytes take up for transpiration. Although all these processes may be lumped into a single parameter for a catchment-scale model, this project aims to gain a better understanding of each mechanism. Ultimately, knowing how each canopy component behaves can help us make a better estimate of the lumped parameter, and how it can vary seasonally or due to changes in land use. In temperate zones, for example, a seasonal variation in canopy storage capacity due to the loss of leaves of deciduous trees could be considered, while in a TMCF, there may be cyclical reductions in canopy biomass due to extended periods of drought or important differences between old growth and secondary growth forests.

Hydrological Balance Setup

To make a hydrological balance of the forest canopy a combination of measured and calculated parameters representing in-fluxes, storages and out-fluxes is outlined (Figure 4.1).

- In-flux
  - Vertical Precipitation
  - Horizontal Precipitation
- Interception and Storage
  - Bromeliads
  - Bryophytes (Mosses)
  - Root masses and Soil
  - Other Epiphytes
  - Tree foliage
- Out-flux
  - Evaporation
  - Transpiration
  - Throughfall
  - Stemflow

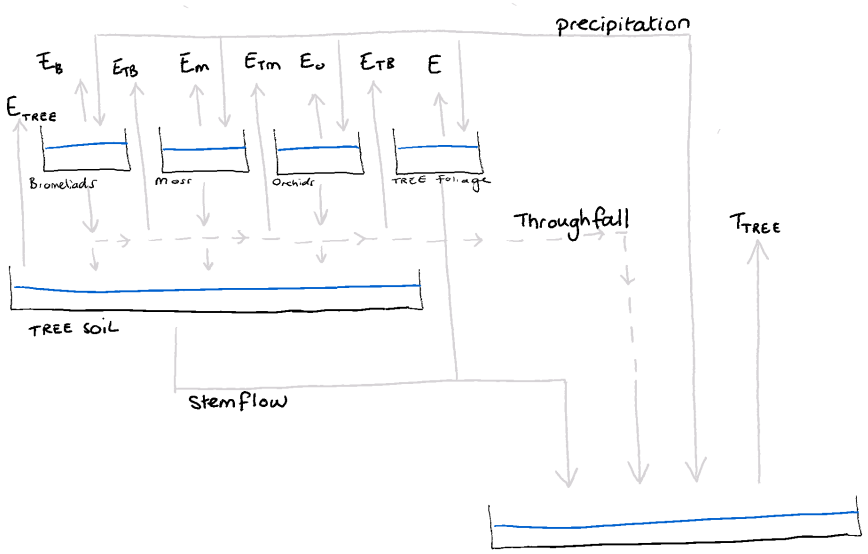

Figure 4.1: Sources and drains in the water balance

4.3. Process Description

4.3.1. In-flux

For the in situ measurements of the hydrological balance, precipitation is the fundamental input process by which water molecules in the atmosphere condense into liquid or solid form and reach the ground. Precipitation is a crucial component in hydrology as it contributes to the Earth's water cycle and provides vital information on climate and atmospheric phenomena. By analyzing the amount, type, and timing of precipitation, insights can be gained into regional climate patterns and the impacts of climate change. The unit used to measure precipitation is the millimetre (mm) and one millimetre is equal to one litre per square meter of surface area (l/m^2). In cloud forests, precipitation can be classified into two categories: vertical and horizontal precipitation. The distinction between these two types of precipitation is based on the angle of descent of the water droplets. Vertical precipitation falls directly from the sky, whereas horizontal precipitation is influenced by the movement of the air.

Vertical precipitation

Vertical precipitation refers to the process by which atmospheric water vapour condenses and falls directly to the ground as rain, snow, sleet, or hail. This precipitation occurs when the temperature and pressure conditions in the atmosphere cause the water vapour to become saturated, resulting in the formation of cloud droplets or ice crystals that fall to the ground due to gravity (58) Since it is not possible to catch the total rainfall over a study area in specific, in the hydrology field different methods are used that attend to estimate the amount of water that precipitates over a given area.

Horizontal Precipitation

Horizontal precipitation occurs when water droplets are carried horizontally by the wind before falling to the ground. Examples of horizontal precipitation may include drizzle, mist, and fog or cloud immersion. These types of precipitation occur when the wind carries water droplets over long distances, and they fall to the ground due to gravity when the wind speed decreases or when they encounter obstacles such as mountains or buildings. Cloud immersion happens when a cloud is pushed by the wind towards a hill or mountain range, causing it to move up and over the obstacle. As the cloud moves up, the air cools, causing the water droplets in the cloud to condense and form larger droplets. The clouds contain aerosolized water droplets suspended in the fog. Fog as an input for the water balance is a parameter that is of specific importance in tropical montane cloud forests.

4.3.2. Interception

Interception in the natural environment is a key process that occurs in forested ecosystems and is defined as precipitation that is redistributed by vegetative surfaces. The vegetation intercepts precipitation and stores it on leaves, branches, stems, and other surfaces before it reaches the forest floor. Cloud forests, which are characterized by persistent fog and high levels of precipitation, are particularly important sites for interception research. The interception process in cloud forests is complex, and there are different types of interception that occur, including canopy interception, stemflow, and moss interception. Its contribution to the hydrological cycle is of importance for forest floor moisture, and for accurate estimations of peak discharge (35).

In this review, the focus lies on the canopy interception of a cloud forest. Canopy interception is the precipitation caught by the trees, branches, and bushes above the forest floor. It is categorized into different types, such as free throughfall, drip and splash throughfall, and stemflow. A special case for the cloud forest is fog drip interception, which is the interception of water droplets from clouds. A part of the intercepted water will be lost due to evaporation, which is referred to as evaporative interception loss. The amount of intercepted precipitation is dependent on the characteristics of the vegetation and rainfall, and of the evaporative demand. An overview of interception in a cloud forest tree is shown in Figure 4.2.

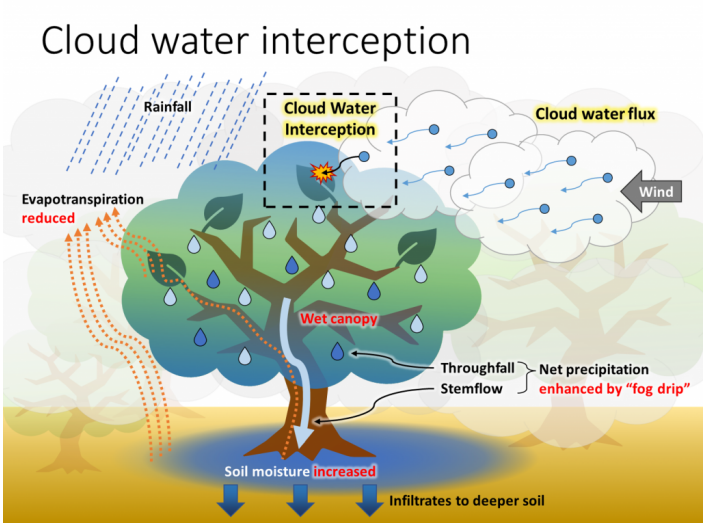

Figure 4.2: Overview of interception in a cloud forest
Source: (1)

Canopy storage capacity

Canopy storage capacity refers to the amount of water that can be stored temporarily on the leaves, branches, and stems of vegetation. When precipitation falls on a vegetated area, a portion of it can be intercepted by the vegetation and stored on the surfaces of the leaves, stems, and branches. This stored water can evaporate or be transpired back to the atmosphere (74). Epiphytic biomass, canopy humus, tree limbs, and foliage all intercept and store water in the canopy. Of these components, the epiphytic biomass and canopy humus are the least studied. In a pioneering study of hydrological properties of epiphyte mass in the TMCF of Colombia in 1990, (101) found that masses of epiphytes intercept high volumes of rainfall, with a slow release through drainage and evaporation. (101) weighted branches and samples of epiphytes after rainfall, while draining, and oven drying; they extrapolated the behaviour of the samples to quantify the total storage capacity of the forest canopy. In 2004, (43) studied and modelled canopy interception including epiphytes in Costa Rica using in situ measurements of moisture. One of the most recent (and ongoing) canopy hydrology research projects in Costa Rica has approached the same question by making a canopy water balance in trees full of epiphytes and trees completely stripped of epiphytes (Gotsch).

Regardless of the approach, in order to estimate the total storage capacity and evaporation rates in the canopy, it is helpful to break it down into key components as shown in figure 4.3:

- Bromeliads
  Bromeliads (Bromeliaceae) are plants that are commonly epiphytic (growing in trees) or epilithic (growing on rocks) but can also be terrestrial. The structure of bromeliads is typically a rosette of leaves around a round water storage area called a phytotelma (104), however, in hydrology, it is referred to as a bucket or tank (63). At our study site, both epiphytic and terrestrial or epilithic occur. However, sometimes it is hard to distinguish due to the shallow topsoil and organic matter accumulation on rocks.
- Non-vascular epiphytes (Bryophytes/Mosses)
  Non-vascular epiphytes such as mosses and lichens are very common in the cloud Forest, they are present nearly everywhere, covering tree trunks, branches and even leaves. Hydrologically, non-vascular epiphytes function as sponges, rapidly absorbing vertical and horizontal precipitation, and then releasing it slowly.
- Root masses and Soil
  Old-growth trees in the TMCF accumulate a carbon rich layer of humus composed of decomposing leaf litter from the tree and epiphytes. This soil is another storage reservoir for moisture.
- Vascular epiphytes
  Vascular epiphytes include non-parasitic dicots and ferns, they are characterized by spending a significant

part of their lifetime without contact with the ground (104).

- Tree foliage
  The leaves of trees are often the first point of interception of rainfall, their storage capacity depends on the phenology of the leaf, and it can vary cyclically with seasons and continuously as the tree grows. Leaf area Index (LAI) is often used as an indicator of the capacity of a canopy. (52)

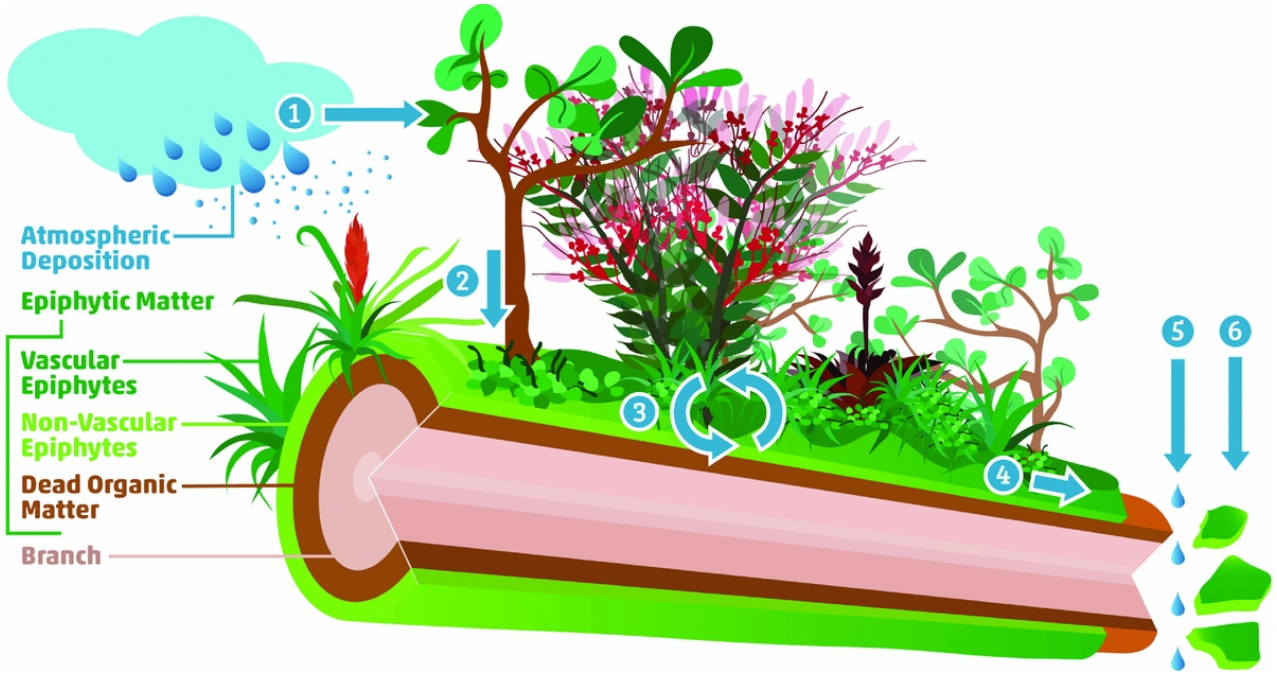

Figure 4.3: Pathways of water and nutrients through Epiphyte Mass by (40)

In order to come up with a total storage capacity for the canopy, the distribution of each of these storages can be quantified per branch, and then extrapolated to a per-tree or per-hectare estimate. In our field site, the forest is fragmented and contains a distribution of young and old trees with different epiphyte contents, as can be seen in Figure 4.4

(a) **(b)**

Figure 4.4: Fragmented Cloud Forest Canopy at our fieldwork site in Satex I. (a) Young tree and fern tree, (b) Old growth tree with high epiphyte content

4.3.3. Out-flux

Evaporation

Evaporation plays a fundamental role in the hydrological balance therefore it is important to understand completely this concept and its mechanisms. In the hydrological processes, evaporation is defined as the mean amount of water that from liquid goes into a vapour state over a given area. The evaporation of water can happen more easily in less saturated air (96). The evaporation can occur by transpiration [E_t], as mentioned

in the next chapter, and by direct evaporation. Open water [E_0], soil [E_s], Interception [E_i] and Snow or ice evaporation [E_sub] are the components of direct evaporation and the sum of these types is known as actual evaporation [E_a].

$$E_a = E_o + E_s + E_i + E_t + E_{sub}* \tag{4.1}$$

$*$ E_{sub} Does not apply for our project

Since it is a complex process where many variables and parameters are taken into account chapter 5 is exposed one of the suggested a method to calculate evaporation.

Transpiration

Transpiration is the process by which water is released into the atmosphere through the leaves of plants. It occurs when water is absorbed by the roots of plants and transported to the leaves, where it is released into the atmosphere during photosynthesis when the stomata are open for the passage of CO_2 and O_2. The loss of water will have a cooling effect on the plants, in particular in warmer weather conditions (68). Water is moved from the roots and stems through the plant tissues towards the leaves where the water vapour is released. The water movement is therefore from the soil, where the roots take up liquid water, to the atmosphere, where the leaves release water vapour into the air. When a leaf is healthy and growing, it can transpire more water than its own weight. A large oak tree can transpire approximately 151,000 liters per year. (96)

The average transpiration rate of a Podocarpus tree can vary depending on various factors such as age, environmental conditions, tree size, and species. However, in general, Podocarpus trees are known for their low to moderate transpiration rates compared to other tree species. Studies have shown that the transpiration rate of Podocarpus trees is generally between 60-120 liters of water per day per tree. However, this can vary depending on factors such as temperature, humidity, soil moisture, and light intensity. It is also important to note that transpiration rates can vary widely between individual trees and even between different parts of the same tree, such as the top versus the bottom of the canopy or different sides of the trunk. Sunlight can have a significant effect on transpiration rates by increasing leaf temperature and driving the opening of stomata. Research has shown that in some plant species, as much as 80% of the variation in transpiration rates can be attributed to sunlight exposure. However, this can vary widely depending on the specific plant species and environmental conditions. Leaf Area Index (LAI) plays a significant role in transpiration rates because it is directly related to the amount of leaf surface area available for transpiration. Leaf Area Index is a measure of the amount of leaf surface area per unit of ground area in a plant canopy. A high LAI value can reduce the amount of solar radiation reaching the ground, leading to a decrease in surface temperature and an increase in the amount of water vapour released by transpiration. A higher LAI value means that there is more leaf surface area per unit ground area, which can increase the overall transpiration rate of the plant canopy. This is because the larger surface area results in more water being evaporated from the leaves, leading to greater water loss from the plant. However, the relationship between LAI and transpiration rates is not always linear. As LAI increases, the canopy becomes denser, reducing the amount of sunlight that reaches the lower leaves. This can reduce the rate of photosynthesis and transpiration in the lower canopy, while the upper canopy continues to transpire at a higher rate. This can lead to a vertical gradient of transpiration rates within the canopy, with the upper leaves transpiring more than the lower leaves. The weather conditions in the corn field and forest will have different characteristics, the relative humidity will be higher and temperatures will generally be lower in the cloud forest compared to the corn field. As a cause of deforestation, the cornfield soil will have less water-holding capacity. The different conditions in both sites are expected to yield different transpiration rates.

Throughfall

Throughfall is the amount of horizontal and vertical precipitation that falls through or from the canopy (86). Throughfall can be divided into three main types, as characterized by the interaction of the water droplet and the canopy. Free throughfall is the number of water droplets that do not come in contact with the canopy surface, whereas splash throughfall and drip throughfall occur due to instant and long contact with the canopy surface respectively. During foggy conditions, the absence of precipitation by rain suggests that free throughfall will not occur. The different types of throughfall have different characteristics, however, the three types will be measured as collective throughfall (86).

Stemflow measurements

Stemflow is a hydrological process that refers to the downward movement of water along the stems and trunks of plants. When precipitation falls on vegetated areas, a portion of the water can be intercepted by the canopy and stored temporarily on the leaves, stems, and branches. As the stored water begins to flow down the stem or trunk, it can pick up additional water and nutrients from the plant surfaces, contributing to the overall water balance of the ecosystem. Stemflow is an important mechanism for transporting water and nutrients from the canopy to the soil surface, where they can be absorbed by the roots of plants. (38).

Stemflow can have important ecological implications, as it can influence the distribution and growth of vegetation, nutrient cycling, and soil moisture dynamics. For example, areas with high stemflow can have increased soil moisture and nutrient availability, which can enhance plant growth and productivity. The stemflow funnelling ratio is a hydrological parameter that describes the proportion of rainfall that is channelled along the stems and trunks of plants and contributes to stemflow. It is calculated by dividing the volume of water collected as stemflow by the total volume of water that falls on the plant canopy as rainfall. Generally, large overstory trees have much higher stemflows than small, understory trees. Often, the contribution of trees with trunk diameters smaller than 1.3 meter is considered negligible (77). However, small, understory trees have a high density and therefore might have a significant influence on stemflow amounts (34) (37). Understory palms and ferns in the cloud forest have a high stem flow due to their geometry which funnels intercepted water towards the stem.

4.4. Conclusion

Modelling the canopy water balance in the Cloud Forest is especially interesting due to its function in intercepting additional precipitation, high storage capacity and delayed evaporation. In the following chapter we report on our work prototyping mechanisms to measure some of the key fluxes and storages identified: Vertical precipitation, Horizontal precipitation, Throughfall, Stemflow, Canopy storage, Evaporation and Transpiration. These parameters have been chosen as they will probably experience changes as a cause of climate change or contribute specifically to the hydrological balance of the Cloud Forest, thus are expected to change in magnitude when there are changes in meteorological conditions and land cover.

4.5. Recommendations for further work

A bucket model (HBV type) could lead to interesting outcomes when studying the complete hydrological balance of the cloud forest ecosystem. The inputs to this model contain -as mentioned before- various parameters, being: snow melt, canopy interception, evaporation, throughfall, unsaturated zone, transpiration, percolation, groundwater flow, preferential flow paths, upwelling, overland flow, and any other process that describes important storages and fluxes. To completely set up and run this model for the hydrological balance of the forest in the area of interest is beyond the scope of this project but would be recommended for further research to gain more insights into the contributions of each of the processes and how they can influence each other.

5

Local Scale Hydrological Balance, Objective D: Prototype in-situ setup for data collection that could be used to calibrate and validate the canopy hydrological balance

5.1. Approach

Using several measuring devices and literature research this chapter aims to find the right techniques to measure the meteorological conditions and components of the hydrological balance of a Cloud Forest for the chosen fieldwork site. The techniques are selected based on significance and feasibility, keeping in mind the continuation of the measurements in the future by CCFC, Rafael Landivar and San Carlos Universities.

5.2. Location Selection

The research location for in-situ hydrological measurements that are included in this project is situated in a cloud forest within the municipality of Coban. The patch of researched land is under the supervision of the community of the village "Aldea Satex 1" at an altitude of 2139 meters. The exact coordinate of the forest is 15°21'14.4"N 90°22'29.8"W. For the open field measurements, a cornfield next to the studied area has been chosen. The open field is situated at an elevation of 2056 meters, at the exact location 15°21'16.4"N 90°22'27.7"W. This location was selected based on previous observations of throughfall (or tuj't ha' in Q'eqchi') during fog events. Setup schematic shown in Figure 5.1. A description of the ecosystem and flora of the site is provided in Appendix G. Future longer-term setup is recommended to be located within the private reserves of Ranchitos del Quetzal or CCFC.

5.3. Data logging, automated and manual options

In the fieldwork, Barometric data loggers (i.e. baro-divers) are used to measure pressure and temperature every 15 minutes. It is strongly advised to use a data logging terminal and more appropriate sensors for each application to avoid the need to empty the container that the diver is placed in.

5.4. Instrumentation and Measurements

The methods and instrumentation are based on literature and information provided in the manual of the course CIE4440 "Hydrological Processes and Measurements", from the Delft University of Technology in combination with methods and approaches found in literature on Tropical and Cloud Forest Hydrology.

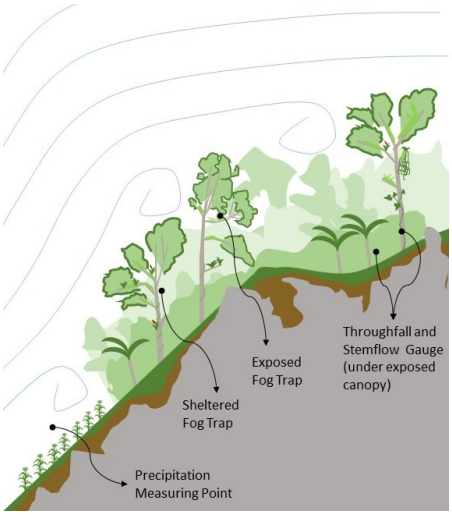

Figure 5.1: Schematic of field and forest location with measuring device placement.

5.4.1. Vertical precipitation

In this study, the rainfall is monitored using homemade rain gauges constructed from 3L water bottles. These gauges are simple, affordable, and easy to use, making them a practical option for gathering data and easy to use in future experiments by local communities. To ensure the accuracy of the measurements, the volumetric content of the homemade gauges is compared to measuring beakers at the beginning and end of the study period. In order to ensure accurate measurements of the rainfall collected in the homemade rain gauges, a barometric diver is used Figure 5.2. The barometric diver works by converting changes in atmospheric pressure into a change in water level, providing a precise measurement of the amount of rainwater collected in the gauge. This method is advantageous because it eliminates the potential for errors that can arise when using manual measurements, such as reading the water level with a ruler. Additionally, the use of a barometric diver allows for real-time monitoring of the rainfall, enabling researchers to track changes in precipitation patterns over time with greater accuracy. A comparative baro-diver is hung in the open air alongside the homemade rain gauges to provide additional measurements of atmospheric pressure. This is done to ensure that any changes in pressure were accurately reflected in the measurements obtained from the rain gauges. By comparing the measurements obtained from the baro-diver to those obtained from the rain gauges, potential sources of error in the data are identified and the needed adjustments could be made. Figure 5.2c shows the 5 rain gauges located in the study zone.

(a) **(b)** **(c)**

Figure 5.2: Placement of divers in the rain gauges and rain gauge set-up in the field.

5.4.2. Horizontal precipitation

The horizontal water flux intercepted by the forest canopy is hard to measure. Due to the high variability in interception capacity of different types of vegetation under different conditions, accurate approximations of fog capture are nearly impossible to measure directly. However, artificial fog gauges are designed to serve as an indicator of the temporal distribution and variation in potential fog deposition. These fog traps do not reflect the characteristics of the vegetation to capture the fog. In this project, the fog gauges are built and tested to determine and gain information on the temporal distribution of fog capture. To study the fog deposition inside the cloud forest, a gauge to canopy factor must be implemented. This factor must be calibrated using a time series of data of sufficient length to isolate the fog interception process in the canopy water balance. Ultimately, it integrates the differences between the efficiency of the fog gauge and the canopy. Previous studies have found that cloud forests and paramo vegetation have higher fog-capturing capabilities per unit area than artificial fog collectors, however, this study does not have sufficient data to determine a gauge-to-canopy factor nor to draw any conclusions on the volume of the fog flux based on the fog trap.(44) (89)

For the design of the artificial fog gauge trap, three types of fog collectors were considered: Square, cylindrical, and modified Juvik. The first considered fog trap is a square fog gauge. These are proven to have the highest yield of water from foggy air. However, square fog traps should be oriented in the prevalent wind direction. As there is expected to be variations in wind direction due to valley breeze effects (katabatic and anabatic winds) and turbulence at the proposed research site, this option is not ideal. The other two fog traps considered are cylindrical. One of these is the cylindrical wire harp. The cylindric catching area guarantees the capture of the fog independent of the wind direction. The last prototype considered is the cylindrical Modified Juvik (JUV), however, for the complexity of its construction, this type of fog gauge is not taken into account (49).

The cylindrical wire harp fog trap prototype is built based on the designs described by (8), (31), and (82).

The efficiency of the fog gauge is dependent on several parameters. The fog gauges catch horizontal precipitation, but there is a chance that vertical precipitation will be measured as well. The implemented roof shields a part of the vertical precipitation, but due to the open structure and the angle of the vertical precipitation, vertical precipitation can influence the measurements (31) Additionally, the efficiency is dependent on the wind speed, drop size and LWC of the fog in the area and the characteristics of the strands of the designed fog gauge. The gauge efficiency will exponentially increase for larger drop sizes and converges approximately at a drop size of 30 ηm. During foggy conditions, the average droplet size is approximately 15 ηm. Wind speed can influence the fog gauge efficiency. Higher wind speeds may cause vibration in the strands and consequently fly off the intercepted droplets (31).

A study performed by (80) determined the efficiency of a cylindrical fog gauge that is similar to ours. This fog gauge is made with a nylon fishing line and had dimensions of 449 mm high, 217 mm outer diameter and 974 cm^2 in cross-sectional area. A model is fitted to describe the upper bound for Fog Water Collection (FWC) [L/m^2] as a function of wind speed and visibility. As the LWC of fog is difficult to predict, it is difficult to find a correlation between these meteorological conditions and the FWC. Wind speed and visibility are more easily measurable variables and thus can provide better estimates (80). The fit of the model and the maximum FWC are shown in Figure 5.3. The statistics for the model are based on the Root Mean Squared Error (RMSE) and the Nash and Sutcliff efficiency ($-\infty \leq NSE \leq 1$) where an $NSE = 1$ means a perfect fitting of the model and $NSE < 0.65$ is an unsatisfactory performance model. (72) The maximum FWC can become unrealistically high (outliers from measurements or pulses of intercepted water during rain events) when there is inclined precipitation that can fall under the angle of the roof and will be caught by the gauge. For this model, the outliers of additional vertical precipitation have been removed but must be taken into account when looking at the data or selecting the storage device (19).

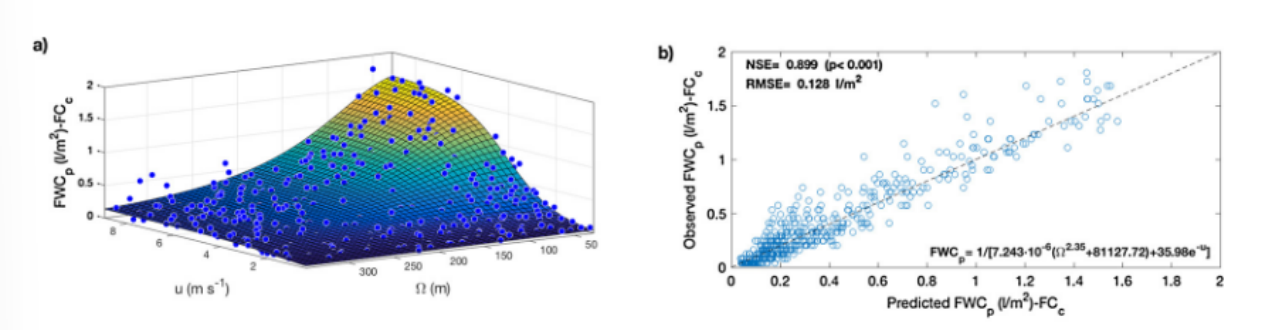

Figure 5.3: The maximum FWC (FWC_p) for a cylindrical wire harp (FC_c) as a function of wind speed ($u[m/s]$) and visibility (Ω [m]) and the goodness-of-fit for the FWC_p model. (80)

The fog gauge prototyped for this project (see Figure 5.4) is 46 cm high, 20 cm in outer diameter and 920 cm^2 in cross-sectional area. The collection surface consists of a 0.5 mm nylon fishing line running vertically and spaced 2 mm apart. The nylon thread is wrapped around a saw blade with a teeth spacing of 2 mm for an even distribution. The fog gauge is hung on a big branch, with an attachment to a lower branch for stabilization. To avoid vertical precipitation, a plastic cover with a diameter of 40 cm is used as protection on the top of the device. Finally, a plastic funnel is attached to direct the collected water. The water level in the container is monitored using a baro-diver(8).

(a) **(b)**

(c) **(d)**

Figure 5.4: Fog trap installation: (a) Assembling of nylon thread on the fog gauge at the CCFC campus, (b) Testing the set-up of fog gauge at the CCFC campus, (c) Prototype of the cylindrical fog harp attached to the tree at the field work site, (d) Set up of the cylindrical fog gauge with the plastic roofs..

5.4.3. Canopy Storage

At our study site, the bulk of epiphytes is present on the primary branches, the mosses make the first substrate or layer of epiphytes that let vascular epiphytes like orchids and bromeliads attach to the branch. The distribution of epiphytes changes from branch to branch e.g.: one covered mainly with orchids, another with bromeliads, and another with ferns. On the longest branches, the composition changes along the length with groups of similar species and mixtures of different kinds of epiphytes.

At our study site, the bulk of epiphytes is present on the primary branches, the mosses make the first substrate or layer of epiphytes that let vascular epiphytes like orchids and bromeliads attach to the branch. The distribution of epiphytes changes from branch to branch e.g.: one covered mainly with orchids, another with bromeliads, and another with ferns. On the longest branches, the composition changes along the length with groups of similar species and mixtures of different kinds of epiphytes.

In order to gain an appreciation for the total canopy storage capacity, each component is simplified into a tank (bromeliads), a surface (vascular epiphytes and tree foliage), or a sponge (mosses and tree soil), as shown in figure 5.5. Each of these components is calculated in this section for one or two of the trees in our study area, and then aggregated into a single value per m^2 of the canopy.

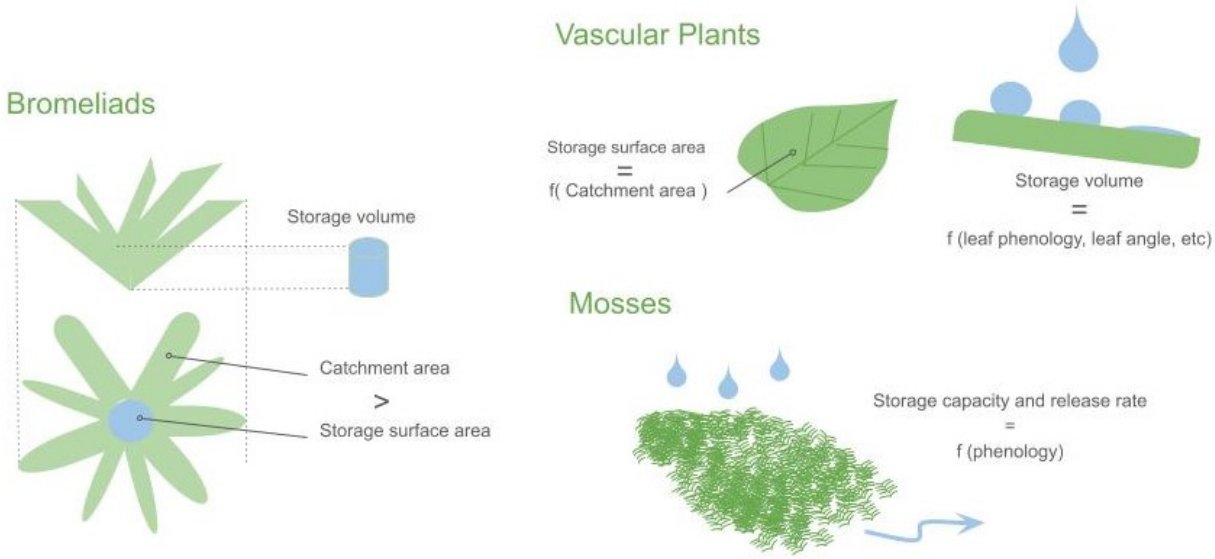

Figure 5.5: Interception behaviour and properties of bromeliads, vascular plant leaves, and mosses

Bromeliads

These tanks function by capturing water over a large area and then storing it in a column with limited and shaded surface area for evaporation. The storage capacity of the bromeliads in the canopy is calculated as the Volume they store over the area that they capture precipitation or throughfall on (Eq. 5.1), the percent reduction factor of evaporation is calculated as the catchment area over the surface area of the storage (Eq. 5.2), and the percentage of the canopy with this storage capacity is calculated as the total area covered with bromeliads in a tree divided by the area of the crown of the tree (Eq. 5.3).

$$I_{max,bromeliad} = \frac{\sum_{i=0}^{n_{categories}} \frac{Vol_{max,bromeliad}}{A_{catch}} \cdot N_{brom,i}}{\sum_{i=0}^{n_{categories}} N_b rom, i} \tag{5.1}$$

$$E_{reduc,bromeliad} = \frac{\sum_{i=0}^{n_{categories}} \frac{A_{storage}}{A_{catch}} \cdot N_{brom,i}}{\sum_{i=0}^{n_{categories}} N_brom, i} \tag{5.2}$$

$$A_{frac,bromeliad} = \frac{\sum_{i=0}^{n_{categories}} A_{catch,i} \cdot N_{brom,i}}{A_{treecrown}} \cdot \frac{A_{treecanopy}}{A_{forest}} \tag{5.3}$$

Bromeliads are classified into four categories by intervals of diameter, at our study site, most of the small to medium bromeliads were of a single epiphytic species (Vriesea montana), while bromeliads in the largest category were terrestrial. See Figure 5.6. For the calculations of interception capacity, evaporation reduction, and bromeliad fraction, the average dimensions of bromeliads in each of the four categories were used, as shown in Table 5.4.3. Based on these values, the maximum interception storage capacity of bromeliad reservoirs, $I_{max,bromeliad} = 4.2$ mm, this interception reservoir will evaporate at a rate of $E_{reduc_bromeliad} = 0.64\%$ of potential evaporation, and bromeliads represent 7.7% of tree crown area for typical old growth trees at our study site, or $A_{frac,bromeliad} = 5.4\%$ of the forest canopy area given that our forest fragment has roughly 70% coverage of old growth trees.

Figure 5.6: Bromeliads from three size categories: (a) Large terrestrial bromeliad (b) Medium bromeliad (c) Small epiphytic bromeliads.

Category	Dia (cm)	Tank Dia (cm)	Catch Area (cm2)	Store Area (cm2)	Vol (cm3)	I_{max} (mm)
Small	30	1.5	225	1.75	105	4.7
Medium	55	2.3	1200	4.15	425	3.5
Large	90	5.5	1950	23.75	800	4.1

Non-vascular epiphytes (Bryophytes/Mosses), root masses and soil

Non-vascular epiphytes (primarily mosses) cover 80% to 90% of tree trunks and branches. The thickness of the moss and tree soil layer varies depending on the angle and dimensions of the branches, at the joint of primary branches with the trunk, it is around 1 or 2 cm, expanding to depths greater than 10 cm at about a meter from the joints, and then decreasing from secondary branch joints. Thin layers of moss (< 1 cm) or lichen (< 2 mm) are present on secondary and tertiary branches. Large (up to 40 cm) hanging balls of moss are also present hanging from vines or suspended from primary branches.

The structure of mosses allows them to expand when they are moist, and shrink when they dry out. During the 11-day dry spell during our fieldwork, mosses were observed to shrink to a fraction of their moist size.

The methodology used to calculate the storage capacity of non-vascular epiphytes is adapted from the study by (101) in high TMCF in Colombia in which the interception capacity of mosses is calculated by a mass balance of moss weights under different moisture content conditions. Samples of moss were measured after gently wringing out ($Weight_{squeezed}$), when saturated ($W_{saturated}$), and after air drying for the length of the 11-day dry spell ($W_{fielddry}$). Air drying rather than oven drying (as done by (101)) is chosen because it reflects the true dry field conditions after periods of drought. Three moss samples of approximately 10 by 10 by 2 cm were measured. The samples reached a steady dry field weight after 5 days. Based on these values, a maximum retention capacity is three times the dry sample weight (Eq. 5.4, however the remaining capacity for well-watered mosses is only twice the dry sample weight (Eq. 5.6), and rapid re-saturation of dry (dormant) moss samples also produced a water retention capacity of twice the dry sample weight (Eq. 5.5).

$$WaterRetention_{max,total} = \frac{W_{squeezedtosaturated} - W_{fielddry}}{W_{fielddry}} \tag{5.4}$$

$$WaterRetention_{max,drymoss} = \frac{W_{drytosaturated} - W_{fielddry}}{W_{fielddry}} \tag{5.5}$$

$$WaterRetention_{max,dampmoss} = \frac{W_{squeezedtosaturated} - W_{squeezed}}{W_{fielddry}} \tag{5.6}$$

In order to measure the evaporation rate from moss, a setup with gravimetric and volumetric measurements is constructed with a fallen epiphyte mass (EM) including roots, soil, moss, and orchids weighing about a half kilogram in field dry conditions (Figure 5.7). To measure the weight, the EM is hung from a produce scale, from which manual readings were taken during field site visits. The volumetric measurement is taken by placing a diver in the bottom of a bucket under the EM. Recordings of pressure at fifteen-minute intervals show a time series of water depth accumulated in the bucket during two consecutive days of rain.

(a) **(b)**

Figure 5.7: (a) Epiphyte Mass Interception and Evaporation estimation setup with gravimetric and volumetric measurements, (b) one of the orchids bloomed during our fieldwork.

Vascular Epiphytes and Tree Foliage

Both the tree foliage and the foliage of vascular epiphytes intercept precipitation, they are assumed to have an interception capacity of 1.5 mm as a typical value for broadleaf trees.

Total Canopy Interception Capacity

The total canopy interception is calculated based on a weighted average of the interception capacities of each type of canopy vegetation, however, because the canopy is highly variable, any calculation based on counting bromeliads and mosses in a few trees is unlikely to be representative of a broader area, therefore, this value can also be calibrated in a hydrological balance model.

5.4.4. Transpiration

In order to calculate the transpiration rate of a tree accurately, it is best to do this according to the sapflow. The sapflow is the movement of water and nutrients from the roots of a plant through the stem or trunk and into the leaves or needles. The rate of sap flow is closely related to transpiration. However, due to time constraints and limited available tools, the sapflow could not be monitored.

To get some insights into the rate of transpiration of the Podocarpus in question, a rough estimation of the transpiration rate has been executed. The transpiration rate of the trees has been estimated by using plastic ziplocks. These ziplocks function as "porometers", indicating how much water a single leaf transpires.

For the calculations, it has been assumed that transpiration is completely dependent on sunlight. To estimate the total surface area of the tree's uppermost branches and leaves, the formula for the surface area of a sphere is used, which is $4r^2$, where r is the radius of the sphere. It is assumed that the tree has a spherical form. Assuming the tree's crown is roughly spherical in shape, its radius has been estimated as half the diameter. The assumed amount of leafs is half the spherical surface.

The Leaf Surface Area of the tree is thus:

$$0.5 * (4r^2)$$

A study by Barajas-Guzman et al. (2017) measured the LAI in the cloud forest of the Sierra de las Minas Biosphere Reserve in Guatemala and reported an average LAI of 4.5. A study by Quiñones-Pérez et al. (2019) in a cloud forest in Honduras reported a maximum LAI value of around 6.0. Therefore, an average LAI of 5 has been used for the calculations. In general, trees are the dominant vegetation type in a cloud forest and contribute the most to the LAI. Studies have reported that trees can contribute up to 70-90% of the total LAI in a cloud forest, depending on the forest structure and composition(4). Epiphytes also contribute significantly to the LAI in cloud forests. These include ferns, bromeliads, and orchids. Studies have reported that epiphytes can contribute up to 15-30% of the total LAI in a cloud forest, depending on the forest type and altitude(110). The contribution of understory vegetation to the LAI in a cloud forest is generally lower than that of trees and epiphytes. However, the exact percentage can vary depending on the density and composition of the understory vegetation. Studies have reported that understory vegetation can contribute up to 10-20% of the total LAI in a cloud forest (109). For the calculation, the percentages of trees, epiphytes and understory have been assumed to be 75%, 15% and 10% respectively.

$$LAI = 0.7 * LeafSurfaceArea_{tree} * 0.15 * LeafSurfaceArea_{epiphytes} * 0.1 * LeafSurfaceArea_{understory}$$

The area covered by the tree is 38^2. The diameter of the tree branches reaches 7.5 meters. It is assumed that the top 4 meters of the spherical tree receive sunlight. According to the formula described in the methodology, this is $88.4m^2$ for tree 2.

Figure 5.8: Transpiration set-up forest - fern leaf.

Transpiration Results

The average transpiration rate of a Podocarpus tree (which was common in the forest at the data collection site) can vary depending on various factors such as age, environmental conditions, tree size, and species. The plastic bags that are used to capture the transpiration of the leafs, cause different climate conditions at the leaf (Figure **??**). Higher temperatures within the bag can result in atypical stomatical functioning and water release. Therefore, the volumes obtained by the plastic bags, are not representative of the actual transpiration rates. To approach a calculation method for the total transpiration of a tree, the values obtained with the above mentioned method are used in the calculations. As all the measured leafs of tree 1 fell off before the final volume was written down, the transpiration volumes retrieved from tree 2 are used.

The first tree leaf has a final volume in the ziplock of 8 mL and a leaf area of 27 cm2, and results in a transpiration of 272 mL per day. The second leaf of the same size has a final volume of 25 mL. This results in total tree transpiration of 849 mL per day. The average of these two is 560 mL per day.

Assuming that the tree within the area of 38 m^2 transpires 560 mL/day, and assuming that the average LAI of the cloud forest of 5 consists of 75% out of the tree, 15% out of epiphytes and 10 % out of understory would result in total transpiration of 560 mL + 112 mL + 75 mL = 327 mL per day within that area. Dividing 747 mL by the area of 38 m2, gives us the estimation of 18.7 mL per m2 per day. Transpiration is typically measured in millimeters over a given time period, or as a rate of water loss per unit of time such as mm/day. 18.7 mL per m2 per day is therefore equivalent to 0.187 mm of transpiration loss per day for the cloud forest of interest.

Transpiration Conclusion

The method used to quantify transpiration, is not representative of the conditions in the cloud forest. A method for the calculation of the total tree transpiration is proposed. However, keep in mind that this is a very rough estimate, with many assumed factors and points in the equation where a wrong or over- or underestimation could be made.

Transpiration Discussion

- It is not possible to accurately calculate the transpiration rate of a tree by measuring the amount of water released by one leaf. This is because transpiration is a process that occurs throughout the entire tree, not just in one leaf. Estimating the number of leaves on a tree can be a challenging task, particularly for large trees with dense canopies. For the estimation of the total amount of leaves in the tree, a sampling method has been used.
- The rate of transpiration has been estimated at 18.2 mm/day. However, other studies conducted in a cloud forest in southern Guatemala found an average transpiration rate of approximately 2.6 mm/day for the dominant tree species, which is one of the highest rates ever reported for a tropical forest. Another study conducted in a cloud forest in northern Guatemala found an average transpiration rate of 1.9 mm/day for the dominant tree species (62; 106; 29; 87). There could be several reasons why your estimation of transpiration for a Guatemalan cloud forest is much higher than the rates reported in scientific studies. One of the reasons for the difference in results could be the differences in environmental conditions: The transpiration rate of a forest can vary depending on environmental conditions such as temperature, humidity, and soil moisture. Our research has been conducted in a relatively dry, warm and sunny period, which could lead to higher transpiration rates. Another reason could be the difference in the time scale of the measurement. Transpiration rates can vary over different time scales, such as hourly, daily, or seasonal. Our estimation is based on a shorter time scale than the studies we're comparing it to. Therefore, the estimation may be higher due to variations in transpiration rates over shorter time intervals. Also, The estimation of the transpiration rates is complex and involves different methods and assumptions. There are many assumptions made, and therefore many inaccuracies which can alter the outcome.

5.4.5. Potential Evaporation

As a first approach for the calculation of the Evaporation, the Penman and Penman-Monteith equations are used. Since the soil and vegetation were continuously wet, our actual evaporation in the forest could be approximately near to the potential evaporation. For this reason, it is assumed that potential evaporation is nearby to actual evaporation. The formula for the two equations and the parameters used are shown below:

Penman

$$E_p = \frac{\frac{s(R_n - G)}{\rho\lambda} + \frac{c_p \rho_a}{\rho\lambda} * \frac{e_s - e_a}{ra}}{S + \gamma} \tag{5.7}$$

Penman-Monteith

$$E_p = \frac{\frac{s(R_n - G)}{\rho\lambda} + \frac{c_p \rho_a}{\rho\lambda} * \frac{e_s - e_a}{ra}}{S + \gamma * (1 + \frac{r_c}{r_a})} \tag{5.8}$$

Where:

- λ The latent heat $[J/kg]$ $(2.45MJ/kg)$
- Rn net radiation on the earth's surface $[Jd^{-1}m^{-2}]$
- s slope of the saturation vapour pressure-temperature curve $[KPa/°C]$
- c_p specific heat of air at constant pressure $[Jkg^{-1}k^{-1})(1004Jkg^{-1}k^{-1})]$
- ρ_a density of air $[Kg/m^3]$ $(1.205kg/m^3)$
- ρ density of water $[Kg/m^3]$ $(1000kg/m^3)$
- e_a actual vapour pressure in the air at $2m$ height $[KPa]$
- e_s saturation vapour pressure for the air at $2m$ height $[KPa]$
- γ psychrometer constant $[KPa]$ $(0.066KPa/°C)$

- r_a aerodynamic resistance $[d/m]$
- r_c crop resistance ≈ 0.9 $[d/m]$
- G Ground heat flux $[W/m^2]$

The calculation of the evaporation event in each place is one of the most challenging calculations in the hydrological processes. This is because the evaporation process is a process that depends on many other variables such as net radiation, temperature, altitude, air humidity, wind speed, and pressure.

This makes Evaporation a complex process and a complex calculation when it comes about to getting the most approximate value on site. Since it can involve too many uncertainties or make many assumptions.

In order to calculate the evaporation, all the values from this parameter that are not constants need to be calculated for the local conditions.

In situ, local data are measured such as temperature, wind speed, and relative humidity. At the weather station located at CFCC, the $R_{s,in}$ radiation is measured.

Calculations for Penman input variables

r_a Aerodynamic resistance $[d/m]$ This parameter depends on the wind velocity v $[m/s]$ measured at 2m height. For the calculation, the average wind speed measured on-site is used.

$$r_a = \frac{245}{0.5 * v + 0.5)} + \frac{1}{86400} \tag{5.9}$$

e_s Saturation vapour pressure for the air at 2m height. Units -> $[KPa]$ kilopascals The saturation vapour pressure e_s is the maximum vapour pressure of water particles before condensation. This value depends on the temperature t.

$$e_s = 0.61(\frac{19.9 * t}{273 + t}) \tag{5.10}$$

s Slope of the saturated vapour pressure vs temperature curve. Units -> $[KPa/°C]$

$$s = \frac{5430 * e_s}{(273 + t)^2} \tag{5.11}$$

e_a Determining the actual vapour pressure by the relative humidity. Units -> $[KPa/°C]$ The actual humidity is expressed as the actual vapour pressure e_a. where e_a (Ta) is the saturation vapour pressure at the current air temperature Ta for a given relative humidity $'h'$ [-].

$$e_a = h * e_s \tag{5.12}$$

Rn, net radiation. To calculate the net radiation is necessary to have a clear Radiation balance as shown in Figure 5.9.

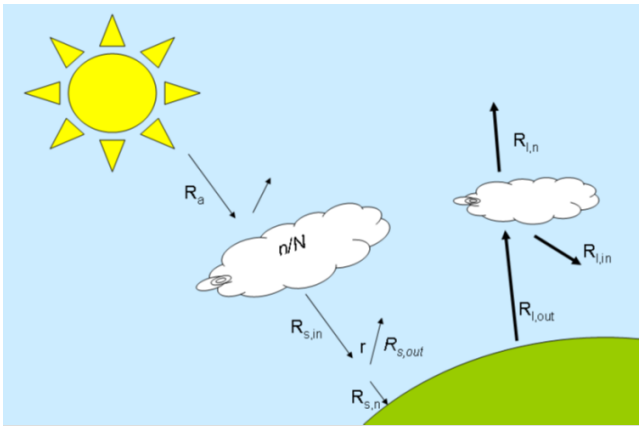

Figure 5.9: Radiation Balance

R_n is the difference between the net short-wave radiation ($R_{s,n}$) and the net longwave radiation ($R_{l,n}$).

$$R_n = R_{s,n} - R_{l,n} \tag{5.13}$$

The net short wave radiation is the difference between the incoming short wave radiation $R_{s,in}$ and the fraction that is reflected that is, $'R'_{s,in}$ times the albedo $'r'$. For this assignment, the theoretical value of $r = 0.18$ is used

Where:

$$R_{s,n} = R_{s,in} - (r * R_{s,in}) \tag{5.14}$$

Then:

$$R_n = [(1 - r) * R_{s,in}] - R_{l,n} \tag{5.15}$$

The meteorological station at CFCC provided us with the R_{in} value.

The net longwave radiation is the difference between the emitted radiation from the surface ($R_{l,out}$) and the long wave radiation that is scattered back by e.g., clouds ($R_{l,in}$). This can be obtained from the empirical expression.

$$R_{l,n} = \sigma * (273 + t)^4 * (0.47 - 0.21 * \sqrt{e_a}) * (0.2 + 0.8\frac{n}{N}) \tag{5.16}$$

where σ is the Stefan-Boltzmann constant with $\sigma = 4.9 * 10^{-3}$ $[J * d^{-1} * m^{-2} * K^{-4}]$; t is the temperature of the air in Celsius and e_a is the actual vapour pressure of the air in kPa.

To full fill with the calculations, it will be assumed that,

$$G \approx 0.1 * R_n[J/d * m^2] \tag{5.17}$$

To calculate n and N
The calculations of this value is approached in two ways. First, the suggested literature is used where the N value depends on the global position as it is shown in figure 5.10.

North Lats. South Lats.	Jan July	Feb. Aug.	Mar. Sept	Apr. Oct.	May Nov.	June Dec.	July Jan.	Aug. Feb.	Sept Mar.	Oct. Apr.	Nov. May	Dec. June
60	6.7	9.0	11.7	14.5	17.1	18.6	17.9	15.5	12.9	10.1	7.5	5.9
58	7.2	9.3	11.7	14.3	16.6	17.9	17.3	15.3	12.8	10.3	7.9	6.5
56	7.6	9.5	11.7	14.1	16.2	17.4	16.9	15.0	12.7	10.4	8.3	7.0
54	7.9	9.7	11.7	13.9	15.9	16.9	16.5	14.8	12.7	10.5	8.5	7.4
52	8.3	9.9	11.8	13.8	15.6	16.5	16.1	14.6	12.7	10.6	8.8	7.8
50	8.5	10.0	11.8	13.7	15.3	16.3	15.9	14.4	12.6	10.7	9.0	8.1
48	8.8	10.2	11.8	13.6	15.2	16.0	15.6	14.3	12.6	10.9	9.3	8.3
46	9.1	10.4	11.9	13.5	14.9	15.7	15.4	14.2	12.6	10.9	9.5	8.7
44	9.3	10.5	11.9	13.4	14.7	15.4	15.2	14.0	12.6	11.0	9.7	8.9
42	9.4	10.6	11.9	13.4	14.6	15.2	14.9	13.9	12.6	11.1	9.8	9.1
40	9.6	10.7	11.9	13.3	14.4	15.0	14.7	13.7	12.4	11.2	10.0	9.3
35	10.1	11.0	11.9	13.1	14.0	14.5	14.3	13.5	12.4	11.9	10.3	9.8
30	10.4	11.1	12.0	12.9	13.6	14.0	13.9	13.2	12.4	12.0	10.6	10.8
25	10.7	11.3	12.0	12.7	13.3	13.7	13.5	13.0	12.3	12.0	10.9	10.6
20	11.0	11.5	12.0	12.6	13.1	13.3	13.2	12.8	12.3	12.0	11.2	10.9
15	11.3	11.6	12.0	12.5	12.8	13.0	12.9	12.6	12.2	12.0	11.4	11.2
10	11.6	11.8	12.0	12.3	12.6	12.7	12.6	12.4	12.1	12.0	11.6	11.5
5	11.8	11.9	12.0	12.2	12.3	12.4	12.3	12.3	12.1	12.0	11.9	11.8
Equator 0	12.0	12.0	12.0	12.0	12.0	12.0	12.0	12.0	12.0	12.0	12.0	12.0

Figure 5.10: Mean daily duration of maximum possible sunshine hours N

Since Guatemala is located latitude of 15.783471 North, in agreement with this table for the month of January, it should be a value of $N \approx 11.3 hours$

The second and implemented approach is the use of the data available from the weather station installed at the CCFC campus. From there, the exact hours with light (maximum) N are observed. These are used for a rough calculation to determine, n the actual hours of sunshine.

From the data of the weather station, it is found that in the study area, the N value corresponds to 12h with 5 minutes. While, $n \approx 9hours$, the value is determined as an average value of the actual hours of sunshine. Figure 5.11 shows the values for the collected evaporation data.

					Penman	Penman-Monteith
Date, January 2023	Rs_in (w/m^2)	t [°C]	h [-]	v [m/s]	E_p (mm/day)	E_p,t (mm/day)
15	167.3	11.9	0.88	0.25	1.3482	1.1138
16	149.3	15	0.84	0.28	1.2568	1.0551
17	155.8	15.4	0.84	0.28	1.3912	1.1692
18	156.6	18.4	0.74	0.56	1.6767	1.3912
19	145.9	15.3	0.83	0.28	1.2222	1.0266
20	135.8	15.5	0.88	0.19	1.0521	0.8948
21	129.4	12	0.97	0.06	0.7482	0.6353
22	132.5	15.7	0.85	0.25	1.0185	0.8607
23	146.9	16.1	0.86	0.36	1.2956	1.0828
24	162.5	14.6	0.84	0.19	1.4381	1.2168
25	163.7	16.9	0.77	0.39	1.6512	1.3819
26	43.6	15.2	0.96	0.11	0	0
27	40.0	14.1	0.99	0.22	0	0
28	182.0	15.1	0.85	0.19	1.7906	1.5194

Figure 5.11: Evaporation per day

5.4.6. Stemflow

Stemflow amounts are collected through in situ measurements. For the measurements, a tree is monitored with characteristics similar to the tree of the horizontal precipitation and transpiration measurements. The tree is located on a low slope and has protection from high winds from other trees. These measures result in more uniform conditions. To collect the stem flow, a PVC pipe of 410 cm and 3 cm width is cut along the length, and attached around the trunk of a tree (Figure 5.12). To optimize the flow, and decrease the loss of water by evaporation, two pipes are attached from the lowest point at the collecting tank to the highest point opposite the collecting tank on the other side of the tree trunk. The PVC pipes are attached to the tree using nails. Small nails of 2.5 cm are used to attach the pipe to the trunk, and larger nails of 4 cm are used to hold the structure of the pipe. The PVC pipe is not sealed using silicon sealant to the tree to reduce leakage along the bark, as this is not allowed by the owner of the property. The water is collected through a funnel in a tank. An atmospheric diver is used to collect time series data of the stem flow. The maximum amount of precipitation is 167 mm/day. In January, there are on average 13 rainy days.

(a) StemFlow close-up: Collecting tank with diver

(b) StemFlow Overview: Stem, PVC pipe, collecting tank

(c) StemFlow Close-Up: PVC pipes into funnel

(d) StemFlow detail: PVC pipe

(e) StemFlow detail: PVC pipe.

(f) StemFlow detail: PVC pipe

Figure 5.12: Stemflow set up.

5.4.7. Throughfall

Due to the high variety of occurrences, size, and height of plants in the canopy of cloud forest, throughfall amounts are not homogeneously covering the surface of the research site. To obtain coverage for the temporal and spatial variability, the throughfall has been measured in two ways. First, the temporal variability is estimated by installing 6 gutters of 1.70m evenly distributed around a collecting tank (Figure 5.13). To prevent leaf litter and organic debris from disturbing the measurements, the gutters and collecting tank have been covered with chickenwire with a gap diameter of 2.5 cm. The total area covered by the gutters and collecting tank is 0.94 m^2. An atmospheric baro-diver is used to gather data in the collection tank. The spatial variability is estimated by installing 6 rain gauges, evenly distributed between the gutters. The spatial variability is used to correct for temporal variability using the formula derived from Gerrits (2010):

$$T_l(t) = T_f, gutter(t) * \left(\frac{\sum_{t=i}^{t=0} T_f, collector}{\sum_{t=i}^{t=0} T_f, gutter(t)} \right) \tag{5.18}$$

The data for the spatial variability could not be measured with baro-divers due to a lack of baro-divers.

Therefore, the throughfall is not corrected for the spatial variability with the formula mentioned above. However, rain gauges have been installed to get a visual idea of the spatial variability.

(a) (b)

Figure 5.13: Throughfall set up, (a) Top View, (b) Side View

5.4.8. Soil Infiltration

In the context of measuring different rainfall and interception inputs, monitoring soil infiltration could provide additional information on the water balance of the forest canopy. By combining measurements of soil infiltration with measurements of throughfall, stemflow, fog interception, and transpiration, researchers could develop a more complete understanding of the hydrological processes that control the water balance of the ecosystem. This could be particularly important in areas where soils are prone to erosion or degradation, as soil infiltration rates may be lower and the water balance of the ecosystem may be more sensitive to changes in precipitation patterns or land use.

While soil infiltration is an important component of the hydrological cycle and can influence the water balance of forest ecosystems, the research can still be relevant. This is because different interception processes can still influence the amount and timing of water that reaches the forest floor, which in turn can affect ecosystem processes such as nutrient cycling, plant growth, and carbon storage (12; 61). Furthermore, understanding the relative importance of different interception processes can provide insights into the hydrology and functioning of the forest canopy, which can be important for predicting how these ecosystems may respond to environmental change (73; 90). Therefore, while soil infiltration is an important component of the hydrological cycle, the research questions formulated based on measuring different rainfall and interception inputs in a cloud forest can still be relevant and informative even if soil infiltration is not explicitly monitored.

5.5. Data collection calibration and errors

To collect data on the water balance in the cloud forest, a series of barometric divers are installed at the study site. These divers recorded changes in the water level over time, allowing to quantify the various inputs to the water balance.

5.5.1. Divers

An overview of all the different measurement devices which contained a dedicated diver is shown. This does not include the weather station Figure 5.14. A period of 4 days is visualized, starting on the 24th of January until the 28th of January. The readings of the divers include multiple parameters like temperature, atmospheric pressure and water pressure. The last one is used in all the following results and is described as millimeters of water (mmH_2O). In addition, the plots show vertical lines indicating the start of a rain event. In the period before the first rain event, an alternating pattern between the fog trap and precipitation is visible, which corresponds to the diurnal cycle. Rain during daytime is expected to have high enough temperatures enable evaporation of the water in the water tanks attached to the fog trap. A nighttime, the water condensed again, leading to an increase of water in the fog trap collecting tank. Moreover, when including the throughfall measurements, a relation is visible between the fog trap and the throughfall, this cyclical ”noise” is removed as shown in Figure 5.15.

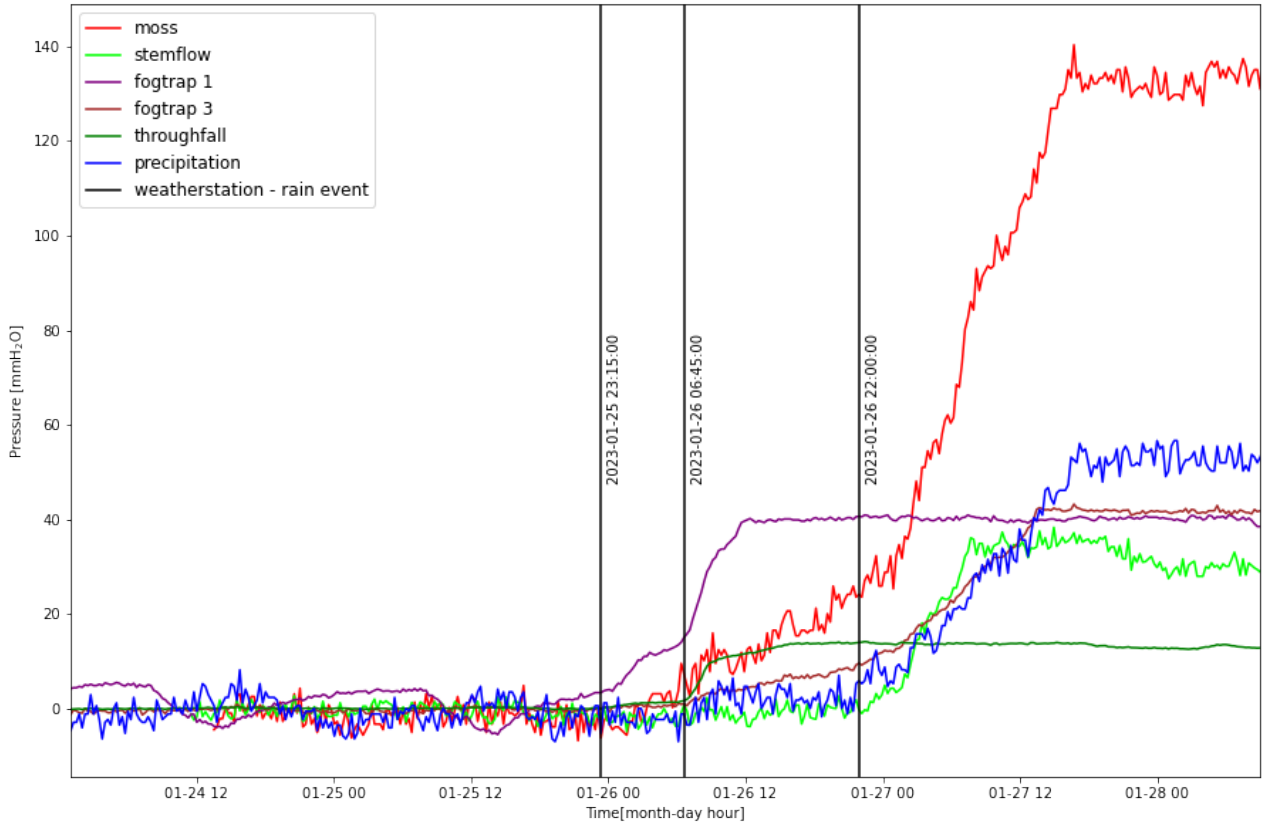

Figure 5.14: Data obtained from the divers installed in the different measurement devices. All measured components are shown in this plot.

In Figure 5.16 the Throughfall and FogTrap 1 capturing is visible in between the first two rain events from the weather station, but before the rain event at the field site begins. As the precipitation measurements do not clearly show significant change, the process of cloud interception on the vegetation and the following throughfall to the ground is likely occuring. This clearly shows the relation between the cloud interception and the resulting throughfall contributing to the hydrological balance in the cloud forest. Fog Trap 1 is far

ahead of the precipitation as it is filled to its maximum value of mmH_2O at noon of the 26th even before the vertical precipitation started in the evening of the same day. This indicates that horizontal precipitation must have filled the fog trap as clouds were already present due to the incoming weather.

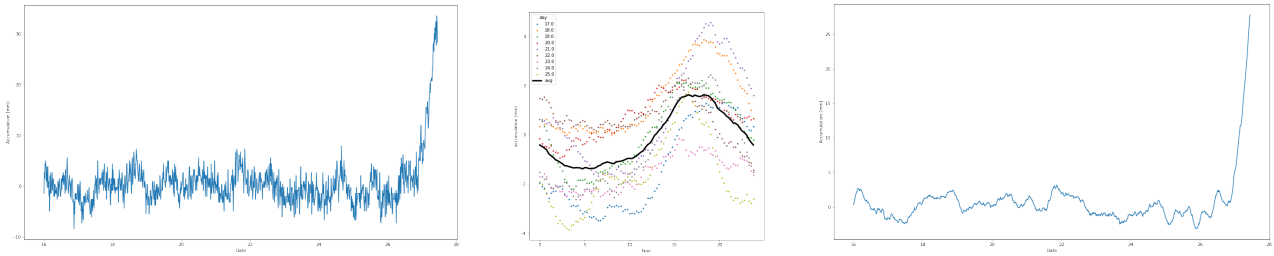

(a) **(b)** **(c)**

Figure 5.15: Removal of daily cyclical variations in diver data.

Meanwhile, both Fog Trap 3 and Moss measurements show an increase in mmH_2O matching the rain event, this makes sense because they are both more sheltered from clouds and wind and therefore are more likely to have intercepted wind-driven rain rather than fog. As the Moss is both catching horizontal and vertical precipitation due to the nature of the setup, it is difficult to distinguish between the different factors involved. Since the moss itself also receives both types of precipitation and the effective area of the moss that contributes to this is difficult to compute, it remains unclear how the different aspects of the moss contributed to the amount of water collected. It does show the importance of vegetation taking up precipitation and being able to transport it further in the water balance.

The stemflow measurements show no flow until the rain event starts, During the fog event there is no stem flow, this makes sense because the canopy was quite dry after the 11-day dryspell. During the heavy rain event starting at the end of the 26th, the stemflow gauge fills quickly. The amount of stemflow is taken over the diameter of the stem, but the precipitation that flows down the stem is caused by the capturing of the branches. Thus, the area of catchment of the water is actually much larger than the diameter of the stem, therefore the depth of water collected in mm cannot be directly compared to the depth of water collected by precipitation or throughfall gauges.

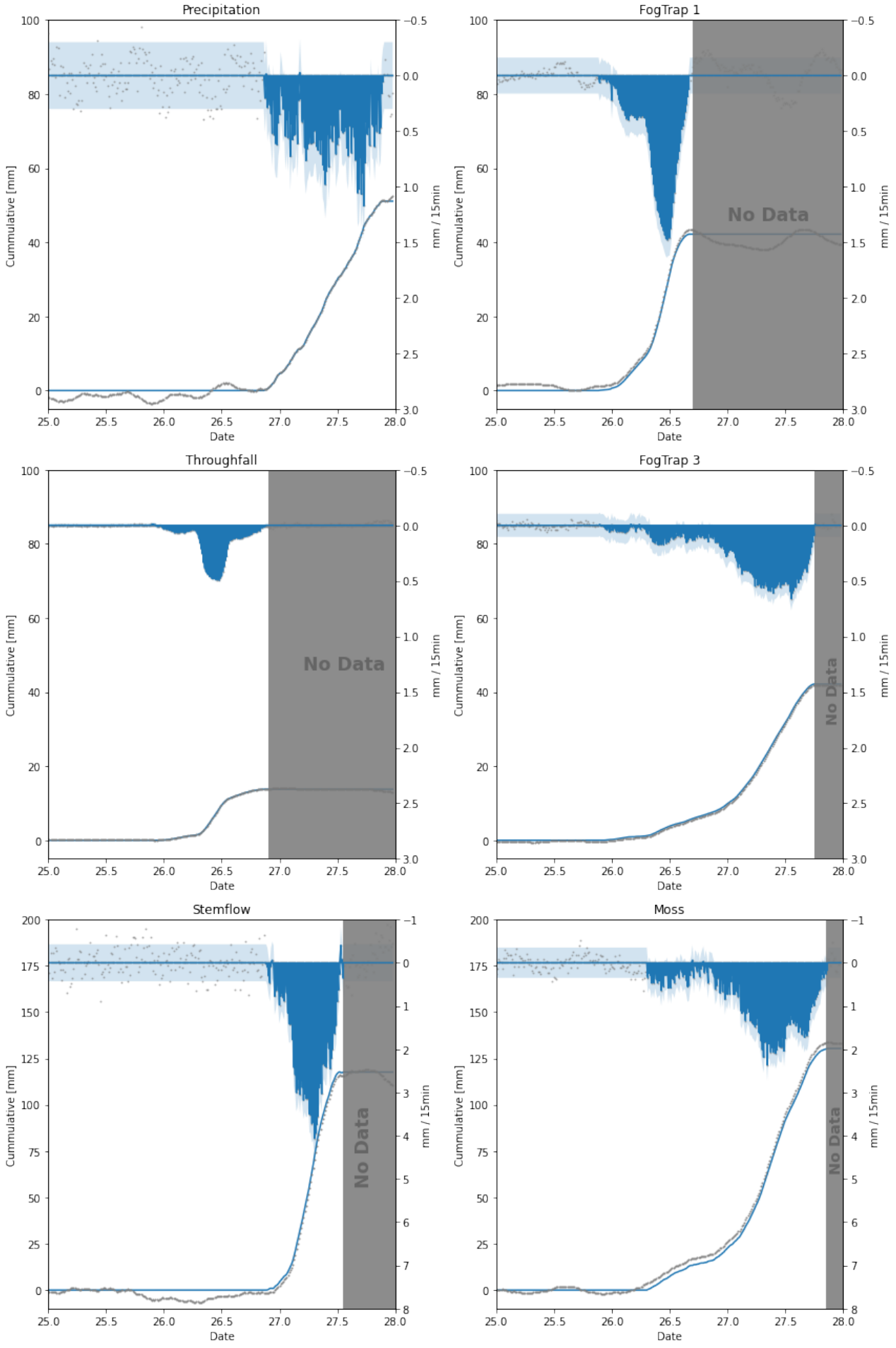

Figure 5.16: Diver data with error filtering for noise and daily cyclical variations due to pressure differences or evaporation within gauges.

5.6. Selecting in-situ measurements vs other available data

5.6.1. Comparison of in-situ measurements of meteorological variables to Weather Station data

To reduce the amount of work in the field, and improve modelling capacity with less manual data collection, it can be helpful to identify meteorological variables that are measured locally, such as the daily measurements by INSIVUMEH, or the 15-minute data available from weather stations on sites such as weather underground (wunderground.com). Figure 5.17 compares measurements at the field sites to the weather station data from a few kilometers away, it appears that there is a consistent offset between the two measurements of dew point. Whereas, for wind speed, the in-situ measurements seem to match the weather station data without an offset. If these patterns remain stable under various conditions, the in-situ measurements could be replaced by the weather station data with a correction factor. This method may be applicable for some variables at certain time scales, but not for others, so any specific study can evaluate the trade-offs between required resolution and accuracy of data. Further comparisons of the weather station and in-situ data collection are shown in Appendix E.

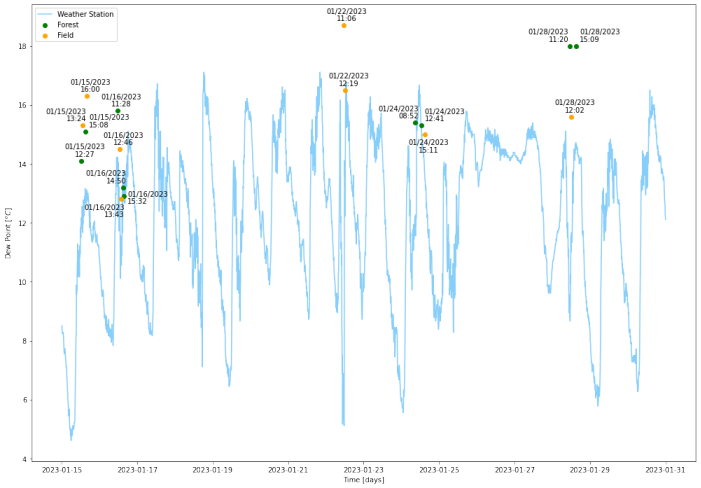

(a)

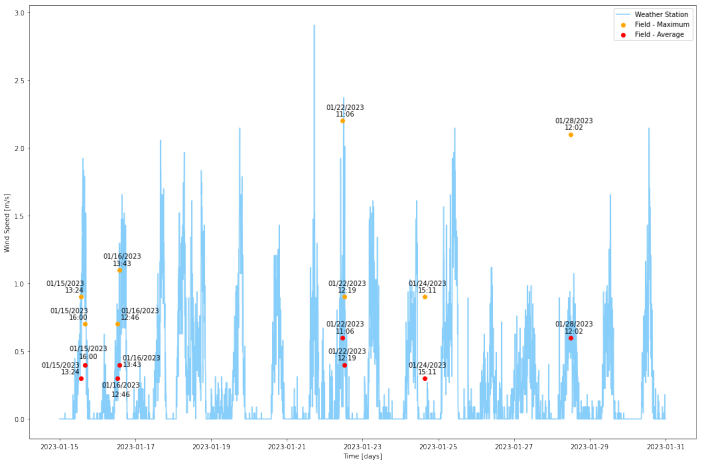

(b)

Figure 5.17: Comparison of weather station to Kestral measurements, (a) Dew Point (b) Wind Speed.

5.7. Comparing FIESTA results to Field Work Results

Because each of the measuring setups only captured one or two events, the only measurement that can be compared to the results of the adapted FIESTA model is Throughfall. 15 mm of Throughfall were captured

under an emergent tree on the 26th. This matches the model well, because although the expected fog interception for the grid cell is between 1.65 mm and 4.28 mm, emergent trees were only modeled as 5% of the grid cell, and they can have two to three times the interception capacity compared to sheltered trees and open field. Recommendations on how to use similar measurement setups to calibrate the FIESTA model are provided in Chapter 6.2

6

Operational Scale: Applying Knowledge

In this Chapter, we summarize the recommendations to CCFC partners in two areas, first, (per **Objective E** we list measures that we recommend based on what we can say with some certainty from a review of literature, data, and experiences in the field, and second, (per **Objective F**) we list suggested paths for future research.

6.1. Objective E: Identify measures that could be encouraged by advocates for water security and forest conservation in order to adapt to the changing global climate through the preservation of microclimates.

Various stakeholders have different reasons to be concerned about land management in the Sierra Yalijux, to highlight the hydrological function of the forest, in this section, some recommendations are provided for each of CCFC's work areas where cloud forest hydrology plays a role.

6.1.1. Water Committee Capacity building

Defining recharge zones for sources of municipal water

Most towns have their own spring or water storage from which the water is collected. However, water management authorities often have little awareness and little to no control over the extent of the recharge zone of their water resource and how land use change can impact water quality and availability. CCFC is advised to work with water committees to identify the recharge zones of important water collection points.

A water catchment is an area over which the collected water is stored and moved along toward a shared outlet. The collected water in this case can be precipitation, both horizontal and vertical. Catchments exist naturally as differences in elevation across an area of land make sure water will flow towards for example one side of a hill. Through using a Digital Elevation and some tools within QGIS, various water catchments within the Cobán region are identified and displayed (Figure 6.1), additional maps of the Mestelá Catchment Properties are shown in Appendix F.

It is important to note that the groundwater flows that end up in these springs do not necessarily follow the predicted catchment area based on surface topography, therefore the true recharge zone extent is somewhere between the outlined areas and the total area on the mountain above the point where the spring is located.

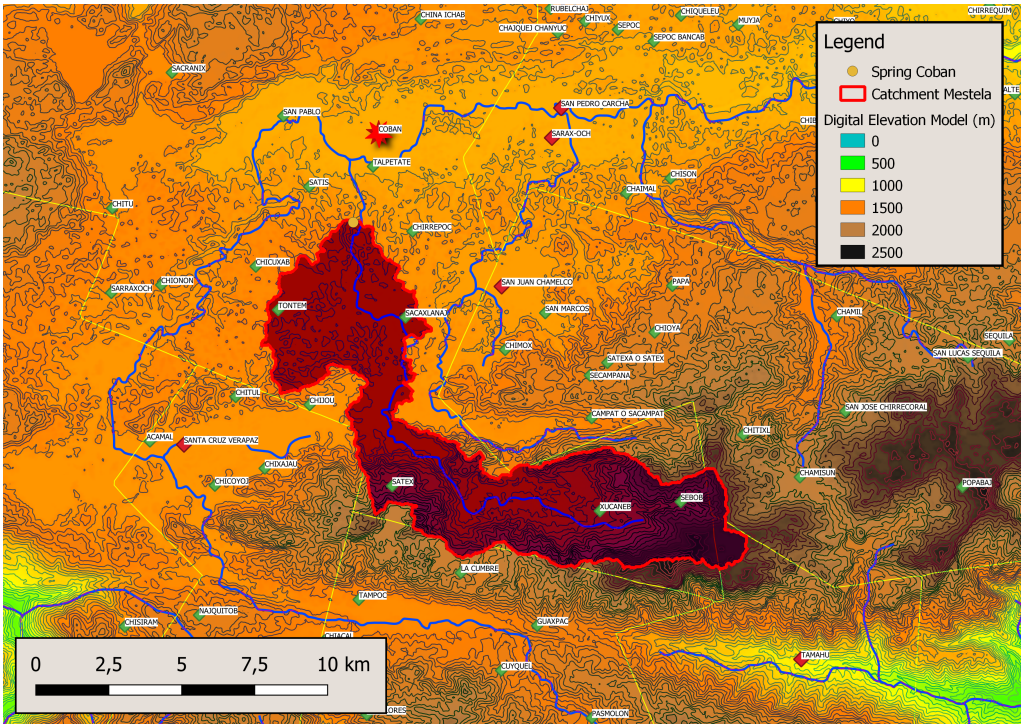

(a)

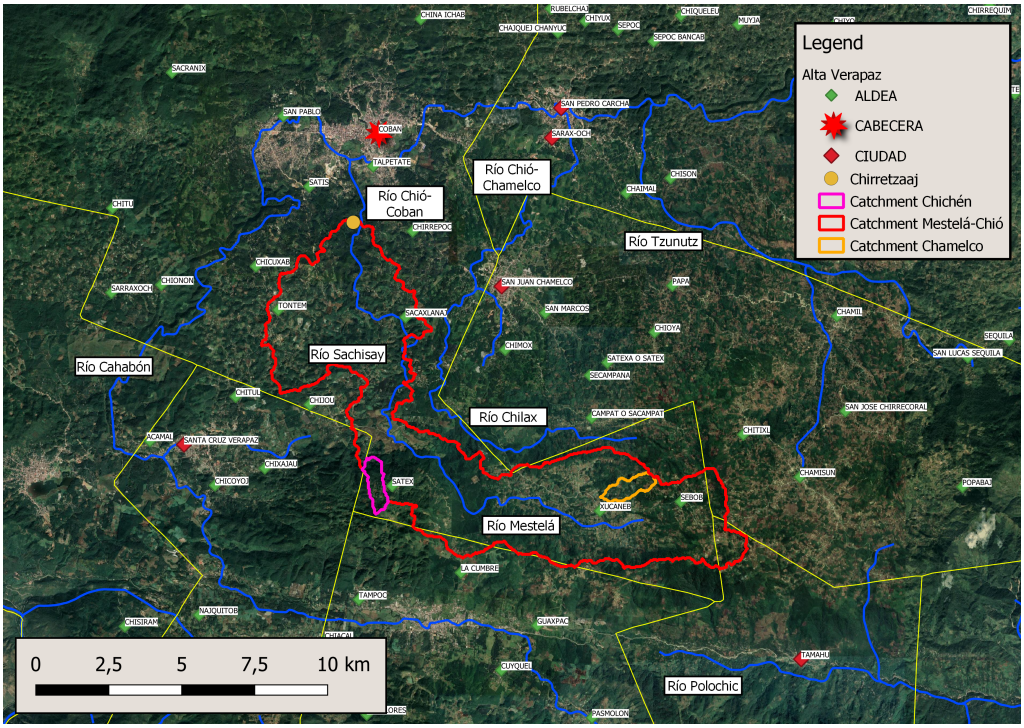

(b)

Figure 6.1: (a) Map of Alta Verapaz showing the Mestelá-Chió catchment ending in the water extraction point, in Chirretzaaj, of the city of Coban,(b) Satellite view of Alta Verapaz showing the Mestelá-Chió catchment and the catchments Chichén and Chamelco.

Using the coordinates from the springs that are delivered by the local water communities, the water catchments that flow into the designated springs or tanks are identified.

These water catchments were then visualized on contour maps and satellite view maps to create a better understanding for the local communities where the boundaries of these catchments were and what the land use is within these boundaries. Land use influences the hydrological inputs and response of a recharge zone. Secondly, these maps are of practical use to enable an easy tool for the local communities to work with and

visualize their environment.

- **Chirretzaaj collection point** on the river Mestelá-Sachisay-Chió is one of the main sources of water for the city of Cobán (81,000 inhab).
- **Chichén Spring** is just next to our research site, it serves 11 villages (prox. 3,000 inhab).Figure 6.2a.
- **Chamelco Spring** is one of the main sources of water for the town San Juan Chamelco (30,000 inhab) gets its water from a spring, Figure 6.2b.

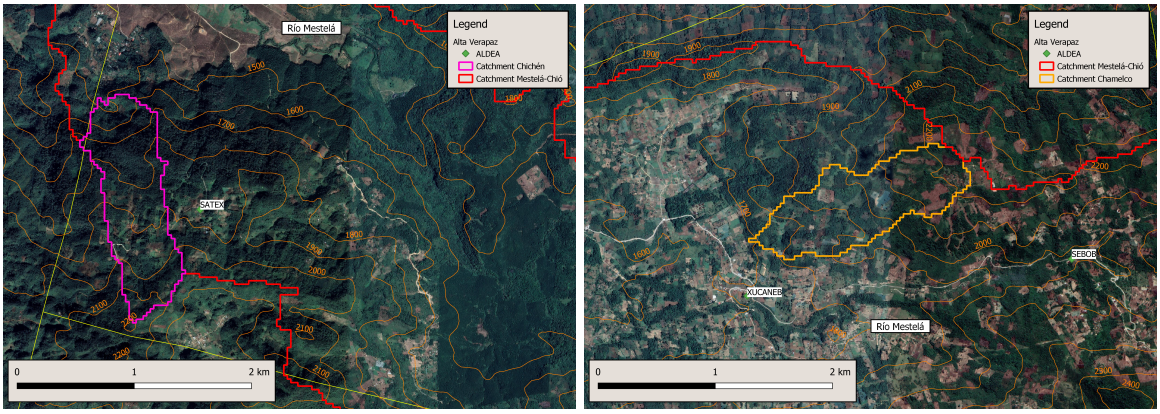

(a) **(b)**

Figure 6.2: (a) Map of Alta Verapaz showing the Mestelá-Chió catchment ending in the water extraction point, in Chirretzaaj, of the city of Coban,(b) Satellite view of Alta Verapaz showing the Mestelá-Chió catchment and the catchments Chichén and Chamelco.

The importance of Cloud Forests as source and regulator of streamflow

The presence of Cloud Forest is expected to increase base flow in springs due to its ability to capture additional hydrological inputs in the dry season, increase moisture recycling after heavy rain events, and store water in the soil. Depending on the size and elevation of a recharge zone, the forest may function more importantly as a regulator of flow or as a source of additional hydrological inputs. Mapping the catchments can help identify which hydrological processes sustain a consistent water supply.

Drought preparedness

While improving recharge zones through reforestation and erosion prevention may have a positive effect on water availability, it may not be sufficient to maintain a constant supply. Village water system tanks and household water reservoirs should be designed to account for extended periods of meteorological drought. In some cases, the sizes of the reservoirs and tanks should increase. The amount of water captured during rain periods can be larger and will prepare the villages better for extended droughts periods. By working with water committees and municipalities, this can be addressed and implemented.

6.1.2. Environmental Education

Adapting environmental education curricula to include a more accurate description of the local water cycle. Besides educational walks in the Cloud Forest, school children can perform experiments testing erosion on patches of soil with and without vegetation, measuring precipitation with homemade gauges, capturing the transpiration of a leaf in a ziplock bag, and showing interception of horizontal precipitation with a spray bottle, see Figure 6.3

(a) (b)

Figure 6.3: Environmental Education (a) Explaining the response of a catchment to deforestation. (b) Experiment on erosion.

6.1.3. Reforestation and Agroecology

To secure water supply to the rural population, targeted reforestation and Agroforestry should be prioritized from the highest and smallest recharge zones downwards because they are most vulnerable to dry spells in vertical precipitation. For example, the village of Sebob in the upper part of the Chamelco spring recharge zone and the village of Satex I in the upper part of the Chichén spring recharge zone. The next priority would be to encourage reforestation or agroforestry with erosion management techniques on the steepest slopes.

6.1.4. Payment for Ecosystem Services

To suggest changes in larger catchments, it often involves asking those upstream to make changes in order to improve conditions downstream. The changes proposed (such as converting slash-and-burn mono-culture to cash-crop agroforestry) are designed to benefit the people implementing them, however, it may be necessary to incentivize these changes. We advise CCFC to explore the possibilities of incorporating knowledge of the role of forest in key recharge zones into any PES (payment for ecosystem services) projects that it is involved in.

6.2. Objective F: Suggest topics for research on the Cloud Forest of the Sierra Yalijux

6.2.1. Moisture Recycling

This phenomenon can be studied at a subcontinental scale using remote sensing data, and weather station data from INSIVUMEH, as attempted in Chapter 3.1 and Appendix B.

6.2.2. Drought Analysis

In this report (Chapter 3.2.4), only dry spells are identified as drought indicators due to their importance in small recharge zones with a rapid hydrological response, however, at larger scales other indicators can give a better understanding of water availaibility, such as the Standard Precipitation Index (SPI).

6.2.3. Hydrological Modeling

Fog Interception Modeling at a local scale: Down-scaling FIESTA model for more applicable results at a village catchment scale in relevant time steps. Logging the meteorological conditions in the local area using a weather station can provide more accurate inputs for the model for temperature, relative humidity, wind, atmospheric pressure, etc.

Infiltration, Runoff, and Erosion: Deforestation of Cloud Forest does not only mean the loss of a canopy that intercepts fog-generating hydrological inputs during the dry season; it also typically causes an increase in total yield from a watershed, but a decrease in base flow (12). Additionally, water supply is not the only need in the region, as a cause of erosion water in the springs can become polluted thus decreasing the quality significantly. (9) Further research on these processes and how they are influenced by deforestation could help show the importance of the forest for water (quality) conservation.

6.2.4. Calibrating models with in-situ measurements

Installing longer-term Data collection in Cloud Forest Canopy: The lack of data in the area makes any analysis difficult, we suggest that CCFC work with partners to install a longer-term setup. The rain gauges, fog traps, stem flow and throughfall devices can be made locally and our findings suggest that these devices can be used for timing and duration of fog and/or rain events. It is strongly advised to use a data logging terminal and more appropriate sensors for each application to avoid the need to empty the container that the diver is placed in. Our containers filled up after one heavy rain event, when this happens the maximum pressure above the diver is reached and further data cannot be provided.

In-situ measurements for adapted FIESTA model calibration The adaptation of the FIESTA model used in this report assumes that the input parameters that were developed for applicability across Central America are valid for the Sierra Yalijux, each of these can be tested using in-situ measurements. The input flux of cloud water as horizontal precipitation is modeled to depend on three factors: (1) whether a cloud is present, (2) how much water it carries, (3) what surface area intercepts it, and, (4) how quickly it moves across/through that surface.

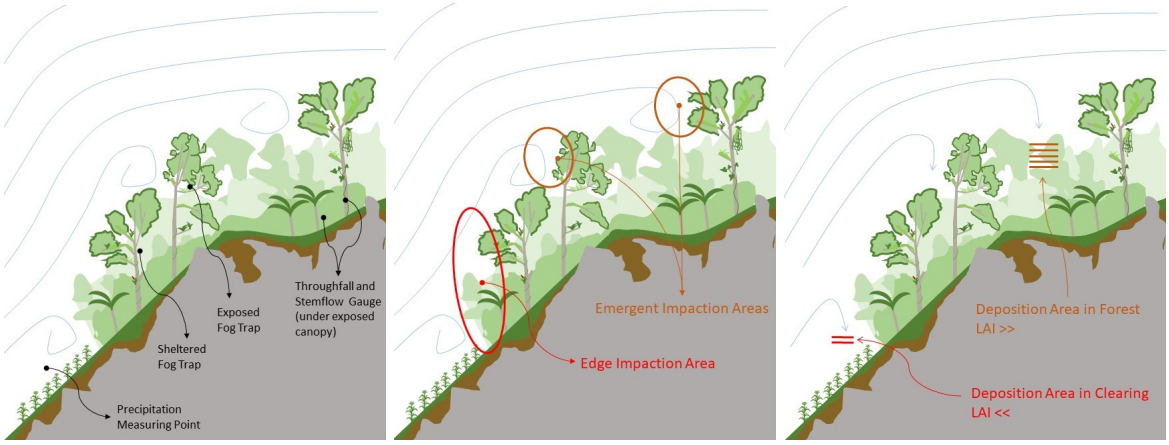

Figure 6.4: Experimental setup for FIESTA calibration (a) Prototype setup Jan 2023 (b) Edge and Emergent edge impaction areas, (c) Deposition areas.

- Determining whether clouds are present at ground level intercept mountains: This is modeled as function of relative humidity and temperature, however, whether the data from INSIVUMEH weather stations located at least 12 km away or the CCFC weather station at least 2 km away is appropriate still needs to be evaluated. However, we expect it to be valid base on observations in the field showing a ”flat” cloud base height across the Cahabón river valley, and reaching the mountains.

- Determining how much water a cloud carries and how it behaves in impactiona and deposition, i.e. Liquid Water Content (LWC): Meteorological constants for Maximum Absolute Humidity (AH_{max}), maximum Liquid Water Content (LWC_{max}), Droplet size, and Droplet Terminal Velocity, can be calibrated by iterating between upper and lower bounds for typical values based on meteorological conditions and cloud type.
- The constants used in determining the surface area that intercepts the clouds in the FIESTA model should be evaluated. because the Sierra Yalijux Cloud Forest is more patchy and more likely to be selectively logged than protected forests, the calculation for forest edge length and assumptions on emergent areas may be underestimated. Average forest edge height can be estimated in-situ, and edge lengths can be measured using satellite imagery. LAI is used as an indicator of fog interception area.
- The constants applied as reduction factors to input wind speed and warping to direction can be calibrated by measuring wind speed and direction in a clearing, at the forest edge, and at the top of the canopy, for the period of measuring the canopy water balance, wind speed can be measured at these points. It can be evaluated whether the weather station data adjusted by reduction factors match these values. If they do not match over the average timestep of FIESTA (6hr), it may be necessary to take additional measurements to calibrate this parameter.
- Finally, to balance the model are direct measurements of precipitation, throughfall, and stem flow, and an estimation of evapotranspiration using FIESTA functions. To capture the three classes of fluxes setups are proposed at three locations, near an edge or emergent tree for impaction, under a sheltered tree for deposition in forest, and in an open area for deposition in clear areas. The expected results for effective precipitation assuming a saturated canopy are shown in Figure 6.5,. Edge/Emergent will have much higher effective precipitation than sheltered whenever there is fog and high wind, whereas for dominant deposition, edge/emergent and sheltered will have similar effective precipitation.

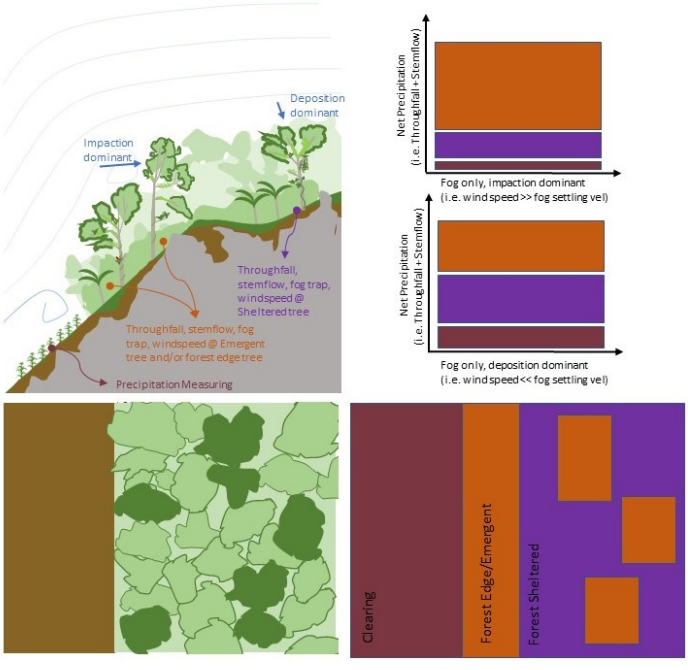

Figure 6.5: Proposed experimental setup for FIESTA calibration. The lower part of the figure shows a gird cell with the spatial distribution of the three types of area, for simplicity each covers one-third of the cell.

Bibliography

aimeesch@hawaii.edu (2021). Cloud Water Interception in Hawaii – Hawai i Climate Data Portal.

Alley, W. M. (1984). The palmer drought severity index: limitations and assumptions. *Journal of Applied Meteorology and Climatology*, 23(7):1100–1109.

Angelidis, P., Maris, F., Kotsovinos, N., and Hrissanthou, V. (2012). Computation of drought index spi with alternative distribution functions. *Water resources management*, 26:2453–2473.

Asbjornsen, H., Goldsmith, G. R., Alvarado-Barrientos, M. S., Rebel, K., Van Osch, F. P., Rietkerk, M., Chen, J., Gotsch, S., Tobón, C., Geissert, D. R., Gómez-Tagle, A., Vache, K., and Dawson, T. E. (2011). Ecohydrological advances and applications in plant–water relations research: a review. *Journal of Plant Ecology*, 4(1-2):3–22.

Assessment, M. E. (2005). *Ecosystems and human well-being: synthesis*. Island Press.

Australia Bureau of Meteorology (2018). Weather Impacts of ENSO. `https://www.weather.gov/jetstream/enso_impacts`. Accessed on Feb 28, 2023.

Barros, V. R. (2013). *Climate change and water resources in the tropical Andes*. Inter-American Development Bank.

Berrones, G., Crespo, P., Wilcox, B. P., Tobón, C., and Célleri, R. (2021). Assessment of fog gauges and their effectiveness in quantifying fog in the andean páramo. *Ecohydrology*, 14(6):e2300.

Bruijnzeel, L., Mulligan, M., and Scatena, F. N. (2011). Hydrometeorology of tropical montane cloud forests: emerging patterns. *Hydrological Processes*, 25(3):465–498.

Bruijnzeel, L. A. (2001a). Hydrology of tropical montane cloud forests: a reassessment. *Land Use and Water Resources Research*, 1:1–17.

Bruijnzeel, L. A. (2001b). Hydrology of tropical montane cloud forests: a reassessment. *Land use and water resources research*, 1(1732-2016-140258):1–1.

Bruijnzeel, L. A. (2004). Hydrological functions of tropical forests: not seeing the soil for the trees? *Agriculture, ecosystems & environment*, 104(1):185–228.

Bruijnzeel, L. A., Scatena, F. N., and Hamilton, L. S. (2010). Hydrological changes in tropical montane cloud forests: responses to climate change and land use. *Forest Ecology and Management*, 259(4):716–728.

Byrne, M. P., O'Gorman, P. A., and Petterssen, C. (2018). Changes in climate extremes, fresh water availability and vulnerability to food insecurity projected at 1.5°c and 2°c global warming with a higher-resolution global climate model. *Philosophical Transactions of the Royal Society A*, 376(2119):20160452.

Calvo-Alvarado, J. C., Nùñez-Avellaneda, M., Vargas-Ríos, O., Jiménez-Rodríguez, C., Martínez-Salas, E., and León-Ortega, M. (2020). Trends and gaps in knowledge of cloud forest biodiversity: A literature review and synthesis. *Forest Ecology and Management*, 460:117832.

Calvo-Rodriguez, S., Ram'ırez, D. A., Gonz'alez-Qui nones, V., Ovando, A., R"osner, S., and S"orensson, A. (2020). Hydrological characterization of the cloud forest in the alta verapaz region of guatemala. *Hydrology and Earth System Sciences*, 24(10):5115–5131.

Cano, E. B., Castillo-Santiago, M. A., and López-Mendoza, R. (2018). Amphibians and reptiles of the cloud forest of alta verapaz, guatemala. *Herpetological Conservation and Biology*, 13(1):77–86.

Castillo-Santiago, M. A., Espinoza-Cabrera, E. A., Higueros-Ciapara, I., Perez, A. G., and Munoz-Salazar, R. (2017). Hydrological functioning of cloud forests in the sierra de las minas biosphere reserve, guatemala. *Forests*, 8(12):492.

Cavelier, J., Solis, D., and Jaramillo, M. A. (1996). Fog interception in montane forests across the central cordillera of panama. *Journal of Tropical Ecology*, 12(3):357–369.

CCFC (2008). Community Cloud Forest Conservation.

Climate.gov, N. (2014). The walker circulation: Enso's atmospheric buddy.

Copernicus Climate Change Service (C3S) (2017). ERA5: Fifth generation of ECMWF atmospheric reanalyses of the global climate. Copernicus Climate Change Service Climate Data Store (CDS). `https://cds.climate.copernicus.eu/cdsapp#!/home`. Accessed on Feb 27, 2023.

Daidzic, N. E. et al. (2019). A new model for lifting condensation levels estimation. *International Journal of Aviation, Aeronautics, and Aerospace*, 6(5):1.

DiLiberto, T. (2014). The Walker Circulation: ENSO's atmospheric buddy. *NOAA Enso Blog*.

Dingman, S. L. (2015). *Physical hydrology*. Waveland press.

Douglas, P. M., Demarest, A. A., Brenner, M., and Canuto, M. A. (2016). Impacts of climate change on the collapse of lowland maya civilization. *Annual Review of Earth and Planetary Sciences*, 44:613–645.

Elgert, L., Austin, P., and Picchione, K. (2016). Improving water security through rainwater harvesting: a case from guatemala and the potential for expanding coverage. *International Journal of Water Resources Development*, 32(5):765–780.

Ellison, A. M., Gotelli, N. J., Farnsworth, E. J., and Simons, T. R. (2007). Ecosystem service assessment of wetlands: Wetland functions and society. *Annual Review of Environment and Resources*, 32:1–25.

Fisher, J. B., Baldocchi, D. D., Misson, L., Dawson, T. E., and Goldstein, A. H. (2007). What the towers don't see at night: nocturnal sap flow in trees and shrubs at two ameriflux sites in california. *Tree Physiology*, 27(4):597–610.

Foster, P. (2001). The potential negative impacts of global climate change on tropical montane cloud forests. *Earth-Science Reviews*, 55(1-2):73–106.

Frumau, K. A., Burkad, R., Schmid, S., Bruijnzeel, L., Tobon-Marin, C., and Calvo, J. (2007). Fog gauge performance under fog and wind-driven rain conditions. *Mountains in the Mist: Science for Conserving and Managing Tropical Montane Cloud Forests, University of Hawaii Press, Honolulu, HI*.

Galdames, R. and Ballesteros, D. (2012). Orchidaceae of Guatemala. In Breedlove, D. E., editor, *Flora of Guatemala, Part X*. Missouri Botanical Garden Press.

Georgakakos, K. P. and Bras, R. L. (1984). A hydrologically useful station precipitation model: 1. formulation. *Water Resources Research*, 20(11):1585–1596.

Germer, S., Werther, L., and Elsenbeer, H. (2010). Have we underestimated stemflow? lessons from an open tropical rainforest. *Journal of Hydrology*, 395(3):169–179.

Gerrits, M. (2019). Na regen komt interceptie. *Stromingen 15*, 1:37–40.

González-Maya, J. F., Ponce-Reyes, R., Polidoro, B., Williams, J. N., and Brown, J. L. (2017). Prioritizing conservation actions for threatened mammals in the highly diverse atlantic slope of mesoamerica. *PloS one*, 12(11):e0188200.

González-Martínez, Williams-Linera, H. (2017). Understory and small trees contribute importantly to stemflow of a lower montane cloud forest. *Hydrological Processes*, 31(5):1174–1183.

González-Martínez, Williams-Linera, H. (2022). Interactive effects of functional traits and rainfall event size on stemflow in a tropical montane cloud forest. *Ecohydrology*, 15(8).

Gotsch, S. Forest ecophysiology lab- university of kentucky.

Gotsch, S. G., Nadkarni, N., and Amici, A. (2016). The functional roles of epiphytes and arboreal soils in tropical montane cloud forests. *Journal of Tropical Ecology*, 32(5):455–468.

Halldin, M. (2006). Intertropical Convergence Zone (ITCZ). `https://skybrary.aero/articles/inter-tropical-convergence-zone-itcz`. Accessed on Feb 21, 2023.

Hijmans et al (2018). Mapa de zonas de vida de Guatemala basado en el sistema de clasificación de Holdridge. `http://www.infoiarna.org.gt/recursos-informativos/mapas/`. Accessed on Jan 21, 2023.

Hölscher, D., Köhler, L., van Dijk, A. I., and Bruijnzeel, L. S. (2004). The importance of epiphytes to total rainfall interception by a tropical montane rain forest in costa rica. *Journal of Hydrology*, 292(1-4):308–322.

Holwerda, F., Bruijnzeel, L., and Scatena, F. (2011). Comparison of passive fog gauges for determining fog duration and fog interception by a puerto rican elfin cloud forest. *Hydrological Processes*, 25(3):367–373.

Instituto Nacional de Sismología, Vulcanología, Meteorología e Hidrología - INSIVUMEH (2023). Perspectiva Climática Cuatrimestral Diciembre 2022 - Marzo 2023. *Departamento de Investigación y Servicios Meteorológicos*.

Irungaray, G. E. P., Monzón, J. C. R., Ibarra, R. E. M., Cabrera, G. A. G., and Ruano, J. G. (2018). *Ecosistemas de Guatemala: basado en el sistema de clasificación de zonas de vida*. Instituto de Investigación y Proyección sobre Ambiente Natural y Sociedad de ….

Jarvis, A. and Mulligan, M. (2011). The climate of cloud forests. *Hydrological Processes*, 25(3):327–343.

Juárez, E., DeClerck, F. A., Giròn, L., Jiménez, E., Sánchez-Azofeifa, A., and Bär, R. (2018). Biodiversity and ecosystem services in guatemalan cloud forests: A systematic review. *Forest Ecology and Management*, 430:209–222.

Juvik, J. O. and Nullet, D. (1995). Comments on" a proposed standard fog collector for use in high-elevation regions". *Journal of Applied Meteorology (1988-2005)*, 34(9):2108–2110.

Kappelle, M. and Brown, A. (2001). Birds of cloud forest in alta verapaz, guatemala. *Conservation Biology*, 15(1):166–176.

Kessler, M. and Krömer, T. (2000). Patterns and causes of species diversity in tropical plant communities. In *The biology of biodiversity*, pages 163–200. Springer.

Klamerus-Iwan, A., Link, T. E., Keim, R. F., and Van Stan II, J. T. (2020). Storage and routing of precipitation through canopies. *Precipitation partitioning by vegetation: A global synthesis*, pages 17–34.

Knoke, T., Hahn-Schilling, K., Wiersma, S., Nugroho, D. A., Sulistyani, E., Hoen, H. F., Korner, P., and Barkmann, J. (2016). Changes in forest ecosystem functions due to land use management practices in humid tropical lowlands of sumatra. *Environmental Management*, 58:961–977.

Köhler, L., Mulligan, M., Schellekens, J., Schmid, S., and Tobón, C. (2006). Final technical report dfid-frp project no. r7991 hydrological impacts of converting tropical montane cloud forest to pasture, with initial reference to northern costa rica.

Lawrence, M. G. (2005). The relationship between relative humidity and the dewpoint temperature in moist air: A simple conversion and applications. *Bulletin of the American Meteorological Society*, 86(2):225–234.

Lawton, R. O., Nair, U. S., Pielke Sr, R. A., and Welch, R. M. (2001a). Climatic impact of tropical lowland deforestation on nearby montane cloud forests. *Science*, 294(5542):584–587.

Lawton, R. O., Nair, U. S., and Welch, R. M. (2001b). Climate change and the hydrology of the humid tropics. *Climatic Change*, 50(3):305–328.

Liu, Y., Chen, J., and Sun, W. (2019). Impact of precipitation types and intensities on urban runoff quality in a coastal city. *Water*, 11(1):115.

Lykes, M. B., Beristain, C. M., and Pérez-Armiñan, M. L. C. (2007). Political Violence, Impunity, and Emotional Climate in Maya Communities. *Journal of Social Issues*, 63(2):369–385.

L'Heureux, M. (2014). What is the El Niño–Southern Oscillation (ENSO) in a nutshell? *NOAA Enso Blog*.

Meentemeyer, R. K., Turner, M. G., and Jones, J. A. (2001). Interception by vegetation can significantly alter the water balance of forested watersheds, even in areas with high rates of infiltration. *Journal of Hydrology*, 240(3-4):230–244.

Meinzer, F., Goldstein, G., Jackson, P., Holbrook, N., and Cavelier, J. (1995). Environmental and physiological regulation of transpiration in tropical forest gap species: the influence of boundary layer and hydraulic properties. *Oecologia*, 101(4):514–522.

Mendieta-Leiva, G., Porada, P., and Bader, M. Y. (2020). Interactions of epiphytes with precipitation partitioning. *Precipitation Partitioning by Vegetation: A Global Synthesis*, pages 133–146.

Merkel, A. (2021a). Climate: GUATEMALA). `https://en.climate-data.org/north-america/guatemala-229/`. Accessed on Feb 23, 2023.

Merkel, A. (2021b). San Juan Chamelco Climate (GUATEMALA). `https://en.climate-data.org/north-america/guatemala/alta-verapaz/san-juan-chamelco-46096/`. Accessed on Feb 22, 2023.

Moghaddam, P. P., Saatchi, S., Erickson, D. J., Moghaddam, M. P., Walker, W. S., and Ardakanian, R. (2016). Conserving montane cloud forests: challenges and opportunities. *Journal of environmental management*, 177:86–93.

Moreno, P., Pawlowski, M., Dominguez, G., Correia, B., and Smith, D. (2008). Contribution of fog to the water relations of sequoia sempervirens (d. don) endl. *Plant, Cell & Environment*, 31(5):463–472.

Mukhopadhyay, A. and Midha, V. (2016). Waterproof breathable fabrics. In *Handbook of technical textiles*, pages 27–55. Elsevier.

Mulligan, M. and Burke, S. (2005). Fiesta fog interception for the enhancement of streamflow in tropical areas final technical report for kcl/amibiotek contirbution to dfid frp project r7991.

Muzylo, A., Llorens, P., Valente, F., Keizer, J., Domingo, F., and Gash, J. (2009). A review of rainfall interception modelling. *Journal of hydrology*, 370(1-4):191–206.

NASA/JPL-Caltech (2018). Intertropical Convergence Zone (ITCZ). `https://scijinks.gov/trade-winds/`. Accessed on Feb 23, 2023.

Nash, J. E. and Sutcliffe, J. V. (1970). River flow forecasting through conceptual models part i—a discussion of principles. *Journal of hydrology*, 10(3):282–290.

Oishi, A., Siccama, T., and Johnson, C. (2010). Interception of rainfall by forest canopies is a major factor controlling the water balance of forest ecosystems, and that changes in interception can have important effects on ecosystem functioning. *Global Change Biology*, 16(10):2715–2728.

Onda, Y., Ito, H., Sakagami, T., and Kato, T. (2016). Interception and storage of rainfall by a japanese cypress plantation forest in comparison with an evergreen broad-leaved forest in japan. *Journal of Hydrology*, 533:380–391.

Parker, C. and Munroe, D. K. (2010). Observations on the interactions among ecosystem services in rural guatemala. *International Journal of Biodiversity Science, Ecosystem Services & Management*, 6(1-2):38–49.

Parker, C., Stabach, J. A., and McNab, R. B. (2004). Natural resource use and conservation in the guatemalan highlands. *Mountain Research and Development*, 24(4):316–321.

Pypker, Delphis, S. V. S. (2011). *Canopy Structure in Relation to Hydrological and Biogeochemical Fluxes*, pages 371–388. Springer Netherlands, Dordrecht.

Ray, D. (2013a). Tropical montane cloud forests. *Climate Vulnerability: Understanding and Addressing Threats to Essential Resources*, 5:79–85.

Ray, D. K. (2013b). Impacts of historical land use change on modern tropical forest cover and implications for carbon storage and biodiversity. *Global Ecology and Biogeography*, 22(3):292–303.

Regalado, C. M. and Ritter, A. (2019). On the estimation of potential fog water collection from meteorological variables. *Agricultural and Forest Meteorology*, 276:107645.

Restall, M. and Solari, A. (2020). *The Maya: a Very Short Introduction*. Oxford University Press, Oxford, United Kingdom.

Ritter, A., Regalado, C. M., and Guerra, J. C. (2015). Quantification of fog water collection in three locations of tenerife (canary islands). *Water*, 7(7):3306–3319.

Rodriguez, V. (2019). Cloud forest conservation and hydrological services in guatemala. *Forest Ecology and Management*, 432:778–789.

Ruano, S. and Milan, A. (2014). Climate change, rainfall patterns, livelihoods and migration in cabricán, guatemala.

Rubel Xucaneb, C. (2022). Reunión sobre la disponibilidad y el acceso al recurso hídrico en las aldeas de rubel xucaneb.

Sadeghi, S. M. M., Gordon, D. A., and Van Stan II, J. T. (2020). A Global Synthesis of Throughfall and Stemflow Hydrometeorology. *Precipitation Partitioning by Vegetation*, pages 49–70.

Sánchez-Azofeifa, G., Quesada, M., Rodríguez, J., Nassar, J., Stoner, K., Castillo, A., and Garvin, T. (2005). Research priorities for neotropical dry forests. *Biotropica*, 37(4):477–485.

Savenije, H. H. (2010). Hess opinions" topography driven conceptual modelling (flex-topo)". *Hydrology and Earth System Sciences*, 14(12):2681–2692.

Schellekens, J., Bruijnzeel, L., Wickel, A., Scatena, F., and Silver, W. (1998). Interception of horizontal precipitation by elfin cloud forest in the luquillo mountains, eastern puerto rico. In *First International Conference on Fog and Fog Collection, ICRC, Ottawa*, pages 29–32.

Staelens, J., De Schrijver, A., and Verheyen, K. (2010). Interception by vegetation is an important factor controlling the water balance of a mountain forest ecosystem, and the importance of interception increased with elevation. *Hydrological Processes*, 24(3):374–385.

Still, C. J., Foster, P. N., and Schneider, S. H. (1999). Simulating the effects of climate change on tropical montane cloud forests. *Nature*, 398(6728):608–610.

Sánchez-Azofeifa, A. and Portillo-Quintero, C. (2011). Climate change in the humid tropics: Impacts and adaptations in neotropical cloud forests. In Kappelle, M. E. and Loo, A. W. K., editors, *Tropical Conservation Science*, volume 4, pages 121–139. University of Costa Rica.

Turner, D. P., Ritts, W. D., Cohen, W. B., Gower, S. T., Running, S. W., Zhao, M., Costa, M. H., Kirschbaum, A. A., Ham, J. M., Saleska, S. R., et al. (2006). Evaluation of modis npp and gpp products across multiple biomes. *Remote sensing of environment*, 102(3-4):282–292.

UNDP (2011). *Indigenous peoples, poverty and human development in Latin America: 1994-2004*. United Nations Development Programme.

UNESCO World Heritage Centre (2017). Cusuco National Park. `https://whc.unesco.org/en/list/1509/`. [Accessed: 15-Feb-2023].

USGS (2018). Evapotranspiration and the water cycle completed.

Van der Ent, R., Tuinenburg, O., Knoche, H.-R., Kunstmann, H., and Savenije, H. (2013). Should we use a simple or complex model for moisture recycling and atmospheric moisture tracking? *Hydrology and Earth System Sciences*, 17(12):4869–4884.

Van der Plas, F., Schrumpf, M., Bruelheide, H., Becker, C., Schwieder, M., Rutten, G., Zuidema, P. A., Koenig, C., Jung, M., Veldkamp, E., et al. (2019). Carbon storage in tropical forests correlates with taxonomic diversity and functional dominance on a global scale. *Global Ecology and Biogeography*, 28(2):211–225.

Vargas, J. M., Pérez-Arce, F., and Valdés-Prieto, S. (2016). Spatial analysis of poverty in guatemala: The case of alta verapaz department. *Economía, Sociedad y Territorio*, 16(51):291–322.

Vecchi, G. A., Soden, B. J., Wittenberg, A. T., Held, I. M., Leetmaa, A., and Harrison, M. J. (2006). Weakening of tropical pacific atmospheric circulation due to anthropogenic forcing. *Nature*, 441(7089):73–76.

Veneklaas, E. J., Zagt, R., Van Leerdam, A., Van Ek, R., Broekhoven, A., and Van Genderen, M. (1990). Hydrological properties of the epiphyte mass of a montane tropical rain forest, colombia. *Vegetatio*, 89:183–192.

Vicente-Serrano, S. M. and Beguería-Portugués, S. (2003). Estimating extreme dry-spell risk in the middle ebro valley (northeastern spain): a comparative analysis of partial duration series with a general pareto distribution and annual maxima series with a gumbel distribution. *International Journal of Climatology: A Journal of the Royal Meteorological Society*, 23(9):1103–1118.

Wang, C., Deser, C., Yu, J.-Y., DiNezio, P., and Clement, A. (2017). *El Niño and Southern Oscillation (ENSO): A Review*, pages 85–106. Springer Netherlands, Dordrecht.

Watson, L. and Dallwitz, M. J. (1999). *The families of flowering plants: descriptions, illustrations, identification, and information retrieval*. University of New Orleans New Orleans, LA.

Wertz-Kanounnikoff, S. and Rankovic, A. (2017). Climate, forests, and water: A synthesis of the scientific literature. *International Journal of Water Resources Development*, 33(6):848–861.

Williams, C., Malhi, Y., Nobre, A., Rastetter, E., Grace, J., Pereira, M., and Harper, A. (1998). Seasonal variation in net carbon exchange and evapotranspiration in a brazilian rainforest: a modelling analysis. *Plant, Cell & Environment*, 21(9):953–968.

Yan, Y. Y. (2005). *Intertropical Convergence Zone (ITCZ)*, pages 429–432. Springer Netherlands, Dordrecht.

Zhang, Y., Kong, D., Gan, R., Chiew, F. H., McVicar, T. R., Zhang, Q., and Yang, Y. (2019). Coupled estimation of 500 m and 8-day resolution global evapotranspiration and gross primary production in 2002–2017. *Remote sensing of environment*, 222:165–182.

Zimmermann, Meir, B. M. C. (2010). Temporal variation and climate dependence of soil respiration and its components along a 3000 m altitudinal tropical forest gradient. *Plant Ecology Diversity*.

Zotz, Hietz, S. (2010). On the extent and significance of epiphyllous liverworts and ferns in cloud forests. *Plant Ecology Diversity*.

A

Appendix: "Back of the envelope" Impact of Lowland Deforestation on Highland Water Balance

According to a global study on Moisture recycling by (97) around 25% to 30% of precipitation in the central highlands of Guatemala comes from evaporation over land. The average distance from Cobán to the ocean in the prevailing wind direction is 200km.

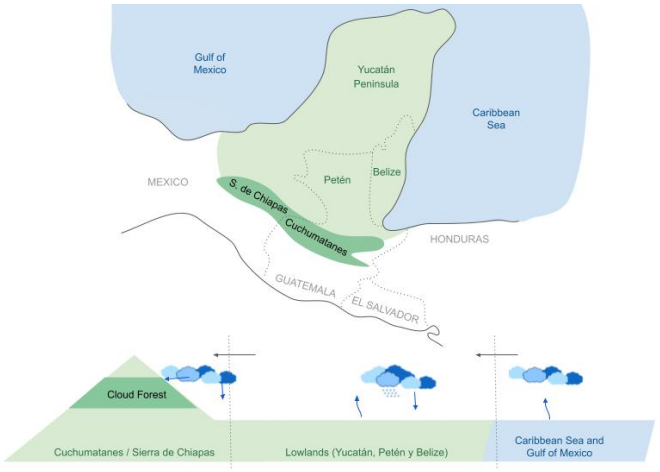

Figure A.1: Study area schematic.

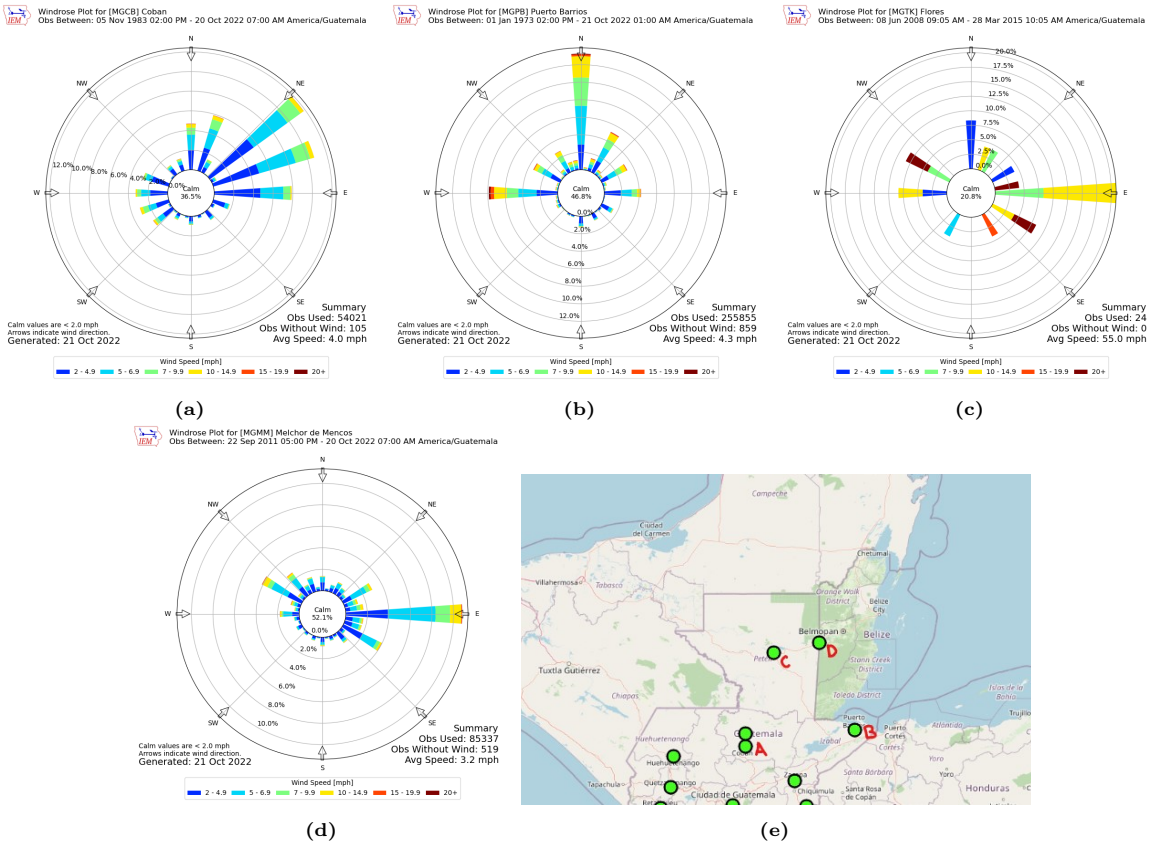

Figure A.2: Prevailing wind direction for (a) Cobán, and other cities upwind (b) Puerto Barrios, (c) Flores, (d) Melchor de Mencos

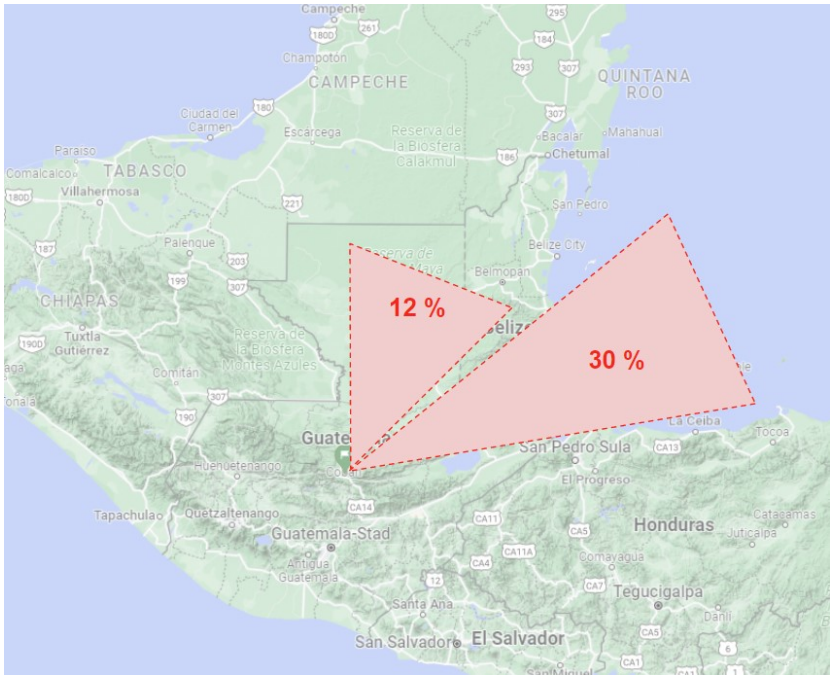

Figure A.3: Percent of time with wind coming from the dominant directions in Cobán.

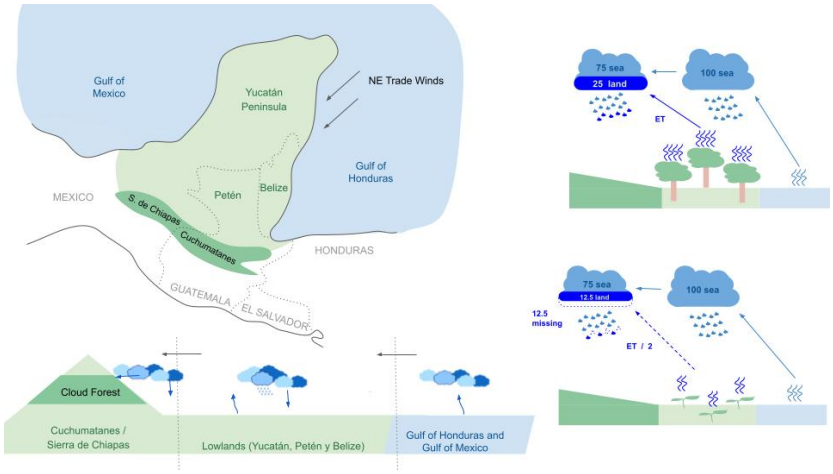

Figure A.4: Back-of-the-envelope approach schematic.

B

Appendix: Dry spell length by month

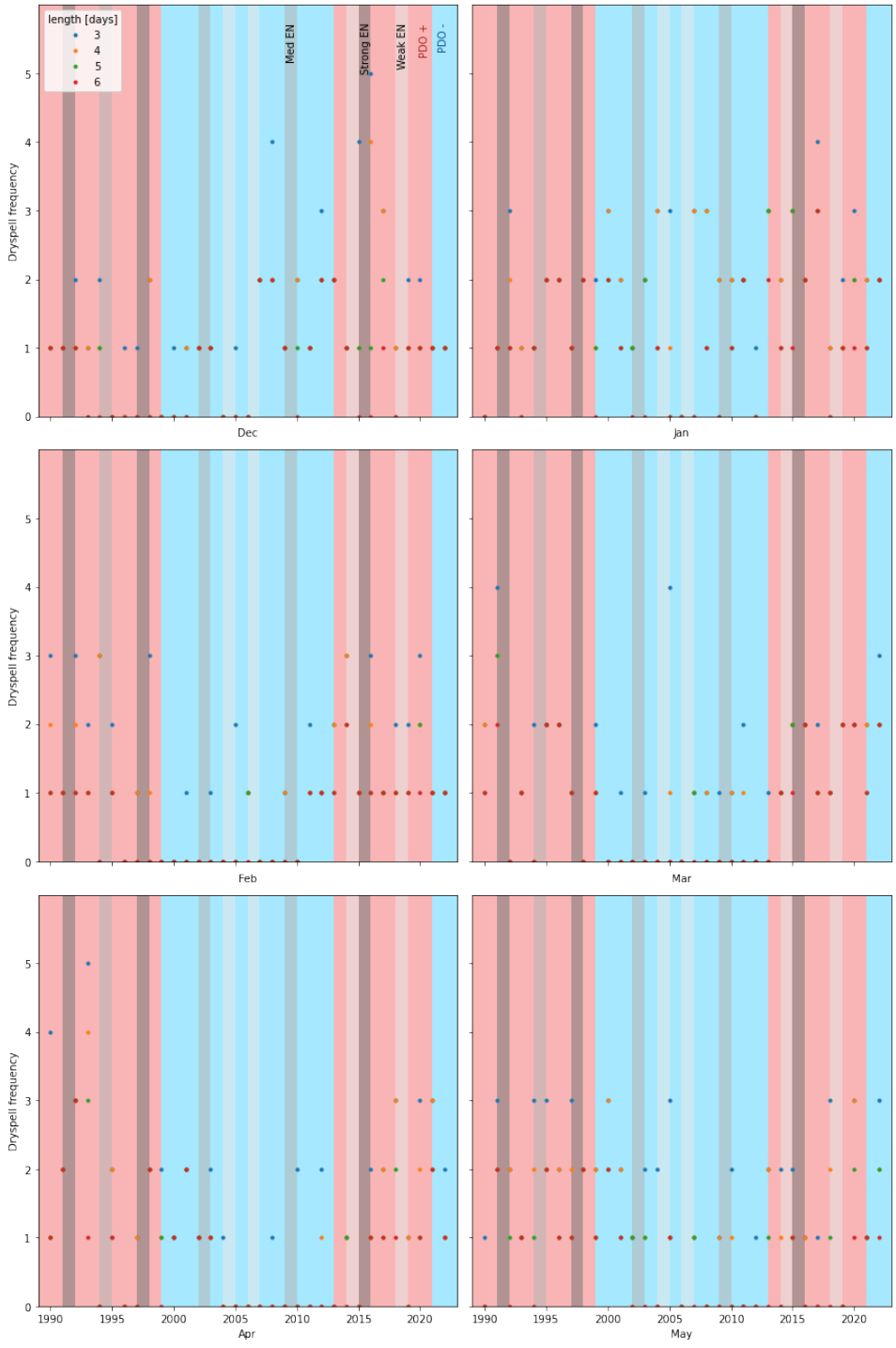

0.50

Figure B.1: Dry spell occurrence from December to May 1990-2022

C

Appendix: FIESTA Model Setup

FIESTA (Fog Interception for the Enhancement of Streamflow in Tropical Areas) by (69), is a spatially distributed model to calculate the fog interception potential of Cloud Forests, for this project we follow the same algorithms with some modifications:

.	**FIESTA**	**MDP Adaptation**
Spatial distribution	Grid (1x1km or 30x30m)	Lumped areas by elevation and slope aspect categories
Temporal distribution	Average values with monthly and daily fluctuations	Daily meteorological data with daily fluctuations

Acquire datasets

- Digital Elevation Model (DEM) from SRTM data downloader in QGIS
- Change in forest cover from 1991 to 2016 from IARNA. (46)
- Map of "Zonas de Vida" from IARNA
- Meteorological data from INSIVUMEH Cobán, Panzos and Cahabón

Geoprocessing QGIS

- Use SAGA geoprocessing tools to calculate the slope aspect from DEM.
- Classify DEM by elevation bands of 100 meter intervals, classify slope aspects in four directions, and create a grid based on the intersection between these layers.
- Use GRASS r.slope.aspect or SAGA to calculate slope, calculate average slope per grid cell
- Calculate 3D surface area as planimetric area / cosine(slope angle)
- Calculate the percentage of types of land use for each grid cell
-

Input Constants

- Droplet size, $DropletSize = 7.5$ um
- Drop terminal velocity, $DropTermVel = 9$ m/s
- Maximum Absolute Humidity $AH_{max} = 0.02717$
- Maximum Liquid Water Content $LWC_{max} = 0.0002$ kg/m3
- Leaf Area Index
  - $LAI_{TMCF} = 4.5$
  - $LAI_{Clear} = 2$
  - $LAI_{Pine} = 2.5$

- Leaf Self-shading (FIESTA uses the same values for all vegetation types, to be revised)
  - $LSS_{TMCF} = 2.1$
  - $LSS_{Clear} = 2.1$
  - $LSS_{Pine} = 2.1$
- Vegetation dimensions and properties
  - Average vegetation height in clear areas $Height_{Grass} = 0.5$ m
  - Average height of trees on forest edge $Height_{Edge} = 10$ m
  - Average height of emergent trees above canopy $Height_{Emergent} = 1.5$ m
  - Reduction factors for wind speed due to friction with the land surface, $ReductionFactor_{Grass} = 0.5030$, $ReductionFactor_{Forest} = 0.6053$

Input Spatial Variables

- Elevation [masl], $Elev$
- Slope
  - Slope angle [degrees], $Slope$
  - Slope Aspect Index, 1 = North, 2 = East, 3=South, and 4 = West, $Aspect$
- Area
  - Planimetric Area, $CellSize$
  - True Area, $Area3d$
- Land use fractions
  - Fraction that was clear for full time span (in this case, 1991-2016), $Frac_{clr}$
  - Fraction that was forested for full time span, $Frac_{frst}$
  - Fraction that was reforested during time span, $Frac_{refrst}$
  - Fraction that was deforested during time span, $Frac_{defrst}$

Input Meteorological Variable Timeseries, daily timestep

- Date, as $Year$, $Month$, Day
- Temperature [C], T_{avg}, T_{min}, T_{max}
- Relative Humidity [%], RH
- Cloud cover on a scale from 0 to 13 [-], Cld
- Radiation at each timestep during the day [W/m^2], $Rad24$, $Rad6$, $Rad12$, $Rad18$
- Wind speed [m/s] Wnd_spd and direction [degrees from North] Wnd_d
- Pressure [kPa], $Presh$
- Precipitation [mm], $Prcp$
- Open Water Evaporation [mm], $Epot$

Land use Scenarios

- Assume 2016 land use conditions are constant through time series, $no - dLULC$ or $Sc1$
- Remove all tree cover, $totaldeforestation$ or $Sc2$
- Cover all area with forest, $totalreforestation$ or $Sc3$
- Assume $dLULC - 1991 - 2016$ or $Sc4$

Model Functions

- Forest edge and emergent edge facing wind direction, these are the exposed edges of vegetation that can receive a fog impaction flux: $forestedgelenfacingm$ or $emergentedgelenfacingm$
- Sedimentation Surface Area, this is a function of fractions of land use, their LAI, and Leaf Self Shading, it returns the fraction of area on which fog can be deposited: $DepositionFrac$
- Transpiration Coefficient using Preistly-Taylor method, returns the Fraction of potential ET that will be intercepted by vegetation, ET_Frac

$$FogSettlingVel = \frac{980 * \frac{DropletSize}{10000}^2 * (1 - 0.0013)}{18 * 0.000185} \tag{C.1}$$

- Fog Settling Velocity is derived from Stokes Law in FIESTA as a function of the droplet size, which in this model is constant (= 7.5 um), in $FogSettlingVel = 0.165$ m/s

$$FogSettlingVel = \frac{980 * \frac{DropletSize}{10000}^2 * (1 - 0.0013)}{18 * 0.000185} \tag{C.2}$$

- Temperatures for 6-hour time steps, fog interception is calculated in 6-hour intervals at 24h, 6h, 12h and 18h.

$$T_{diurnalrange} = T_{max} - T_{min} \tag{C.3}$$

$$T_{24h} = T_{avg} - \frac{T_{diurnalrange}}{4} \tag{C.4}$$

$$T_{6h} = T_{avg} \tag{C.5}$$

$$T_{12h} = T_{avg} + \frac{T_{diurnalrange}}{4} \tag{C.6}$$

$$T_{18h} = T_{avg} \tag{C.7}$$

- Saturated Vapour Pressure

$$Es = \exp 26.66082 - 0.0091379024 * (Tmp + 273.15) - \frac{6106.396}{Tmp + 273.15} \tag{C.8}$$

$$E = \frac{RH}{100} * Es \tag{C.9}$$

- Air Density in kg/m3

$$AirDensity = \frac{Presh * 100}{(Tmp + 273.15) * 287} \tag{C.10}$$

- Absolute Humidity

$$AH = \frac{E * 100}{(Tmp + 273.15) * 461.5} \tag{C.11}$$

- Liquid Water Content, FIESTA models liquid water content as a fraction of the maximum Liquid Water Content proportional to the absolute humidity at the timestep over maximum absolute humidity.

$$LWC = \frac{AH}{AH_{max}} * LWC_{max} \tag{C.12}$$

- Dewpoint

$$T_d = \frac{((26.66082 - log(E)) - \sqrt{((26.66082 - log(E))^2) - 223.1986}}{0.0182758048} - 273.15 \tag{C.13}$$

- Lifting Condensation Level LCL and fog presence fog, FIESTA applies a formula proposed by (33) for the pressure of the lifting condensation level, then this is converted to meters with a formula from the 1976 ISA model.

$$P_{LCL} = \frac{1}{\frac{Tmp - T_d}{223.15}}^{3.5} * P_{surface} \tag{C.14}$$

$$Z_{LCL} = max(44.3308 - 4.94654 * (P_{LCL} * 100)^{0.190263} * 1000, 0) \tag{C.15}$$

$$fog = if(Z_{LCL} < Elev, 1, 0) \tag{C.16}$$

- Effective Solar Radiation function reduces incoming radiation by a proportion of the cloud frequency factor.
- Net Radiation, following the empirical relationship described in FIESTA for Solar to Net Radiation for different types of land cover.
- Adjustment to wind speed and direction, the speed is reduced by 50% if the slope aspect is parallel to the wind direction and by 90% if it is opposite. Wind direction is adjusted from an angle w.r.t North to the angle w.r.t the slope aspect, this returns $Wind_{spd,adj}$ and $Wind_{dir,adj}$
- Precipitation Correction for slope

$$TanRainInclination = \frac{Wind_{spd,adj}}{DropTermVel} \tag{C.17}$$

$$CorrectionFactor = max(1 + Slope * TanRainInclination * cos(Wind_{dir,adj}), 0) \tag{C.18}$$

$$Prcp_{corrected} = Prcp * CorrectionFactor \tag{C.19}$$

- Edge Impaction FLux, the total amount of moisture impacting the vegetation edges in a grid cell

$$WindFlux_{Edge} = (Wind_{spd,adj} * ReductionFactor_{Forest} * 3600) * ForestEdgeLenFacing * Height_{Edge} \tag{C.20}$$

$$ImpactionFlux_{Edge} = LWC * WindFlux_{Edge} \tag{C.21}$$

$$WindFlux_{Emergent} = (Wind_{spd,adj} * 3600) * EmergentEdgeLenFacing * Height_{Emergent} \tag{C.22}$$

$$ImpactionFlux_{Emergent} = LWC * WindFlux_{Emergent} \tag{C.23}$$

- Fog Interception (Deposition and Impaction FLuxes)

$$FogInclination_{Pasture} = \frac{atan(Wind_{spd,adj} * ReductionFactor_{Grass})}{FogSettlingVel} \tag{C.24}$$

$$FogInclination_{Forest} = \frac{atan(Wind_{spd,adj} * ReductionFactor_{Forest})}{FogSettlingVel} \tag{C.25}$$

$$DepositionProportion = cos(FogInclination_{Forest}) * Frac_{Tree} + cos(FogInclination_{Pasture}) * (1 - Frac_{Tree}) \quad \text{(C.26)}$$

$$ImpactionProportion = 1 - DepositionProportion \quad \text{(C.27)}$$

$$GravityFlux = FogSettlingVel * 3600 * Area3d \quad \text{(C.28)}$$

$$SettlingFlux = LWC * GravityFlux \quad \text{(C.29)}$$

$$Interception_{deposition} = fog * SettlingFlux * DepositionProportion * DepositionFraction \quad \text{(C.30)}$$

$$WindFlux_{Grass} = Wind_{spd,adj} * ReductionFactor_{Grass} * 3600 * (1 - Frac_{Tree}) * CellSize * height_{Grass} \quad \text{(C.31)}$$

$$ImpactionFlux_{Grass} = LWC * WindFLux_{Grass} \quad \text{(C.32)}$$

$$ImpactionFraction = AirRising * ForestTrappingSurfaceArea \quad \text{(C.33)}$$

$$ImpactionFlux_{total} = ImpactionFlux_{Emergent} + ImpactionFlux_{Edge} + ImpactionFlux_{Grass} \quad \text{(C.34)}$$

$$Interception_{impaction} = fog * ImpactionFlux_{total} * ImpactionProportion + ImpactionFraction \quad \text{(C.35)}$$

$$Fog_{interception} = Interception_{deposition} + Interception_{impact} \quad \text{(C.36)}$$

$$Fog_{interception,mm} = \frac{Fog_{interception}}{Area3d} * Cld \quad \text{(C.37)}$$

Calculation for expected input on the 26th of January at our fieldwork site

- Inputs
  - Area = 1 ha
  - Slope = 45 degrees, Aspect = north facing
  - Land Use fractions = 0.5 TMCF, 0.5 Clear
  - Elevation = 2070 masl
  - Temperature max = 13.2 C, min = 9.5 C, avg = 11.2 C
  - Relative Humidity = 99

  - Pressure = 1025 hPa
  - Cloud cover = 100 %
  - Radiation, $Rad24 = 0$, $Rad6 = 10$, $Rad12 = 245$, $Rad18 = 10$
  - Wind, $Wnd_spd = 5$ m/s $Wnd_d = 0$ degrees from North
  - Precipitation, $Prcp = 0$ mm

- Result

  - For the conditions on January 26, with LWC based on rising humidity forming at lifting condensation level, the model resulted in fog interception of 1.65 mm /day
  - Given that the clouds present on the 26th were not only from humidity rising locally, but the estimated LWC may also be lower than reality, and upper bound to possible fog interception was found by applying a liquid water content of .25 g/m3, this resulted in fog interception of 4.28 mm /day

Cahabón Fog Capture Model

Analysis Set up

This calculation of Fog Interception is based on the model developed by Mark Mulligan and Sophia Burke for FIESTA (Fog Interception for the Enhancement of Streamflow in Tropical Areas). Mulligan, M. and Burke, S. (2005). Fiesta fog interception for the enhancement of streamflow in tropical areas final technical report for kcl/amibiotek contirbution to dfid frp project r799. (https://www.researchgate.net/publication/237574142_Final_Technical_Report_DFID-FRP_Project_no_R7991_Hydrological_impacts_of_converting_tropical_montane_cloud_forest_to_pasture_with_initial_reference_to_northern_Costa_Rica)

Data

INSIVUMEH - Meteorological data from Estación Cobán 1991-2022. Retreived from public information request to INSIVUMEH via email

Libraries

In [179…

```
import numpy as np
import matplotlib.pyplot as plt
from matplotlib.pyplot import cm
import datetime
import math
import pandas as pd
#colors https://www.webucator.com/article/python-color-constants-module/
```

Constants

In [180…

```
#Constants
MSLP = 1 #[mb] Mean sea level pressure
kWh_MJ = 3.6 #Conversion from kWh to MJ multiply
SecondsInMonth = np.array([2678400, 2419200, 2678400, 2592000, 2678400, 2592000, 2678400, 2678400, 2592000, 2678400, 2592000, 2678400, 2505
droplet_size = 7.5 #dorplet size  [um]
DropTermVel = 9 #m/s. Average terminal velocity of raindrop. TBD --> adjust depending on cloud height and type of rain.
#Define LAI of each land use:
LAI_TMCF = 4.5
LAI_Clear = 2
LAI_Pine = 2.5
#Leaf Self Shading for each land use
lss_TMCF = -0.7 * 0.3 * 10
lss_Pine = -0.7 * 0.3 * 10
lss_Clear  = -0.7 * 6.0 *  0.5
```

Functions

In [182…

```python
def LULC_scenario(scenario, LUclass_len, ts_len, Frac_clr, Frac_defrst, Frac_frst, Frac_refrst):
    # 2016 Conditions, No Land Use Change
    if scenario == 'no_dLULC':
        TreeFrac    = np.zeros([LUclass_len, ts_len])
        FracClear   = np.zeros([LUclass_len, ts_len])
        FracTMCF    = np.zeros([LUclass_len, ts_len])
        FracPine    = np.zeros([LUclass_len, ts_len])
        for k in range(LUclass_len):
            FracClear[k, :]   = Frac_clr[k] + Frac_defrst[k]
            FracTMCF[k, :]    = Frac_frst[k]
            FracPine[k, :]    = Frac_refrst[k]
        TreeFrac = FracTMCF + FracPine

    #Complete Deforestation, No Land Use Change
    if scenario == 'totaldeforestation':
        TreeFrac    = np.ones([LUclass_len, ts_len]) * 0.05
        FracClear   = np.ones([LUclass_len, ts_len]) * 0.95
        FracTMCF    = np.ones([LUclass_len, ts_len]) * 0.025
        FracPine    = np.ones([LUclass_len, ts_len]) * 0.025

    #Complete Reforestation, No Land Use Change
    if scenario == 'totalreforestation':
        TreeFrac    = np.ones([LUclass_len, ts_len]) * 0.975
        FracClear   = np.ones([LUclass_len, ts_len]) * 0.025
        FracTMCF    = np.ones([LUclass_len, ts_len]) * 0.95
        FracPine    = np.ones([LUclass_len, ts_len]) * 0.025

    #Gradual Change in Deforestation and Reforeattion from 1991 to 2016 (real conditions)
    if scenario == 'dLULC_1991_2016':
        # t0
        #    --> FracClear = Frac_clr + Frac_reforested
        #    --> FracPine  = 0
        #    --> TreeTMCF  = Fracfrst
        #    --> TreeFrac  = FracTMCF + FracPine
        # t_end
        #    --> FracClear = Frac_clr + Frac_deforested
        #    --> FracPine  = Frac_reforested
        #    --> TreeTMCF  = Fracfrst - Frac_deforested
        #    --> TreeFrac  = FracTMCF + FracPine

        FracClear   = np.zeros([LUclass_len, ts_len])
        FracTMCF    = np.zeros([LUclass_len, ts_len])
        FracPine    = np.zeros([LUclass_len, ts_len])

        for k in range(LUclass_len):
            #At t = 0
            frac0_Clear = Frac_clr[k]
            frac0_TMCF  = Frac_frst[k]
```

```
            frac0_Pine  = 0
            #At t = end
            fracN_Clear = Frac_clr[k] + Frac_defrst[k]
            fracN_TMCF  = Frac_frst[k] - Frac_defrst[k]
            fracN_Pine  = Frac_refrst[k]
            for i in range(ts_len):
                FracClear[k,i] = frac0_Clear + (fracN_Clear - frac0_Clear) / ts_len * i
                FracTMCF[k,i]  = frac0_TMCF  + (fracN_TMCF  - frac0_TMCF)  / ts_len * i
                FracPine[k,i]  = frac0_Pine  + (fracN_Pine  - frac0_Pine)  / ts_len * i
        TreeFrac = FracTMCF + FracPine
    return FracClear, FracTMCF, FracPine, TreeFrac

def Forest_Edge(Treefraction, Cellarea):
    #FIESTA = The formula relates two different grid cell size due to the data sources used in FIESTA,
    #         this is not necessary in our model.
    #         forestedgefrac = -3 * 10 ** (-5) * Treefraction ** 2 + 0.0036 * Treefraction
    #         forestedgelenm = forestedgefrac * ((Cellarea ** 2)/(25 * 25)) * 100
    #         emergentedgelenm = (0.05 * Treefraction)*((Cellarea ** 2)/(25 * 25)) * 100 #calculated as 5% of fraction of area covered by t
    #         forestedgelenfacingm = forestedgelenm / 4
    #         emergentedgelenfacing = emergentedgelenm / 4
    #MDP =
    forestedgefrac = -0.0001 * ((Treefraction*100) ** 2) + 0.0144 * (Treefraction*100) #From Figure 59, (Mulligan & Burke, 2005)
    forestedgelenm = forestedgefrac * np.sqrt(Cellarea) * 4 #edge faction in a fraction of the total edge of the cell.
    emergentedgelenm = (0.05 * Treefraction) * np.sqrt(Cellarea) * 4
    forestedgelenfacingm = forestedgelenm / 4
    emergentedgelenfacingm = emergentedgelenm / 4
    # Output units = meters
    return forestedgelenfacingm, emergentedgelenfacingm

def Sedimentation_Surface_Area(Frac_frst, Frac_clr, Frac_pine, LAI_frst, LAI_clr, LAI_pine, lss_frst, lss_pine, lss_clr):
    #Sedimentation Surface area
    # F = Key assumption : That the whole unshaded (one sided) leaf surface area is available for sedimentation (deposition)
    #Surface area for each land use:
    #FIESTA uses these constants:
    #lss_frst = -0.7 * 0.3 * 10, leaf self shading forest
    #lss_pine = -0.7 * 0.3 * 10, leaf slef shading pine
    #lss_clr  = -0.7 * 6.0 *  0.5, leaf self shading clear
    TrappingSfcArea_frst = (1 - (np.exp(lss_frst)))
    TrappingSfcArea_pine = (1 - (np.exp(lss_pine)))
    TrappingSfcArea_clr = (1 - (np.exp(lss_clr)))
    #Total deposition area per grid cell
    DepositionFrac = (Frac_frst * TrappingSfcArea_frst * LAI_frst) + (Frac_pine * TrappingSfcArea_pine * LAI_pine) + (Frac_clr * TrappingSf
    # Output Units = Fraction
    return DepositionFrac

def ET_LU(Frac_frst, Frac_clr, Frac_pine, LAI_frst, LAI_clr, LAI_pine):
    #Intercepted Energy Fractions
    # Key assumption : That evapotranspiration is effectively modelled at
```

```
    # this coarse spatial and temporal scale from consideration of energy
    # availablility and atmospheric demand for water only. Leaf area is
    # sufficient to represent plant processes and aerodynamic resistances can safely be ignored.
    ExpLAI_frst = 1-np.exp(-0.7*max(1,LAI_frst))
    ExpLAI_pine = 1-np.exp(-0.7*max(1,LAI_pine))
    ExpLAI_clr  = 1-np.exp(-0.7*max(1,LAI_clr))

    EtFrac_frst = Frac_frst * ExpLAI_frst
    EtFrac_pine = Frac_pine * ExpLAI_pine
    EtFrac_clr  = Frac_clr  * ExpLAI_clr

    EtFrac_total = EtFrac_frst + EtFrac_pine + EtFrac_clr

    # Output Units = Fraction
    return EtFrac_total

def FogSettlingVel(droplet_size):
    #Fog Settling
    #Eq 2. FIESTA =  That fog settling occurs under calm conditions and upwards fog
    #          turbulent diffusion is limited compared with this downward flux,
    #          Fog settling velocity is calculated according to Stokes Law based
    #          on the mean particle size for fog.
    # MDP   =  Same as FIESTA, Stokes law
    FogSettlingVel = (980 * ((droplet_size/10000)**2)*(1-0.0013))/(18*0.000185)
    # Output units = m/s
    return FogSettlingVel

def T_elev_shift(Elev_cell, T_var_C=-0.6, Elev_station=1320):
    # Temperature
    # INSIVUMEH
    # FIESTA = regular diurnal range variation.
    # MDP    = same as FIESTA.
    #T_var_C = -0.6 C/100m
    T_shift = (Elev_cell - Elev_station) * T_var_C / 100
    return T_shift

def Temps(Hour, T_max, T_min, T_mean_in, Elev):
    # Inputs:
    #       - Hour = 1, 2, 3, or 4: the four timesteps through the day.
    #       - T_max, T_min, T_mean = Read from INSIVUMEH
    #       - T_shift = change in temperature for cell's elevation band
    # Output:
    #       - Tmp = Temperature at time step, adjusted for elevation
    #T_mean = T_mean_in + T_elev_shift(Elev, T_var_C=-0.6, Elev_station=1320)
    T_mean = T_mean_in
    DiurnalTRange = T_max-T_min
    if(Hour == 1):
        Tmp = T_mean - 0.25 * DiurnalTRange
```

```
        AirRising = 0
    elif (Hour == 2):
        Tmp = T_mean
        AirRising = 1
    elif (Hour == 3):
        Tmp = T_mean + 0.25 * DiurnalTRange
        AirRising = 1
    else:
        Tmp = T_mean
        AirRising = 0
    #Output Units = Degrees Celsius
    return Tmp, AirRising

def Saturated_vapur_press(Tmp, RH):
    # Dewpoint
    # Inputs:
    #       - Tmp = tamperature (C)
    #       - RH = relative humidity (%)
    # Outputs:
    #       - Es = saturated vapour pressure (mb)
    #       - E  = vapour pressure (mb)
    Es = np.exp(26.66082-0.0091379024*(Tmp + 273.15)-(6106.396/(Tmp+273.15))) #Saturated Vapour Pressure (mb)
    E = (RH/100)*Es #Vapour Pressure (mb)
    # Output units = mb
    return E


def Air_density(MSLP, Tmp, E):
    # Air Density
    # Inputs:
    #      - MSLP = mean sea level pressure (mb)
    #      - Tmp  = Temperature
    #      - E    = Vapour Pressure
    # Outputs:
    #      -
    AirDensity = (MSLP*100)/((Tmp+273.15)*287) #Air density [kg/m3]
    AH = (E*100)/((Tmp+273.15)*461.5) #Absolute humidity [kg/m3]
    # Output units = Air density [kg/m3],
    return AirDensity, AH

def LiqWaterContent(AH_n, AH_max, maxLWC=0.0002):
    # Liquid Water Content
    # Cloud liquid water content is proportional to absolute atmospheric humidity.
    # maxLWC = 0.0002 #usually observed maximum AH [kg/m3]
    LWC = (AH_n/AH_max)* maxLWC
    # Output Units = kg/m3
    return LWC
```

```
def Dewpoint(E):
    #Function to calculate Dewpoint Temperature (Td) [C]
    # Inputs:
    #       - E = Vapour Pressure [mb]
    # Outpouts:
    #       - Td = Dew Point Temperature [C]
    btemp = 26.66082 - np.log(E)
    Td    = ((btemp-np.sqrt((btemp**2)-223.1986))/0.0182758048)-273.15
    # Output Units = Degrees Celsius
    return Td

def LiftingCondensationLevel(Tmp, Td, MSLP, Elevation):
    # Function to calculate Lifting Condensation Level (LCL) [m]
    # Inputs:
    #      - Tmp = Ground Temperature [C]
    #      - Td  = Dew point temperature [C]
    # Outputs:
    #      - LCL = Lifting Condensation Level [masl]
    #      - fog = Presence of fog (0 or 1) [-]
    LCL_mb = (1/(((Tmp-Td)/223.15)+1)**3.5)*MSLP
    LCL_masl   = max((44.3308-4.94654*((LCL_mb*100)**0.190263))*1000, 0)
    if (LCL_masl < Elevation):
        fog = 1
    else:
        fog = 0
    return LCL_masl, fog

def EffectiveSolarRad(CloudFreqFrac, fog, SolarR_toa):
    if(fog==1):
        TransmissionLoss = (CloudFreqFrac*0.678)+((1-CloudFreqFrac)*-0.143)
    else:
        TransmissionLoss = (CloudFreqFrac*0.525)+((1-CloudFreqFrac)*-0.143)
    SolarR_ground = SolarR_toa * (1 - TransmissionLoss)
    #Output units = W/m2
    return SolarR_ground

def NetRad(SolarR_ground, Frac_frst, Frac_pine, Frac_clr, Month, LR, SecondsInMonth):
    # Key assumption from FIESTA: The solar to net radiation conversion functions measured under
    #   forest and grassland are representative for larger areas and other covers of similar density.
    SIM = SecondsInMonth[int(Month)]
    if (Month == 2) and (LR == 1): #February, Leap Year
        SIM = SecondsInMonth[12]
    #Some empirical constants from FIESTA -->
    #Based on the linear relationship between solar and net radiation for forest and field sites in the study location in CR.
    FIESTA_C_tree_b = -27.9
    FIESTA_C_tree_m = 0.9
    FIESTA_C_clr_b  = -27.5
    FIESTA_C_clr_m  = 0.8
```

```
    SolarWm = SolarR_ground #(SolarR_ground*1000000)/(SIM/2) #This is the function from FIESTA, but their input is in MJ, our input is kWh
    #SolarWm = SolarR_ground / 3600
    NetMap_frst = ((Frac_frst)*(FIESTA_C_tree_b+(FIESTA_C_tree_m*SolarWm)))
    NetMap_pine = ((Frac_pine)*(FIESTA_C_tree_b+(FIESTA_C_tree_m*SolarWm)))
    NetMap_clr  = ((Frac_clr) *(FIESTA_C_clr_b +(FIESTA_C_clr_m *SolarWm)))
    NetMap  = NetMap_frst +  NetMap_pine + NetMap_clr
    return NetMap

def WindSpeed(Wind_d, Wind_spd, Aspect):
    #Not following FIESTA.
    aspect_dir = [[1, 315, 45], [2, 45, 135], [3, 135, 225], [4, 225, 315]] #slope aspect and bounding angles for perpendicular wind
    #Key Assumption: perpendicular aspect = 100%, parallel aspect = 50%, opposite aspect = 1
    factor_perp = 1
    factor_par  = 0.5
    factor_opp  = 0.1
    if (Wind_d > aspect_dir[int(Aspect)-1][1] and Wind_d < aspect_dir[int(Aspect)-1][1]):
        Wind_spd_adj = Wind_spd * factor_perp
        Wind_dir_adj   = 0
    elif Wind_d > (aspect_dir[int(Aspect)-1][1]-90) and Wind_d < aspect_dir[int(Aspect)-1][2] or Wind_d > (aspect_dir[int(Aspect)-1][2]) an
        Wind_spd_adj = Wind_spd * factor_par
        Wind_dir_adj   = 45
    else:
        Wind_spd_adj = Wind_spd * factor_opp
        Wind_dir_adj   = 90
    # Wind Speed - Next steps:
    #   - Set wind exposure at higher elevations, due to prevailing wind direction perpendicular to catchment valley.
    #   - Interpolate Cobán and Panzos weather station wind directions.
    #   - Apply daily variation based on average daily range from ICOBN4 weather station
    #Output units = m/s
    return Wind_spd_adj, Wind_dir_adj

def RainMod(Prec, Wind_spd_adj, Wind_dir_adj, slope, DropTermVel):
    # Same as Fiesta Eq 15
    TanRainInclination = 0
    if Prec > 0:
        TanRainInclination = Wind_spd_adj/DropTermVel
        check = 1 + slope * TanRainInclination * math.cos(Wind_dir_adj)
        WindSlopeCorrectionFactor = max(check,0)
    else:
        TanRainInclination = 0
        WindSlopeCorrectionFactor = 0
    Prec_corrected = Prec * WindSlopeCorrectionFactor
    #Output
    return Prec_corrected

def EdgeImpactFlux(Wind_spd_adj, forestedgelenfacingm, emergentedgelenfacingm, LWC):
    #Copied from FIESTA
    #Eq 16. This equation calculates the kg/hr/cell of water passing through forest edges.
```

```
    reduc_factor = 0.6053 # is a factor which reduces wind speeds as a result of frictional losses with the forest
                        #  and is calculate from comparison of forest and pasture site vertical wind profiles.
    H_mean_forest_edge = 10 # represents the mean height of forest edges (10m)
    H_mean_emergent = 1.5 #is the average height of emergents above the surrounding canopy (1.5m)
    WindFlux_Edg = (Wind_spd_adj*reduc_factor*3600)*forestedgelenfacingm * H_mean_forest_edge
    EdgeImpactionFlux = LWC * WindFlux_Edg
    WindFlux_Emrg = (Wind_spd_adj*3600)*emergentedgelenfacingm * H_mean_emergent
    EmergentImpactionFLux = LWC * WindFlux_Emrg
    #Output units = kg/hr/gridcell
    return  EdgeImpactionFlux, EmergentImpactionFLux

def FogDeposition(Wind_spd_adj, TreeFrac, CellSize, LWC, FogSettlingVel, CellTrueArea, EdgeImpactionFlux, EmergentImpactionFlux, AirRising,
    #Copied from FIESTA
    #Eq 17. A fog inclination angle for fog inputs over forest and pasture is calculated, based on
    #       their respective wind speeds. A vertical flux is calculated as the fog settling velocity
    #       over the whole cell surface area (rather than any vertical catching surfaces). proportion
    #       of fog inputs that are deposited rather than impacted depends upon the cosine of the fog
    #       inclination angle over grassland and forest fractions.

    #Angles
    reduc_factor_forest = 0.6053 # is a factor which reduces wind speeds as a result of frictional losses with the forest
    reduc_factor_grass = 0.5030 # is a factor which reduces wind speeds as a result of frictional losses with the pasture
    ForestFogInclinationAngle = math.atan((Wind_spd_adj * reduc_factor_forest)/FogSettlingVel)
    PastureFogInclinationAngle = math.atan((Wind_spd_adj * reduc_factor_grass)/FogSettlingVel)
    #Proportions of Deposition vs Impaction
    DeposProportion = ((math.cos(ForestFogInclinationAngle))*TreeFrac)+((math.cos(PastureFogInclinationAngle))*(1-TreeFrac))
    ImpactionProportion = 1 - DeposProportion


    #Total Deposition
    #Settling
    GravityFlux = (FogSettlingVel*3600)*CellTrueArea
    SettlingFlux = LWC * GravityFlux #[kg/gridcell]
    DeposInterc = fog * ( SettlingFlux * DeposProportion) * DepositionFrac

    #Eq 18. Vegetation Areas for Fog Interception
    #Grass
    Grass_height = 0.5
    WindFLux_Dep_Grass = (Wind_spd_adj*reduc_factor_grass*3600)*(1-TreeFrac)*CellSize*Grass_height
    GrassImpactionFlux = LWC * WindFLux_Dep_Grass #Units = [kg/cell]

    # AirRising
    # In FIESTA, the parameter AirRising is true for situation where upwind elevations are greater than the downwind cell
    # In this adaptation, because mountain breeze dominates over the prevailing wind,AirRising is true during the day and false at night
    ForestTrappingSfcArea = (1-np.exp((-0.7*0.3*(TreeFrac))/math.cos(ForestFogInclinationAngle)))
    PastureTrappingSfcArea = (1-np.exp((-0.7*6*(1-(TreeFrac)))/math.cos(PastureFogInclinationAngle)))
    #Impaction Flux
    ImpactionFrac = (AirRising * ForestTrappingSfcArea)
```

```
    ImpactionFlux = (EmergentImpactionFlux + EdgeImpactionFlux + GrassImpactionFlux)
    ImpactionInterc = fog * (ImpactionFlux * ImpactionProportion) * ImpactionFrac

    #Total Fog FLux
    FogInterc = DeposInterc + ImpactionInterc #kg/m2/hr
    FogIntmm = (FogInterc/CellTrueArea)*(CloudFreqFrac)

    return FogIntmm

def Evap(NewTemp, NetMap, EtFrac_total):
    #Copied from FIESTA
    #Eq 21 = Thus evaporation is calculated on the basis of available energy and atmospheric
    #        demand to give potential evaporation and this is then combined with the non self
    #        shaded surface area available for the interception of radiation/evaporation of water to
    #        give something closer to actual evaporation, which is responsive to vegetation type
    #        and cover as well as climate conditions
    #Input Variables:
    #        NewTemp = Air temp
    #        NetMap = Radiation [W/m2]
    #Output Variables:
    #       ActEvap = Actual Evaporation
    lat_hvap = 2.45 #Latent Heat of Vaporization [MJ/kg]
    Ea = (611 * np.exp((17.27 * NewTemp)/(273.15+NewTemp)))/1000 #Vapor Pressure in [KPa]
    SlopeSatCurveK = (4098*Ea)/((273.15+NewTemp)**2) #Slope of the Saturation Vapour Pressure Curve [KPaC]
    PotEvap_m_d = (SlopeSatCurveK/(SlopeSatCurveK+0.066))*NetMap
    PotEvap = PotEvap_m_d * (60 * 60 / 1000000)
    if PotEvap > 0:
        PotEvap_adj = PotEvap / lat_hvap
        ActEvap = PotEvap_adj * EtFrac_total
    else:
        PotEvap_adj = 0
        ActEvap = 0
    return ActEvap

def Budgets(Prec, FogIntmm, ActEvap):
    #Copied from FIESTA
    #Eq. 22
    Budget = ((Prec + FogIntmm)-ActEvap)
    return Budget


#Monthly, Hourly, Slope Variations for Solar Radiation
rad_vars   = np.loadtxt('solar_rad_slope_scaling.csv', delimiter=',')
# The solar radiation data for 4 time steps in the time series file is
# for south facing slopes, for N, E amd W, the values must be mutliplied by scaling factors in this file
# Data columns--> (E, W, N, S) * (24, 6, 11, 17)
#          E    E       E       E       W       W       W       W       N       N       N       N       S       S       S       S
#         24    6       11      17      24      6       11      17      24      6       11      17      24      6       11      17
```

```
# Data rows --> Jan to Dec
#         J     F       M       A       M       J       J       A       S       O       N       D
#Fill arrays with values, radS * scalar.
def rad_EWN(rad_S, Month):
    #Building Solar Radiation Arrays for each slope direction:
    rad_E = np.zeros(np.shape(rad_S))
    rad_W = np.zeros(np.shape(rad_S))
    rad_N = np.zeros(np.shape(rad_S))
    rad = np.zeros(np.shape(rad_S))
    for i in range(len(rad_S)):
        for j in range(4):
            rad_E[i, j] = rad_S[i, j] * rad_vars[int(Month[i])-1, j] * kWh_MJ
        for j in range(4,8):
            rad_W[i, j] = rad_S[i, j] * rad_vars[int(Month[i])-1, j] * kWh_MJ
        for j in range(8,12):
            rad_N[i, j] = rad_S[i, j] * rad_vars[int(Month[i])-1, j] * kWh_MJ
        for j in range(12,16):
            rad_S[i, j] = rad_S[i, j] * rad_vars[int(Month[i])-1, j] * kWh_MJ
    return rad_E, rad_W, rad_N, rad_S
```

Inputs: Meteorology from INSIVUMEH

In [183…

```
INSIVUMEH_Coban_in = np.loadtxt('INSIVUMEH_Meteo.csv', delimiter=',')
#Año    Mes     Día     LR      T_max   T_min   T_mean  Rh      CloudFrac13     Rad24   Rad6    Rad12   Rad18
# Wind_d        Wind_v  Press   ENSO    Precip  EvapPot

INSIVUMEH_Coban = INSIVUMEH_Coban_in[3256:-1, :]
ts_len = len(INSIVUMEH_Coban)
Year  = INSIVUMEH_Coban[:, 0]
Month = INSIVUMEH_Coban[:, 1]
Day   = INSIVUMEH_Coban[:, 2]
LR    = INSIVUMEH_Coban[:, 3]
T_max = INSIVUMEH_Coban[:, 4]
T_min = INSIVUMEH_Coban[:, 5]
T_avg = INSIVUMEH_Coban[:, 6]
RH    = INSIVUMEH_Coban[:, 7]
Cld   = (INSIVUMEH_Coban[:, 8])/13
Rad24 = INSIVUMEH_Coban[:, 9]
Rad6  = INSIVUMEH_Coban[:, 10]
Rad12 = INSIVUMEH_Coban[:, 11]
Rad18 = INSIVUMEH_Coban[:, 12]
Wnd_d = INSIVUMEH_Coban[:, 13]
Wnd_spd = INSIVUMEH_Coban[:, 14]
Presh_in = INSIVUMEH_Coban[:, 15]
Presh = (Presh_in - (113)) * 1.333223874 #Shifting and converting to mb
ENSO  = INSIVUMEH_Coban[:, 16]
```

```
Prcp  = INSIVUMEH_Coban[:, 17]
Epot  = INSIVUMEH_Coban[:, 18]
```

Inputs: Topography data based on Slope Aspect, Elevation and Land Use Change Classification

In [184…

```
#Gridcells
Gridcells = np.loadtxt('QGIS_LandClass_fracs.csv', delimiter=',')
LUclass_len = len(Gridcells)
#Elev   Aspect  Area    Area3D  Slope   Frac_clr        Frac_frst       Frac_refrst     Frac_defrst
Elev        = Gridcells[:,0]
Aspect      = Gridcells[:,1]
CellSize    = Gridcells[:,2]
Area3d      = Gridcells[:,3]
Slope       = Gridcells[:,4]
Frac_clr    = Gridcells[:,5]
Frac_frst   = Gridcells[:,6]
Frac_refrst = Gridcells[:,7]
Frac_defrst = Gridcells[:,8]
```

LULC Scenarios

In [198…

```
#scenario = 'no_dLULC'
#scenario = 'totaldeforestation'
#scenario = 'totalreforestation'
scenario = 'dLULC_1991_2016'
```

In [199…

```
FogSettlingVelocity = FogSettlingVel(droplet_size)
FracClear, FracTMCF, FracPine, TreeFrac = LULC_scenario(scenario, LUclass_len, ts_len, Frac_clr, Frac_defrst, Frac_frst, Frac_refrst)
```

Data Frame Setup

In [200…

```
FogSettlingVelocity = FogSettlingVel(droplet_size)
FracClear, FracTMCF, FracPine, TreeFrac = LULC_scenario(scenario, LUclass_len, ts_len, Frac_clr, Frac_defrst, Frac_frst, Frac_refrst)
Fog_Evap_Budg = np.zeros((LUclass_len, ts_len, 3))
fog_val = np.zeros((LUclass_len, ts_len, 4))
LCL_val = np.zeros((LUclass_len, ts_len, 4))
for k in range(len(Elev)):
    for i in range(len(Year)):
        Daily_deposition = np.zeros(4)
        Daily_evap = np.zeros(4)
        Daily_budget = np.zeros(4)
        for j in range(1, 5):
            forestedgelenfacingm, emergentedgelenfacingm = Forest_Edge(TreeFrac[k,i], CellSize[k])
            DepositionFrac   = Sedimentation_Surface_Area(FracTMCF[k,i], FracClear[k,i], FracPine[k,i], LAI_TMCF, LAI_Clear, LAI_Pine, lss_
            EtFrac_total     = ET_LU(FracTMCF[k,i], FracClear[k,i], FracPine[k,i], LAI_TMCF, LAI_Clear, LAI_Pine)
```

```
            Tmp, AirRising   = Temps(j, T_max[i], T_min[i], T_avg[i], Elev[k]) #Tmp [C]
            E                = Saturated_vapur_press(Tmp, RH[i]) #E [mb]
            AirDensity, AH   = Air_density(Presh[i], Tmp, E)
            LWC              = LiqWaterContent(AH, AH_max=0.02717, maxLWC=0.0002)
            Td               = Dewpoint(E) # Td [C]
            LCL, fog         = LiftingCondensationLevel(Tmp, Td, Presh[i], Elev[k])
            if   j == 1:
                SolarR_ground = EffectiveSolarRad(Cld[i], fog, Rad24[i])
            elif j == 2:
                SolarR_ground = EffectiveSolarRad(Cld[i], fog, Rad6[i])
            elif j == 3:
                SolarR_ground = EffectiveSolarRad(Cld[i], fog, Rad12[i])
            elif j == 4:
                SolarR_ground = EffectiveSolarRad(Cld[i], fog, Rad18[i]) # SolarR_ground [W/m2]
            NetMap           = NetRad(SolarR_ground, FracTMCF[k, i], FracPine[k, i], FracClear[k, i], Month[i], LR[i], SecondsInMonth) #Ne

            Wind_spd_adj, Wind_dir_adj = WindSpeed(Wnd_d[i], Wnd_spd[i], Aspect[k])
            Prec_corrected    = RainMod(Prcp[i], Wind_spd_adj, Wind_dir_adj, Slope[k], DropTermVel)
            EdgeImpactionFlux, EmergentImpactionFLux = EdgeImpactFlux(Wind_spd_adj, forestedgelenfacingm, emergentedgelenfacingm, LWC)
            FogIntmm         = FogDeposition(Wind_spd_adj, TreeFrac[k, i], CellSize[k], LWC, FogSettlingVelocity, Area3d[k], EdgeImpaction
            ActEvap          = Evap(Tmp, NetMap, EtFrac_total)
            Budget           = Budgets(Prec_corrected, FogIntmm, ActEvap)
            #Store Outputs
            Daily_deposition[j-1] = FogIntmm * 6 #6 hours per timestep
            Daily_evap[j-1] = ActEvap
            Daily_budget[j-1] = Budget
            fog_val[k, i, j-1] = fog
            LCL_val[k, i, j-1] = LCL
        Fog_Evap_Budg[k, i, 0] = np.sum(Daily_deposition)
        Fog_Evap_Budg[k, i, 1] = np.sum(Daily_evap)
        Fog_Evap_Budg[k, i, 2] = np.sum(Budget)

Fog_Evap_Budg_Scn4 =  Fog_Evap_Budg
TreeFrac_Scn4 = TreeFrac
```

In [172…

```
#plt.plot(LCL_val[:, :, 2], '. ')
foggy_days = np.count_nonzero(fog_val[1, :, 2])
```

In [173…

```
print(foggy_days)
print(np.shape(fog_val[:, :, 2]))
```

```
8497
(40, 8796)
```

Stats and Visualization

Inputs:

D

Appendix: Instrumental set-up

D.1. Challenges and Decisions

D.1.1. Fieldsite location

The choice of this site for our prototyping phase was based on the following constraints:

- Had to decide between a cloud forest of higher elevation but lower accessibility (Los Ranchito) or lower elevation and higher accessibility (Satex I). Lower elevation can result in a lower amount of cloudy days.
- had to decide between a tree which was not affected by other trees but more exposed to sun, or a tree which was more in a cloud forest climate but the measurements were influenced by other trees. Eventually, the stemflow and throughfall measurements have been performed for the tree in the forest and the other measurements for the individual tree

D.1.2. Design of Devices

- We failed to estimate the necessary volume of containers correctly
-

D.2. Transpiration

Figure D.1: Transpiration set-up field - Arnica leaf.

Figure D.2: Transpiration set-up field - Hortencia leaf.

Figure D.3: Transpiration set-up field - Grass leaf.

Figure D.4: Transpiration set-up field - Helecho (fern) leaf.

Figure D.5: Transpiration set-up tree 1 - orchid leaf.

Figure D.6: Transpiration set-up tree 1 - tree leaf.

Figure D.7: Transpiration set-up tree 1 - tree leaf.

Figure D.8: Transpiration set-up tree 2 - tree leaf.

Figure D.9: Transpiration set-up tree 2 - tree leaf.

Figure D.10: Transpiration set-up tree 2 - tree leaf.

Figure D.11: Transpiration set-up forest - leaf from tree 3.

Figure D.12: Transpiration set-up forest - fern leaf.

Figure D.13: Transpiration set-up forest - tree leaf.

D.3. Diver Data

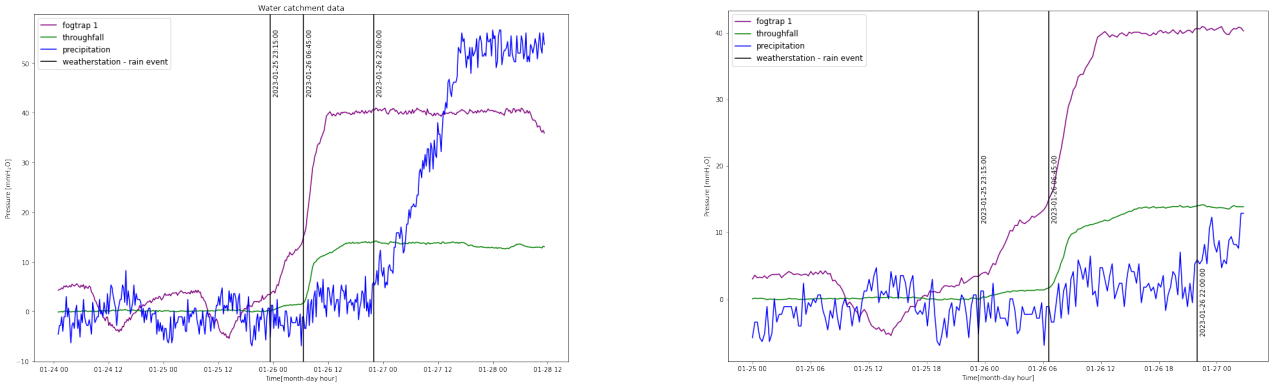

(a) **(b)**

Figure D.14: Data obtained from the divers installed in the measurements. Precipitation gauges and throughfall are shown for the entire period (a) and zoomed in on the first rain event (b).

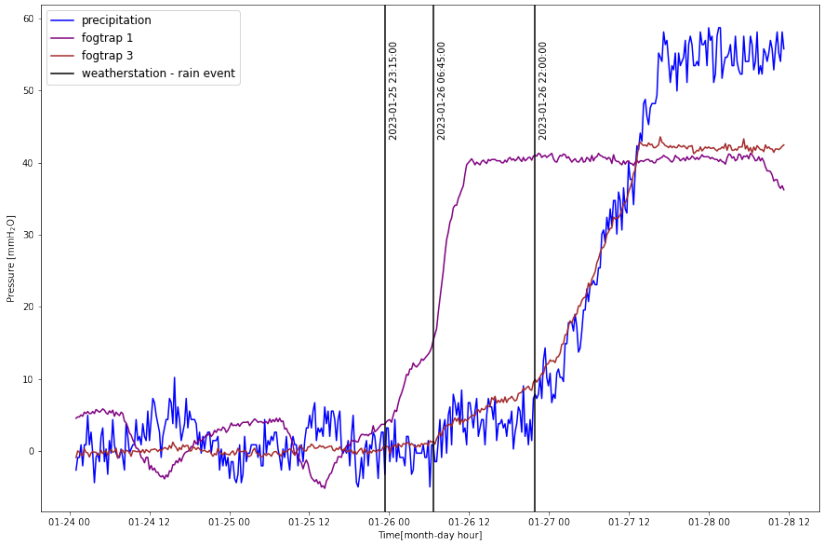

(a)

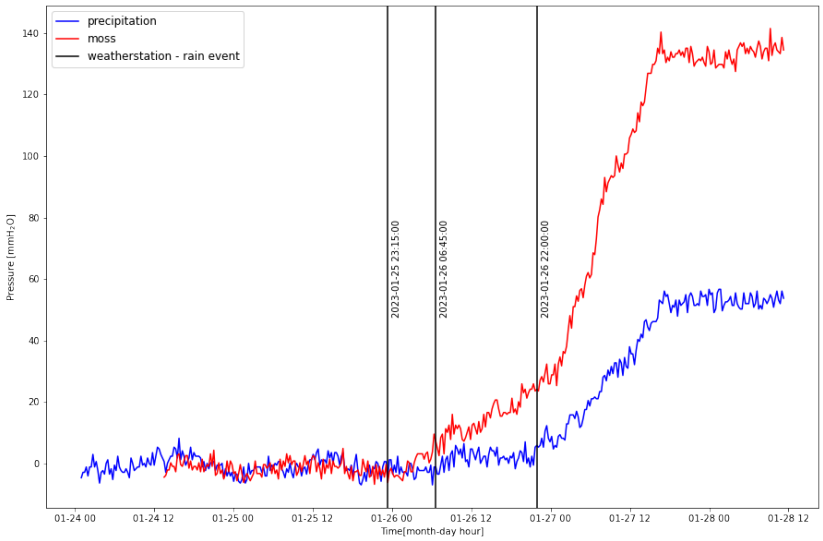

(b)

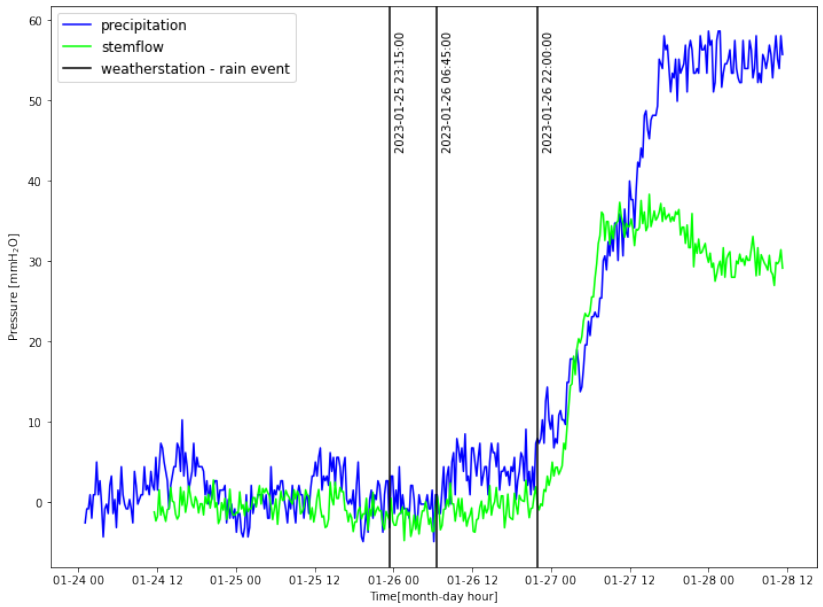

(c)

Figure D.15: Data obtained from the divers installed in the measurements shown during the total measuring event (a) Precipitation gauges and fog traps, (b) Precipitation gauges and moss fog trap (c) recipitation gauges and stem flow.

E

Appendix: Comparison of in-situ meteorological variables to weather station data

Figure E.1: Temperature from the weather station and scattered points of the data taken with the Kestral device.

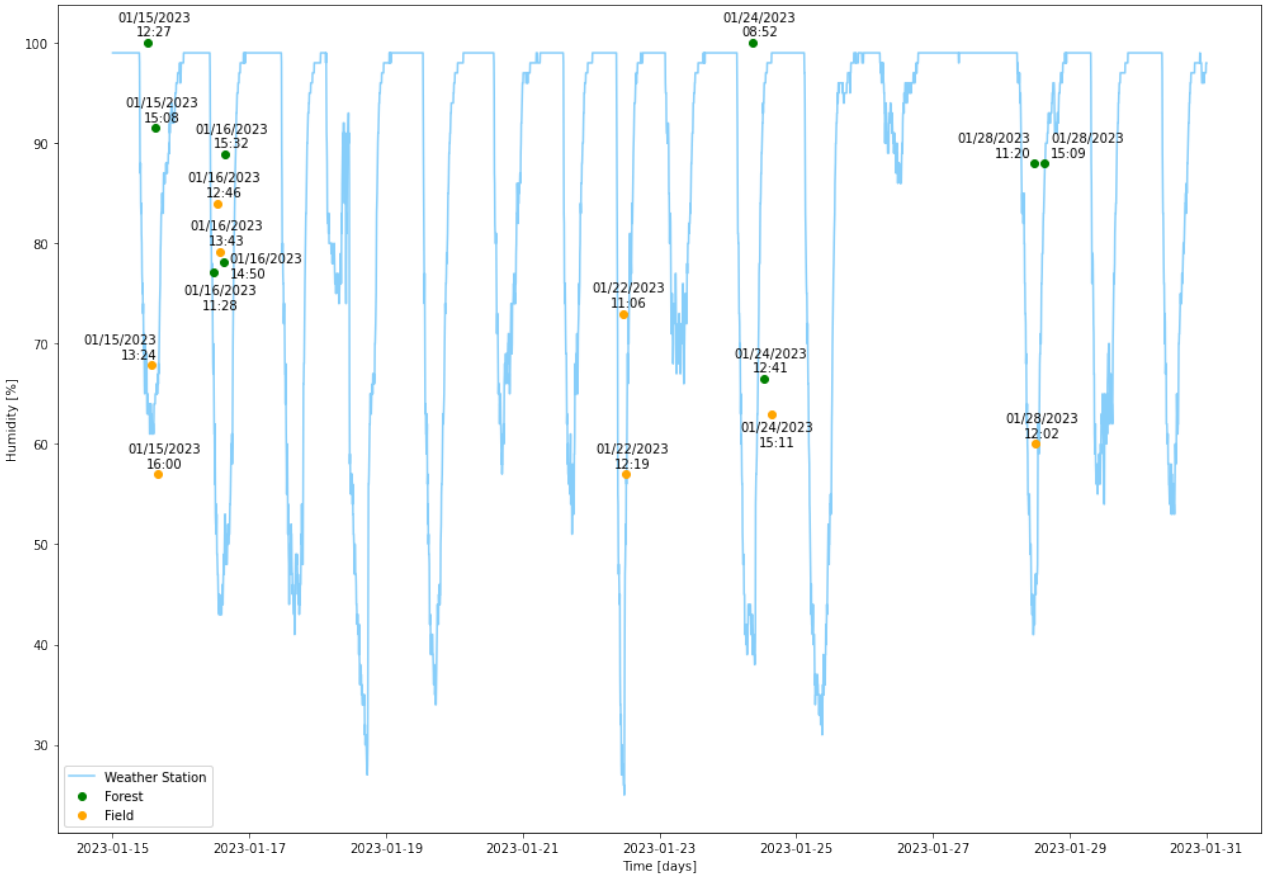

Figure E.2: Relative Humidity from the weather station and scattered points of the data taken with the Kestral device.

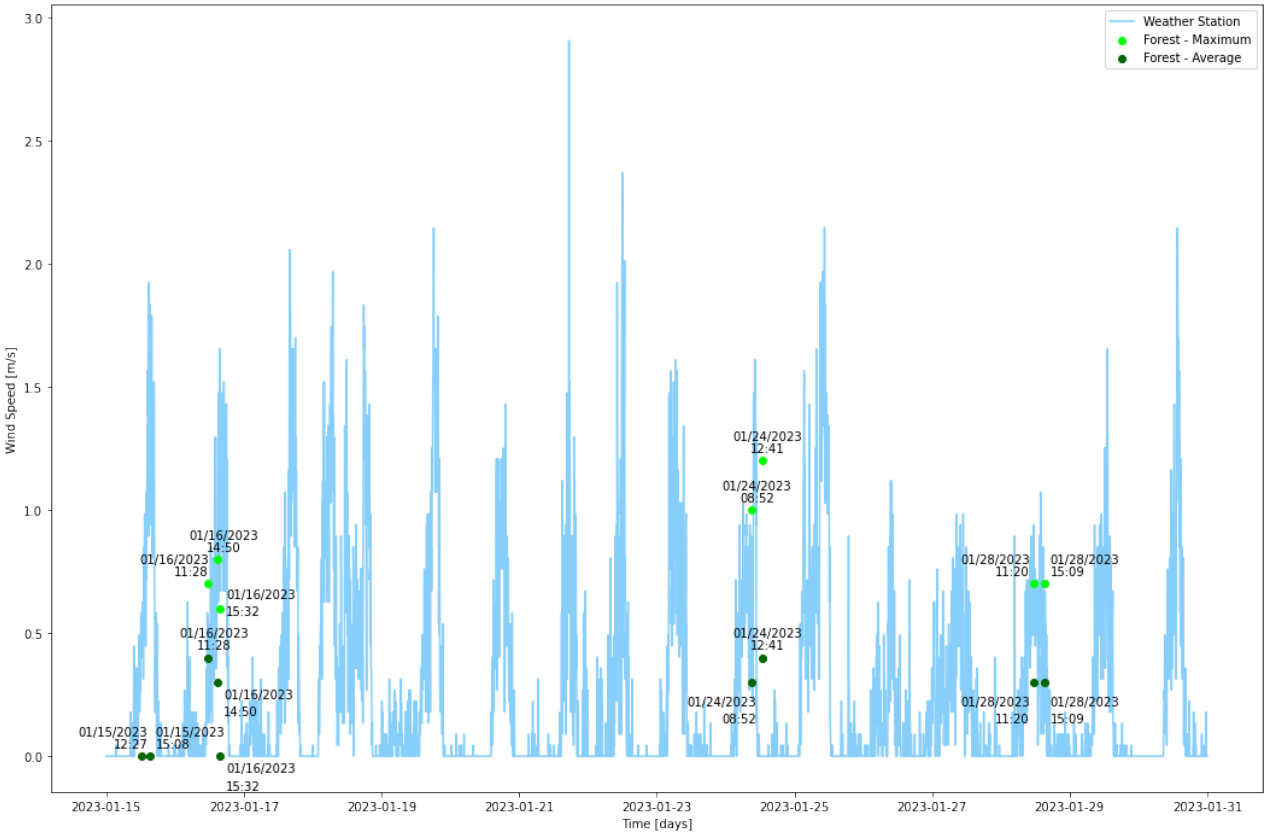

Figure E.3: Wind Speed from the weather station and scattered points of the data taken with the Kestral device.

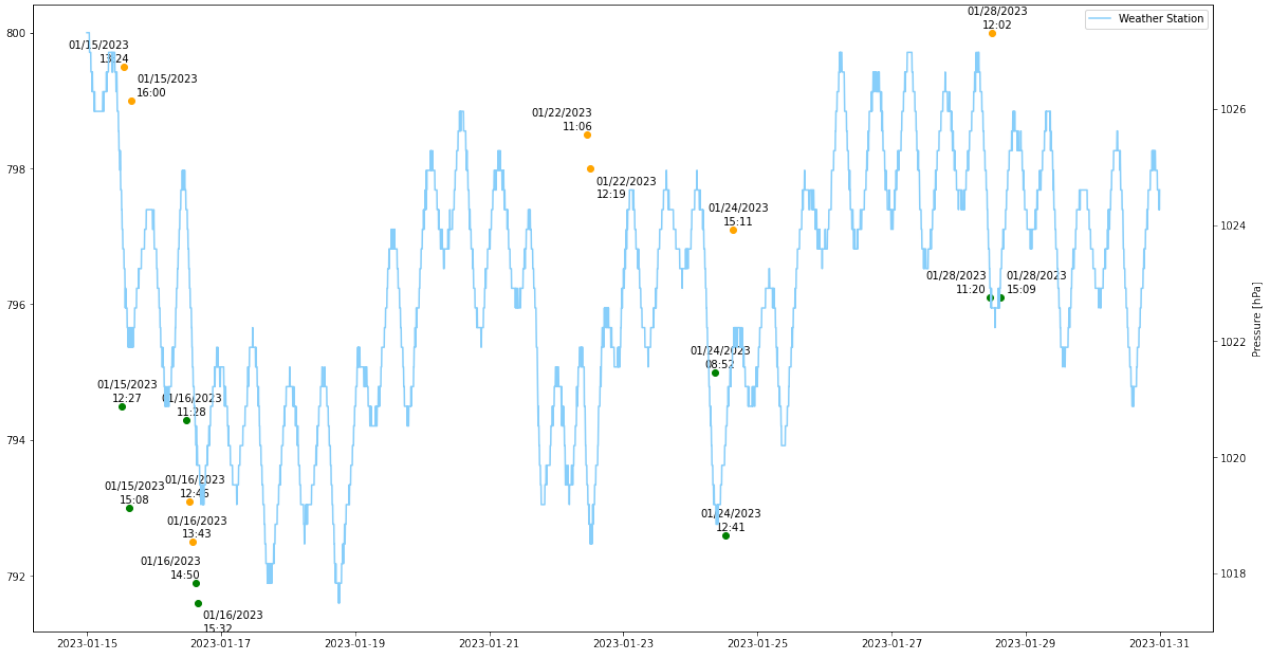

Figure E.4: Pressure from the weather station and scattered points of the data taken with the Kestral device.

F

Appendix: Mestela Catchment Maps

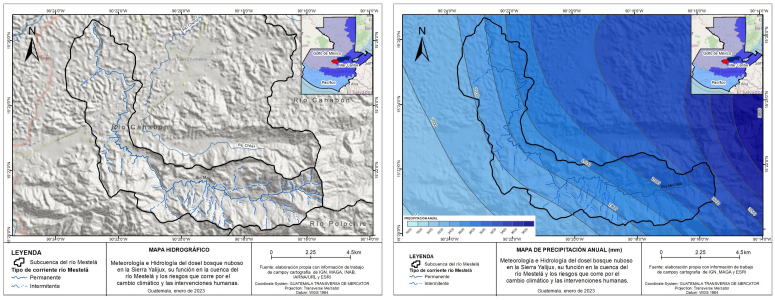

(a) **(b)** **(c)**

Figure F.1: Mestela Catchment Properties (a) flow paths, (b) yearly precipitation, (c) geology (Ochoa, 2023).

G

Appendix: Ecological and botanical site description

Dr. Fredy Archila
Lic. Javier Archila

INFORME VISITA A BOSQUE NUBOSO

Los bosques nubosos en términos generales se consideran **Bosques tropicales Montanos**. Reciben el nombre de “Bosques Lluviosos” por la característica de las lluvias horizontales o niebla. Desde el punto de vista ecológico estos bosques son zonas de captación de humedad y cabeceras de cuencas hidrográficas, desde el punto de vista de Biodiversidad los bosques nubosos funcionan como islas en los procesos de especiación vegetal debido a su sistema de dispersión de semillas cerrado. Existen grandes ejemplos de su importancia para la diversidad biológica y grandes iconos ambientales como los gorilas en el Congo, el oso de anteojos y la orquídea *Sudamerlycaste* en Sudamérica (Archila, 2002) el Quetzal en los bosques nubosos de México y centro América, la *Lycaste virginalis* en Guatemala y muchas especies endémicas de *Lepanthes* en el neotrópico.

El bosque que se visitó es un bosque transicional entre dos Zonas de Vida:

1) Bosque muy Húmedo subtropical frío.
2) Bosque pluvial Montano Bajo Subtropical (Archila, 2001).

Lo anterior lo podemos observar por su ubicación intermedia entre estas zonas y por las especies vegetales que se encuentran en el lugar que normalmente son indicadoras de ambas zonas, principalmente las miembros de la Familia Orchidaceae y algunas Bromeliaceae.

Durante la visita se pudo observar remanentes boscosos en los que la principal composición arbórea es:

Podocarpus-Quercus-Gordonia-Ormosia

La composición arbustiva está integrada por:

Dicksonia-Deppea-Cyathea-Geonoma* y *Chamaedorea

Un estrato bajo terrestre:

Lycianthes-Hohenbergiopsis-Greigia

Y un estrato epifito abundante en:

Cavendishia-Arpophyllum-Epidendrum-Anathallis-Guzmania

Al analizar la clasificación de tipos de vegetación de Guatemala este bosque pertenece a: "***Selvas Medianas siempreverdes de Tierras templadas***" (Méndez & Véliz, 2017)

LAS ORQUÍDEAS EN GUATEMALA

Guatemala es considerado uno de los 20 países megadiversos (Vázquez *et al*, 2021), los fenómenos que han moldeado la biodiversidad vegetal de esta tierra han sido múltiples en periodos largos de tiempo, causando extinciones masivas y presiones de selección que nos llevan a la flora actual (Archila & Tribouillier, 2020).

En los últimos 33 años La Estación Experimental de Orquídeas de la Familia Archila se ha dedicado a preservar e investigar plantas pertenecientes a la familia botánica Orchidaceae De Jussieu dado como resultado un incremento considerable del número de especies. Tomando en cuenta los datos de Ames & Correll, que indicaron que existían 527 especies (Ames & Correll, 1953) se comenzó con la actualización de los nombres y el incremento al explorar nuevas áreas y encontrar nuevos registros, es así como se presentó la primer actualización a 800 especies (Archila, 1992) posteriormente 1237 (Archila, 2014) y luego 1300 (Archila *et al*, 2018) y recientemente fue publicado un Checklist con 1400 especies un número considerable e interesante de especies considerando lo pequeño en espacio geográfico del país (Archila, 2022).

Lista de Orquídeas presentes en árboles muestreados:

- ***Oncidium tenuipes*** Kraenzl
- ***Rhynchostele cordata*** (Lindl.) Soto Arenas & Salazar
- ***Epidendrum Chloe*** Rchb.f.
- ***Arpophyllum medium*** Rchb.f.
- ***Anathallis platystylis*** (Schltr.) Solano & Soto Arenas
- ***Maxillaria praestans*** Rchb.f.
- ***Lepanthes matudana*** Salazar & Soto Arenas
- ***Epidendrum ramosum*** Jacq
- ***Epidendrum sp. verrucosum*** Sw.
- ***Epidendrum aberrans*** Schltr.
- ***Zosterophyllanthos pansamalae*** (Schltr.) Szlach. & Marg.
- ***Specklinia segregatifolia*** (Ames & C. Schweinf.) Solano & Soto Arenas
- ***Dichaea aff. muricatoides***

ZONAS DE VIDA

BOSQUE MUY HÚMEDO SUBTROPICAL (FRÍO) (bmh-S (f)).

Localización y extensión:
Constituye un segmento del muy húmedo Subtropical, representándose con una (f) de más para la zona de mayor altura donde las temperaturas medias son iguales a la biotemperatura. Este segmento abarca los alrededores de Cobán, siguiendo una faja angosta de 2 a 4 kilómetros de ancho para Baja Verapaz, pasando por la cumbre de Santa Elena. Luego se separa la faja para seguir bordeando la Sierra de Las Minas por un lado y por el otro sigue rumbo a la cumbre de El Chol en Baja Verapaz. Existe una pequeña área en el Cerro Monte Cristo frontera Salvador y Honduras; asimismo en el Volcán Chingo frontera con El Salvador. La superficie total de esta zona de vida es de 2,584 kilómetros cuadrados, lo que representa el 2.37 por ciento de la superficie total del país.

Condiciones climáticas:
El régimen de lluvias como en la zona anterior, el de mayor duración, lo que influye en la vegetación. El patrón de lluvia varía de 2,045 a 2,514 mm promediando 2,284 mm de precipitación total anual. Las biotemperaturas van de 16 grados a 23 grados C. La evapotranspiración potencial puede estimarse en promedio de 0.50.

Topografía y vegetación:
La topografía es generalmente ondulada llegando en algunos casos a ser accidentada. La elevación varía entre1100 m. En la Finca Las Victorias, hasta 1,800 m s. n. m. en Xoncé, Nebaj, Quiché. La vegetación natural que se considera como indicadora, está representada por: *Liquidambar styraciflua, Persea donnellsmithii, Pinus pseudostrobus, Persea schiediana, Myrsine ferruginea, Clethra spp, Morella spp, Croton draco, Eurya seemanii.*

Consideraciones generales sobre su uso apropiado:
Esta formación está siendo utilizada tanto para fitocultivos como para el aprovechamiento de sus bosques. Se cultivan, aparte de maíz y frijol, que son tradicionales, café, cardamomo, caña de azúcar, pacaya y árboles frutales como: cítricos, aguacate, coyou, injerto. También agave, pimienta y otros. Esta zona de vida es utilizada, a la vez para pastos criollos con ganadería en pequeña escala. En cuanto al aprovechamiento forestal, la especie más utilizada es *Pinus pseudostrobus*. Es necesario proteger y manejar adecuadamente los bosques para mantener el equilibrio, porque los suelos no son del todo vocacionales para fitocultivos y ganadería (Holdridge, 1978)

BOSQUE PLUVIAL MONTANO BAJO SUBTROPICAL (bp-MB)

Localización y extensión:
Comprende un área pequeña arriba de Tucurú y Tamahú en Alta Verapaz, pasando por Purulhá, Unión Barrios y Chilascó en Baja Verapaz, continua en la parte alta de la Sierra de Las Minas. La superficie total es de 908 kilómetros cuadrados lo que representa el 0.83 % de la superficie total del país.

Condiciones climáticas:
El patrón de lluvias es un poco difícil de determinar, por no disponerse de mayores datos, sin embargo, puede decirse que sobrepasa los 4,100 mm de precipitación anual. La biotemperatura oscila alrededor de los 19 grados C. La evapotranspiración potencial se estima en 0.25.

Topografía y vegetación:
La topografía es accidentada, teniendo elevaciones que van desde 1,500 hasta 2,700 m s. n. m. La vegetación natural predominante indicadora de esta zona de vida es: *Podocarpus oleifolius, Alfaroa costarincesis, Oreomunnea spp., Billia hippocastrum, Magnolia guatemalensis* y *Brunellia spp*. *Oreopanax xalapensis, Hedyosmun mexicanum* y *Gunnera sp*., que es una planta herbácea de hojas bien grandes.

Consideraciones generales sobre su uso apropiado:
La cubierta boscosa de esta zona reviste gran importancia por ser reguladora en el escurrimiento del agua. La presión demográfica puede llegar a reducir los bosques, y resulta necesario hacer notar que es mala economía para la nación dejar que se destruyan, pues al desaparecer se producen grandes erosiones, con las consecuencias ya conocidas.

Aparte de esto, puede comprobarse que son estos bosques los que prefiere El Quetzal (ave símbolo) para vivir. El uso apropiado de la zona, entonces, se conservaría como área de protección forestal. (Holdridge, 1978)

TIPO DE VEGETACIÓN:

Selva mediana siempreverde de tierras templadas
En Guatemala, se encuentran en el arco húmedo del norte, sobre rocas cristalinas, y en el pie de monte volcánico en el Pacifico, por lo general su dosel se encuentra entre los 15-30 m de altura, se desarrollaron en áreas con pendientes, desde los 1200 a 2500 m s. n. m, con niebla frecuente y con gran abundancia de helechos, epífitas y musgos.

Los ensambles de las especies difieren entre el arco húmedo norte y la cadena volcánica, algunos ejemplos de ello, son especies como *Brunellia mexicana* Standl., *Weinmannia pinnata* L., *Bejaria guatemalensis Camp., Toxicodendron striatum* (Ruiz & Pav) Kuntze, *Clethra suavelens* Turcz., *Podocarpus oleifolius*D. Don. ex Lamb., *Styrax spp, Persea sessilifolia* Standl. & Steyerm., *Cyathea divergens var tuerckheimii* (Maxon)R. M. Tryon, *Matudaea sp, Oreopanax steyermakii* A. C. Smith, *Saurauia pseudoscabrida* Buscalioni, *S. pseudorubiformis* Buscalioni, *Ternstroemia hemsleyi* Hochr, *Laplacea coriácea* L. Wms., *Liquidambar styraciflua* L., *Magnolia guatemalensis* Donn. Sm., *Oreomunnea guatemalensis* (Standl.) J.F. Leroy, *Styrax conterminius* Donn. Sm. *y S. steyermarkii* P. W. Fristch, especies con alta frecuencia en el arco húmedo del norte.

El sotobosque por lo general está poblado de distintas familias de helechos, incluyendo los arborescentes de las familias Cyatheaceae y Dicksoniaceae. En la cadena volcánica son

frecuentes especies como *Chiranthodendron pentadactylon,* Larreategi, *Clethra pachecoana* Standl. & Steyerm.*, Saurauia oreophila* Hemsl.*, Gunnera mexicana* Brandegee*, Oreopanax sanderianus* Hemsl.*, O. xalapensis* (Kunth)Dcne. & Planch.*, Prunus salasi* Standl.*, Cinnamomum salvinii* (Mez)Kosterm.*, Olmediella betschleriana,* (Goepp.)Loes, *Cedrela tonduzii* Harms*, Citharexylon donnell-smithii* Greenm.*, Quercus acatenangensis* Trel. *e Ilex tolucana* Hemsl*.*

El estrato arbustivo por lo general cuenta con helechos arborescentes de los géneros *Alsophila, Cyathea, Sphaeropteris y Dicksonia*, con mayor frecuencia en el arco húmedo norte.

Otros grupos frecuentes son: Arecaceae (*Geonoma* y *Chamaedorea* spp), Begoniaceae (*Begonia* spp), Ericaceae (*Cavendishia, Sphyrospermum y Vaccinium*), Rubiaceae (géneros *Hoffmania, Rondeltia, Palicourea y Psychotria*) y Gesneriaceae (géneros *Besleria, Solenophora y Achimenes*).

El estrato epífito es muy rico, siendo las regiones de mayor diversidad de Guatemala, especialmente la región del arco húmedo norte, como se observa en la figura 1, la diversidad y densidad en especies de las familias Orchidaceae, Ericaceae, Hymenophyllaceae, Lycopodiaceae y Bromeliaceae es muy alta, encontrando hasta 100 especies en este estrato. En la cadena volcánica, también existen muchas especies, pero la composición difiere, aparecen las mismas familias, pero menos diversas y además otras, como Crassulaceae (*Sedum y Echeveria*) y Scrophulariaceae. Véliz (1993), cita 47 especies en este estrato.

En la figura 1 se presenta dos topologías de ensambles idealizados de las epifitas, ello como ejemplo sobre las diferencias de las dos regiones lluviosas. Se conocen pocos estudios de este tipo de vegetación y regular número de registros de las plantas superiores. De grupos de plantas inferiores hay pocas colectas en Guatemala.

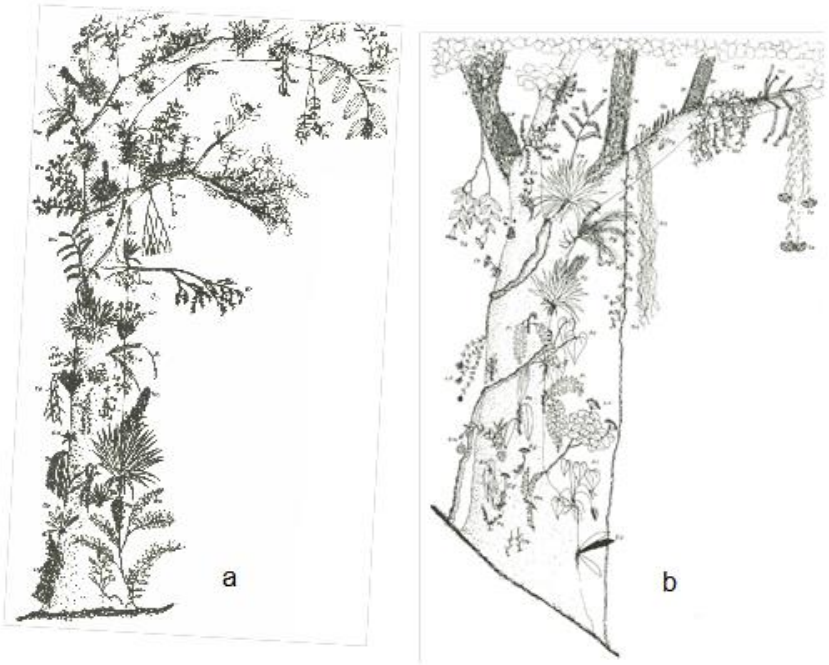

Figura 1. Topología de la distribución de epífitas de dos selvas medianas perennifolias templadas, (a) Epífitas del Biotopo del Quetzal, Purulha. B.V en el Arco húmedo Norte, 1900 m s. n. m. (b) Epífitas de la comunidad *Chiranthodendron* en al volcán Acatenango, en la cadena volcánica, 2300 m s.n.m. (Fuente: Méndez y Véliz, 2017).

BIBLIOGRAFÍA

Ames, O. & Correll, D. 1953. Orchids of Guatemala. Fieldiana: Botany, Volume 31. 779 pp.

Archila F. 1992. Recolección, cultivo y reproducción de orquídeas. Escuela Nacional Central de Agricultura ENCA, Informe técnico. 37 pp.

Archila F. 2001. *Lepanthes* de Guatemala. Monografía del género *Lepanthes* S.W. Guatemalensis Suplemento especial No, 2 281 pp.

Archila F. 2002. *Sudamerlycaste* Archila, Un género nuevo para Sudamérica. Revista Guatemalensis, Año 5(2). 16-34 pp.

Archila F. 2014. Listado de orquídeas de Guatemala. Revista Guatemalensis año 17 (2). 32-71 pp.

Archila, F.; Chiron, G.; Szlachetko, D.; Lipinska, M.; Bertolini, V. & Mystkowska, K. 2018. Orchid Genera and Species in Guatemala. Koeltz Botanical Books, Germany. 724 pp.

Archila F. 2022. Listado actualizado de orquídeas de Guatemala. Revista Guatemalensis año 25 (1 y 2). 129-419 pp.

Archila F. & Tribouillier E. 2020. Biogeografía y Evolución de la Flora de Guatemala. Revista Guatemalensis año 23 (1 y 2) 1-79 pp.

Holdridge L.R. 1978. Ecología basada en Zonas de Vida. IICA. San José, Costa Rica.

Méndez C. & Véliz M. 2017. Tipos de Vegetación en Guatemala. Revista Guatemalensis, año 20 (1 y 2). 155-165 pp.

Vásquez-García A.; Tribouillier E.; Archila F.; Véliz M.; Ortega S. & Shalisko V. 2021. Three new species of Magnolia (Magnoliaceae) endemic to the nort-wet-are in the Maya Highlands of Guatemala. Phytotaxa 529 (1) 57-70 pp.